GOVERNMENT OF INDIA
MINISTRY OF POWER

PREPARING DISTRIBUTION UTILITIES FOR UTILITY-SCALE STORAGE AND ELECTRIC VEHICLES

A Novel Analytical Framework

GREENING THE GRID (GTG)
A Partnership Between USAID and Ministry of Power, Government of India

Photo from iStock 1177095707

Prepared by

NREL

PREPARING DISTRIBUTION UTILITIES FOR UTILITY-SCALE STORAGE AND ELECTRIC VEHICLES

A Novel Analytical Framework

Authors

Adarsh Nagarajan, Shibani Ghosh, Akshay K. Jain, Sertac Akar, Richard Bryce, Michael Emmanuel, Timothy Remo, Aadil Latif, David Palchak, Jaquelin Cochran, *National Renewable Energy Laboratory (NREL)*

Abhishek Ranjan, Naveen Nagpal, *BSES Rajdhani Power Ltd.*

ACKNOWLEDGMENTS

ABSTRACT

Emerging distributed energy resources (DERs)—such as solar photovoltaics (PV), battery energy storage systems (BESS), and electric vehicles (EVs)—are expected to increase substantially in India in the coming years following policy-driven targets of the Government of India to modernize its electricity system, reduce greenhouse gas emissions (GHGs), and improve air quality. These emerging technologies can pose challenges to distribution utilities, forcing overhauls in planning and operational practices. They can also create challenges in power system infrastructure planning and cause more frequent system operational violations (e.g., network voltage bounds and loading thresholds) if not properly integrated.

The impacts on the localized power distribution grid from these emerging technologies manifest in increased infrastructure investments and erratic shifts in demand patterns. These impacts are not yet well understood, and analytic solutions are not readily available. To address these challenges, the National Renewable Energy Laboratory (NREL), in collaboration with BSES Rajdhani Power Ltd. (BRPL), developed an advanced power distribution system impact analysis framework of BRPL's distribution system. This framework helps analyze the readiness of the power distribution network to accommodate emerging technologies and the potential opportunities they might introduce. The framework has been predominantly set up to evaluate distributed PV, BESS, and EVs. In this collaboration between NREL and BRPL, we developed and evaluated the framework on two distribution feeders in the BRPL territory for various scenarios of BESS and EVs. BESS are evaluated for their effectiveness on the grid to mitigate present and future feeder overloading scenarios, and they are subsequently analyzed for their costs compared to the costs of traditional upgradation measures. Scenarios include assessing the effects of EV density on grid infrastructure upgrades and interlinking EV management with BESS integration.

List of Acronyms

BESS	battery energy storage systems
BNEF	Bloomberg New Energy Finance
BRPL	BSES Rajdhani Power Ltd
DER	distributed energy resources
DT	distribution transformer
EV	electric vehicles
GIS	geographic information system
GTG	Greening the Grid
HPC	high-performance computing
LCOE	levelized cost of energy
Li-ion	lithium-ion
NREL	National Renewable Energy Laboratory
PPA	power purchase agreement
PV	photovoltaics
RISE	Renewable Integration and Sustainable Energy
SAM	System Advisor Model
SAVFI	system average voltage fluctuation index
SAVMVI	system average voltage magnitude violation index
SAVUI	system average voltage unbalance index
SCADA	supervisory control and data acquisition
SCDOI	system control device operation index
SELI	system energy loss index
SOC	state of charge
SRPDI	system reactive power demand index

Executive Summary

Context and Problem Descriptions

Emerging distributed energy resources (DERs)—such as solar photovoltaics (PV), battery energy storage systems (BESS), and electric vehicles (EVs)—are expected to increase substantially in India in the coming years following policy-driven targets of the Government of India to modernize its electricity system, reduce greenhouse gas emissions (GHGs), and improve air quality. These emerging technologies can pose challenges to distribution utilities, forcing overhauls in planning and operational practices. They can also create challenges in power system infrastructure planning and cause more frequent system operational violations (e.g., network voltage bounds and loading thresholds) if not properly integrated.

The impacts on the localized power distribution grid from these emerging technologies manifest in increased infrastructure investments and erratic shifts in demand patterns. These impacts are not yet well understood, and analytic solutions are not readily available. To address these challenges, the National Renewable Energy Laboratory (NREL), in collaboration with BSES Rajdhani Power Ltd. (BRPL), developed an advanced power distribution system impact analysis framework of BRPL's distribution system. This framework helps analyze the readiness of the power distribution network to accommodate emerging technologies and the potential opportunities they might introduce. The framework has been predominantly set up to evaluate distributed PV, BESS, and EVs.

Methodology

In this collaboration between NREL and BRPL, we evaluated the framework on two distribution feeders in the BRPL territory for various scenarios of BESS and EVs. BESS are evaluated for their effectiveness on the grid to mitigate present and future feeder overloading scenarios, and they are subsequently analyzed for their costs compared to the costs of traditional upgradation measures. Scenarios include assessing the effects of EV density on grid infrastructure upgrades and interlinking EV management with BESS integration. Key outcomes of this research are as follows:

- Developed and validated an accurate, scalable end-to-end framework for evaluating the impacts of emerging technologies (BESS, PV, and EVs) on power distribution systems

- Developed models to characterize utility-scale BESS operations and economics across different use cases and developed methods to analyze isolated and stacked benefits of BESS with different control patterns

- Characterized various EV technologies deployed at different penetration levels for public, private, and commercial vehicles in terms of their aggregate demand profiles

- Identified and computed a suite of grid-readiness metrics for techno-economic assessments of network operation impacts under BESS control use cases and EV penetration scenarios

- Defined upgrade requirements for network infrastructure to mitigate possible violations of grid-readiness metrics and reduce potential customer service interruptions caused by an increase in overall system loading from EVs.

The work conducted for this project leverages many tools and capabilities unique to NREL. Data provided by BRPL—including feeder head and distribution transformer loading data along with all the technical specifications and schematics of two feeders in Delhi—underpin the model development and validation work.

After using specialized algorithms to improve the quality of the data, the distribution transformer profiles are used to perform multiyear, quasi-static time-series power flow analyses on detailed three-phase feeder

models. NREL's high-performance computing (HPC) system is leveraged to allow for the parallel analysis of many potential future scenarios. Additionally, the developed architecture provides a reusable framework to analyze the impact of integrating increasing numbers of EVs and utility-scale batteries into distribution networks.

Results

Results discussed in this report show the effective application of the developed framework. Included in are critical building blocks for the analyses, such as aggregated EV demand profiles and preliminary voltage impacts. Energy storage integration for peak-shaving applications are also evaluated. These platforms are then integrated for simulation on NREL's HPC system for subsequent cost-benefit analyses. Using the simulation results and corresponding impact-metrics analyses, network upgrade recommendation models are developed and assessed for two Delhi feeders and the costs of an emerging technology upgradation approach is compared to a traditional upgradation approach.

These types of assessments will help BRPL and other utilities gauge the readiness of their feeders for integrating increasing numbers of EVs and energy storage as the distribution sector continues to transform.

The following four topics are investigated in this study, which have relevance for policymakers, utility planners and other decision makers beyond the case study analyzed:

- Reusable framework for distribution utilities
- Impact of BESS on distribution system losses
- Minimally sizing and controlling BESS for maximum benefits
- Essential and cost-effective pathways to deploy BESS (staged vs. all at once).

Scalability of reusable framework for distribution utilities: This effort developed a reusable framework for distribution utilities to assess the impact of emerging technologies (BESS, EV, and PV) on their power distribution grids. The framework contains three layers, as shown in Figure ES-1. The first and base layer is the distribution feeder topology assessment. The second layer is for distributed generation, such as rooftop PV or any generation resources commonly referred to as a DER. The third layer is dedicated to BESS. The fourth layer is built to include EVs. Overall, all four layers interact and provide a comprehensive assessment of challenges and opportunities from emerging technologies.
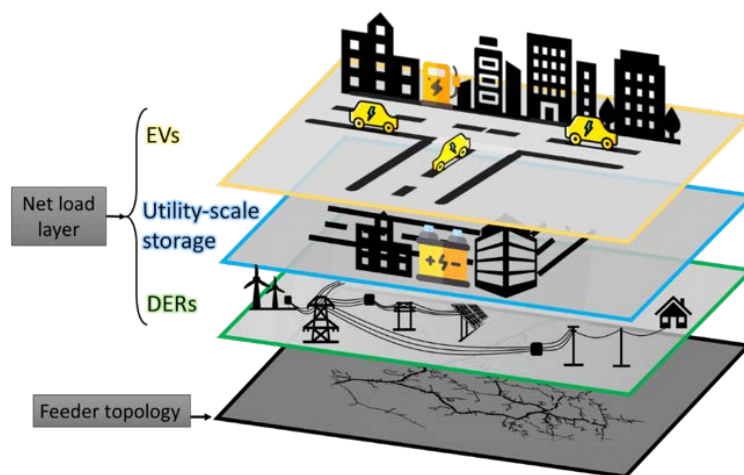

Figure ES-1. Modular layers in our reusable distribution analysis framework

This framework was simulated on NRELs HPC, and simulation runs exceeded 500 hours; however, the computational requirements for using this framework are not beyond a typical server or modern laptop. It is expected that BRPL engineers could run distribution feeder operation scenarios without the need for upgrades or simplification of models.

Analysis using this framework can be conducted outside of a supercomputing system or by purchasing software licenses given that we would like many utilities and other interested users to have access to this type of analysis. The solution framework is built entirely on open-source platforms and programming language.

Impact of BESS on distribution system losses: The main case study performed in this effort is on helping distribution utilities understand the possibility of deferring a distribution transformer upgrade by deploying a BESS in the neighborhood. Hence, the presiding question was understanding how a BESS affects system losses. Distribution transformers are generally designed to operate with maximum efficiency at or near 70% of rated power—in other words, transformer efficiency is affected by its loading. Appropriate battery charge/discharge settings on the test distribution feeders lead to reduced system losses. The reason being battery energy storage successfully displaces the transformer loading from less efficient part of the load curve to more efficient part of the load curve. Figure ES-2 depicts from our research results that for selected distribution transformers, combined system losses reduced when the BESS was performing peak shaving.
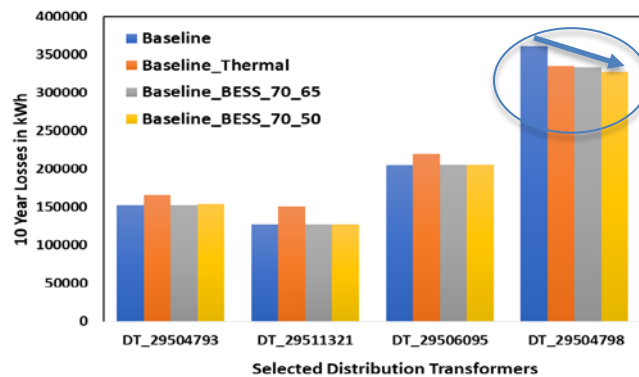

Figure ES-2. Impact of different battery control strategies on system losses

Minimally sizing and controlling BESS for maximum benefits: The peak-shaving mode of BESS requires the service operator to provide trigger values for peak shaving and base loading. The BESS will discharge power into the grid if the total power demand at the measured point—in this case, the distribution transformer—is greater than the peak-shaving upper reference limit. Conversely, the BESS will charge if the total power consumption at the measured point is less than the base-loading limit. It is important to ensure that charging the BESS occurs during the baseload loading periods (i.e., the valleys) to avoid overloading the distribution transformer during peak periods. After simulating various use cases, Figure ES-3 was generated to showcase the ability to achieve upgrade deferral with appropriate battery controls. Figure ES-3 depicts that for a certain distribution transformer, two different peak-shaving battery trigger points had varying impacts on overloading instances over 10 years of simulation.
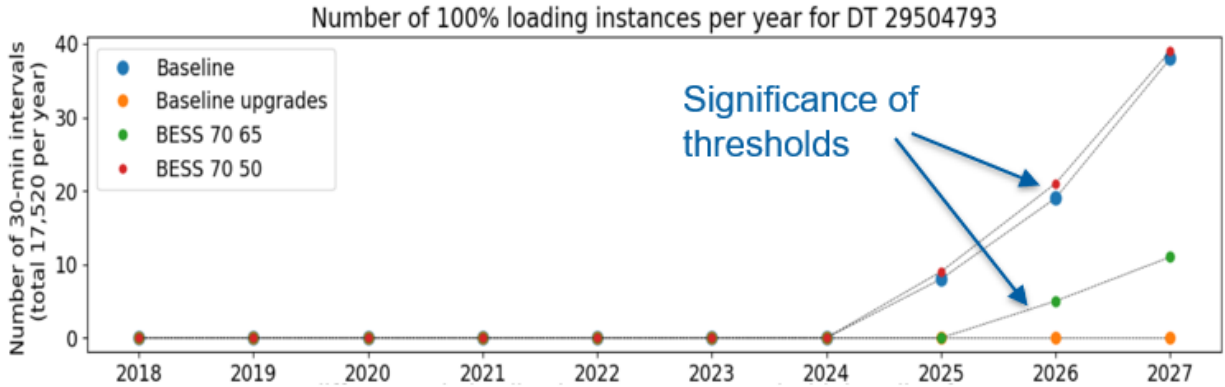
Figure ES-3. Count of 100% loading instances per year for selected transformer for different battery peak-shaving trigger points

Note: BESS 70 65 represents a control scheme where the battery operates to keep the loading of the distribution transformer between 70% and 65%. Simillarly for BESS 70 50, the battery operates to keep the distribution transformer between 70% and 50%.

Essential and cost-effective pathways to deploy BESS (staged vs. all at once): BESS are typically sized and deployed as full size; however, as a research exercise, we created three deployment scenarios (as shown in Figure ES-4): (1) standard deployment during the first year of the project (3,600 kWh), (2) staged deployment to meet the battery requirements, and (3) staged deployment by adding 200 kWh every year. The results of the staged deployment scenarios showed that capital costs can be 9.7% less for Scenario 2 and 13% less for Scenario 3 (Figure 87). Section 6.3.2 contains detailed descriptions on how we reached this result.
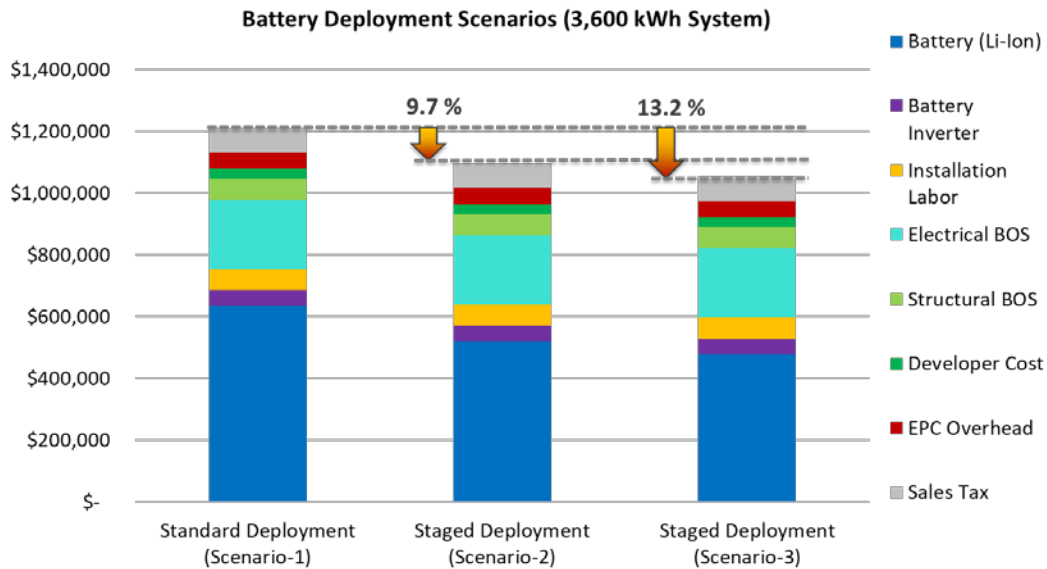

Figure ES-4. Capital cost comparison for different battery deployment scenarios

These topics are addressed throughout this report. Chapter 7 summarizes the notable outcomes.

Table of Contents

List of Figures

List of Tables

1 Introduction

In addition to behind-the-meter photovoltaics (PV) and battery energy storage systems (BESS), the integration of electric vehicles (EVs) is expected to increase substantially in India in the coming years as a result of clean energy policy targets from the Government of India. The impact of such rapid growth of distributed energy resources (DERs) on the electric grid needs to be understood and quantified to reinforce informed planning and ensure reliable grid operation. To address this, the National Renewable Energy Laboratory (NREL), in collaboration with BSES Rajdhani Power Ltd. (BRPL), has developed an analysis framework that uses state-of-the-art modeling techniques to anticipate the potential impacts on distribution systems in an evolving energy sector. This work is conducted under a broader program, Greening the Grid, which is an initiative co-led by the Government of India's Ministry of Power and the United States Agency for International Development.

This report presents initial findings of the research collaboration between NREL and BRPL and addresses key research questions about the integration of these emerging technologies onto BRPL's distribution grid. The objective is to build a framework for analyzing the economic and technical benefits and challenges of the integration of EVs and BESS and to help optimize infrastructure development costs for BRPL.

1.1 Background

Reducing BESS costs and increased growth in EV penetration are the primary drivers of this research collaboration. BRPL anticipates installing BESS in their distribution transformers (DTs) and a rapid EV rollout soon. BESS deployments and EV rollouts are encouraged by national- and state-level policies to increase renewable integration and reduce emission intensity.

This framework developed by NREL and BRPL captures the combination of this simultaneous evolution (BESS and EV) in distribution system planning so that potential grid impacts can be anticipated, and cost-effective measures can be taken to address potential issues. In addition to developing the framework, NREL adapted grid-readiness metrics that help characterize the scale of system impacts on various measures of grid health.

The cost-benefit analyses of BESS integration are performed on two feeders in BRPL's service territory, chosen for their potential to host a BESS pilot project or strategic investment. Storage technologies are expensive assets and have the potential to provide multiple services to the grid. NREL identifies value streams of utility-scale, grid-interactive BESS for load-leveling applications on transformers, which are similarly applicable across diverse use cases (such as capacity firming and energy arbitrage) for local grid-support services. Along with BESS, realistic models of various EV technologies (such as e-rickshaws and plug-in EVs) are deployed at various penetration levels for public, private, and commercial vehicles. These models will translate the EV fleet on the streets into grid-connected temporal load curves. For techno-economic assessments of grid impacts, this framework computes suites of grid-readiness metrics under different BESS use cases and EV integration scenarios.

Under this collaborative effort with the United States Agency for International Development and BRPL, NREL achieved the following project objectives:

- Developed and validated an accurate and scalable end-to-end framework for simulating various present and future scenarios of the selected feeders

- Developed models to characterize utility-scale BESS operations and economics across different use cases and developed methods to analyze isolated and stacked benefits of the BESS with different control patterns
- Characterized various EV technologies deployed at different penetration levels for public, private, and commercial vehicles in terms of their aggregate demand profiles
- Identified and computed a suite of grid-readiness metrics for techno-economic assessments of network operation impacts under BESS control use cases and EV penetration scenarios
- Defined upgrade requirements for network infrastructure to mitigate possible violations of grid-readiness metrics and reduced potential customer service interruptions caused by an increase in overall system loading from EVs.

These objectives were designed to realize combined value streams of the BESS, which requires careful consideration of use case prioritization, double counts, and time- and location-based constraints. From these analyses, decision makers might benefit from understanding the economic impacts of operational decisions of service providers. Without a robust understanding of trade-offs, during peak periods, for instance, service providers and operators might prioritize load leveling irrespective of how lucrative the energy market prices are within this period. For EV integration scenarios, understanding where, when, and how much consumers charge their vehicles will assist the utility in developing realistic charging-station demand profiles and projections to provide a robust solution for mapping distributed and centralized charging concepts within their service territory. Based on these EV and baseload projections, utilities could develop their network upgrade plans. To that end, NREL carried out sensitivity analyses on possible network upgrades across BESS use cases with stacked benefits valuations specific to the selected distribution feeders.

1.2 Analysis Approach

NREL developed robust simulation-based methodologies and analytic methods for a techno-economic evaluation of grid-interactive energy storage assets across diverse use cases while combining the integration of EV technologies in two selected feeders of the BRPL network. This approach also required maintaining grid reliability and resilience.

This framework can help utilities analyze their network readiness for emerging technologies, the impact of EV penetration on the grid, and the potential solutions introduced by front-of-the meter BESS. Together with technical benefits, this framework allows for an assessment of the economics of conventional (lines/transformers) and advanced network upgrades (storage). Case studies for this framework are designed around New Delhi feeders under various levels of projected growth in EV penetration and charging scenarios.

1.3 Use Cases

This research evaluates the interactions between BESS and EV technologies across diverse use cases and penetration levels, as shown in Figure 1.
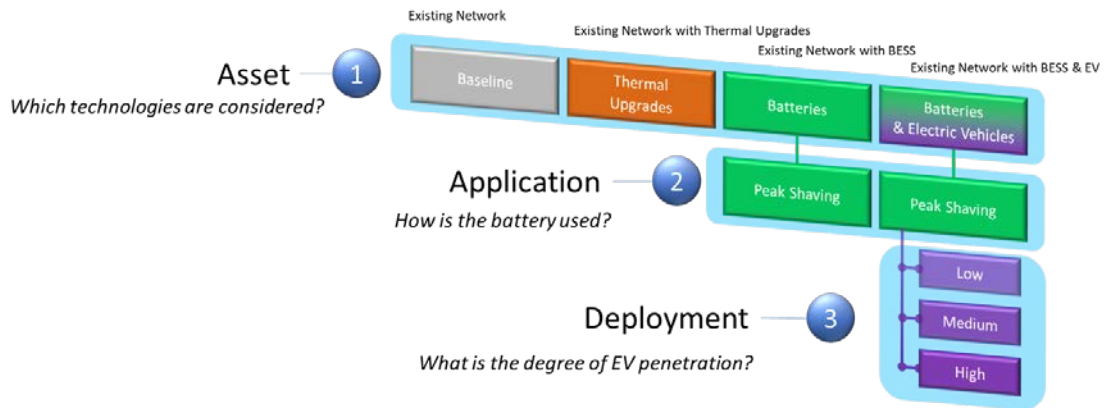
Figure 1. Different use cases and scenarios to consider for the EV/BESS pilot

To obtain all combinations of these technologies, NREL performed the study under a bassline and three major use cases:

1. Baseline: The baseline scenario uses the existing network architecture and feeder loading, which helps differentiate the changes caused by new technologies on the local grid in the subsequent simulation scenarios.

2. Traditional upgrades: This use case considers line or transformer upgrades as needed to prevent network violations. Yearly load growth can exacerbate network operation and cause thermal violations for these devices.

3. BESS and control applications: This use case considers utility-scale BESS, sized as recommended by BRPL, on the baseline model. The intent is to analyze and evaluate the achievable value streams from the integrated energy storage asset. Peak shaving is considered with staged (yearly addition of battery packs) and fixed deployment strategies. EVs are not included in this use case.

4. EVs: Varying levels of EV penetration are considered in this use case. Two subcategories of this use case are:

   A. With peak-shaving BESS

   B. Without BESS (baseline and with traditional upgrades).

   Each subcategory considers three EV penetration levels: low, moderate, and high. Initial assumptions for these levels come from the total number of vehicles within the territories of the given feeder(s). Because these scenarios represent future scenarios, corresponding load growth and expected PV are also considered.

These use cases are included as layers on base feeder models, as shown in Figure 2. Any existing DERs can be integrated in the net load layer.
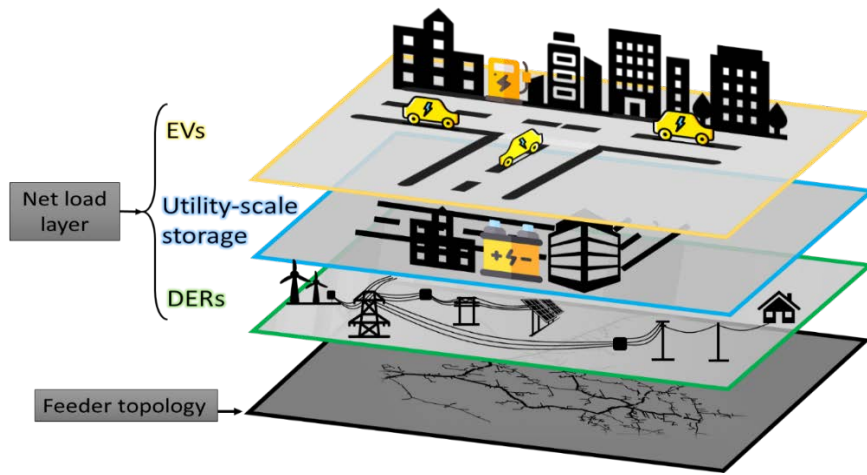
Figure 2. Various layers for modeling loads, EVs, and other DERs for centralized charging concept

2 Distribution Feeder Modeling

This chapter describes the methodologies used for building analyses-ready feeder models, including allocating and cleaning data for the EV integration and BESS impact studies. Two distribution feeders (Feeder 1 and Feeder 2) in Delhi were identified by BRPL and were therefore selected as case studies to better understand the impact of BESS and EVs. Using the topological and network configuration data provided by BRPL, NREL modeled the network in OpenDSS, an open-source software for simulating electric distribution systems.

2.1 Distribution System Analyses Tool

For the purpose of performing distribution system power flows OpenDSS is used. The OpenDSS is a comprehensive electrical power system simulation tool for electric utility power distribution systems. It supports nearly all frequency domain (sinusoidal steady-state) analyses commonly performed on electric utility power distribution systems. In addition, it supports many new types of analyses that are designed to meet future needs related to smart grid, grid modernization, and renewable energy research. Primary purpose to choose OpenDSS is that OpenDSS is designed to be scalable so that it can be easily modified to meet required needs as opposed to other off-the-shelf solutions such as Synergi, CYMEDIST.

2.2 Distribution Network Modeling

The building blocks of this feeder analysis framework require multiple data sets to be compiled into a usable distribution network model, as shown in Figure 3. The network topology is created from the geographic information system (GIS) database that manages all network assets. Equipment databases are used to identify and model attributes of different network assets, such as distribution lines, transformers, capacitor banks, and existing PV systems. Demand is also a critical component of this model. Base demand profiles are created from supervisory control and data acquisition (SCADA) data and consumer energy consumption patterns.
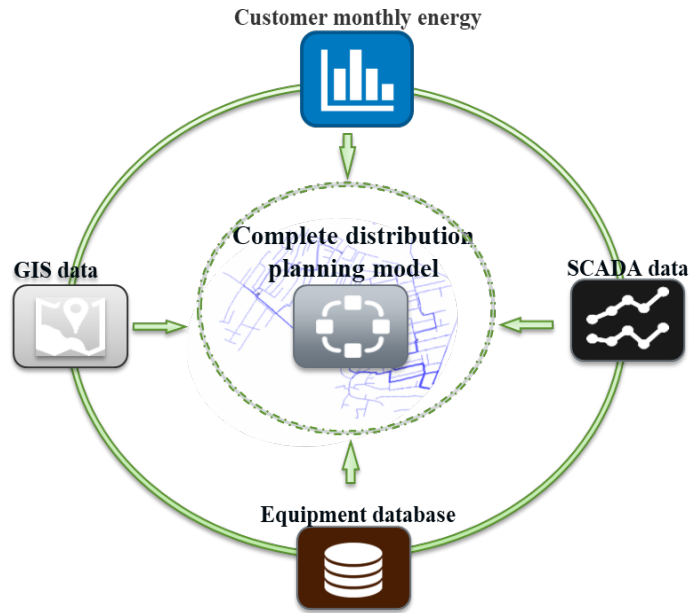
Figure 3. Network model development for the planning framework

In many instances, utilities do not have real electric models for network segment modeling, simulation, and power flow studies. Instead, they maintain a GIS database to manage network assets for their service territories. A pivotal step to enable accurate characterization of feeder operations is to convert the GIS data into a format suitable for OpenDSS. GIS-based shapefiles provide visualization for the feeder topology and typical path and engineering design of wires and towers (Stephen, 2014); however, a critical issue with GIS-based network diagrams is in the accuracy of network segment connectivity. For example, line segments that appear to be connected in GIS visualization could be separated by a minute distance, which might not be obvious to visual perception and therefore might result in an unsuitable model for power flow analysis (Espinosa, 2015).

2.2.1 Converting Geographic Information System Files to a Connected Network

The distribution network segments are represented within the GIS database by layers, which have different numbers of features (i.e., attributes) and geometry types, as shown in Table 1. These data layers are processed in QGIS software, an open-source platform to analyze and visualize geospatial information.

Table 1. Features and Types of Network Segments			
Layer ID	**Layer Name**	**Number of Features**	**Geometry Type**
0	Busbar	69	Line string
1	Circuit breaker	23	Point
2	Distribution transformer	7	Point
3	Extra-high voltage lines	1	Polygon
4	High-tension cable	21	Line string
5	Low-tension cable	27	Line string

6	Overhead conductors	165	Line string
7	Substation	7	Polygon
8	Switch	60	Point

The QGIS software uses line strings to represent line segments in the network, some of which are polylines, as shown in Figure 4 making it difficult to access all the features of each segment. Also, these polylines, which are continuous lines with one (or more than one) line segments, are represented as a single object in QGIS. These polylines have a single source and end point coordinates, which do not fully represent them and are therefore insufficient to build electrical models in power network modeling and simulation tools.
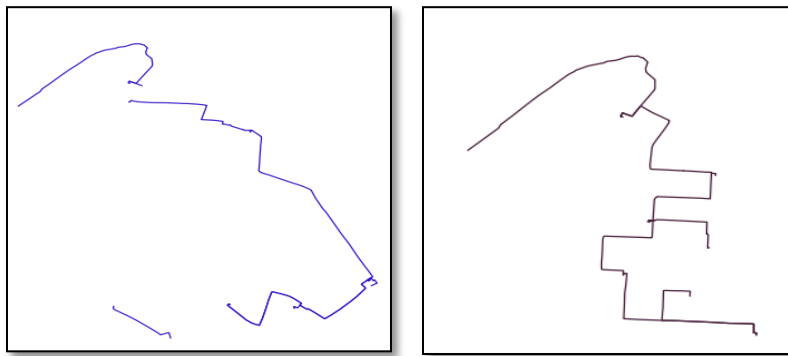
Figure 4. Line string example of feeder sections with multiple polylines

To address the issue with polylines, the following procedure was implemented in QGIS:

1. Explode each line layer. This takes each line and creates a set of new lines representing segments of the original line. The new lines have a start and an end point without intermediate nodes.

2. Export the geometry of the exploded layer to nodes and attribute files using the MMQGIS plugin. The resulting line segments from Step 1 have nodes with source and end coordinates.

3. Add the coordinates of all the line layers from Step 2 to form the network line topology as shown in Figure 5 and Figure 6 for Feeder 1 and Feeder 2, respectively.
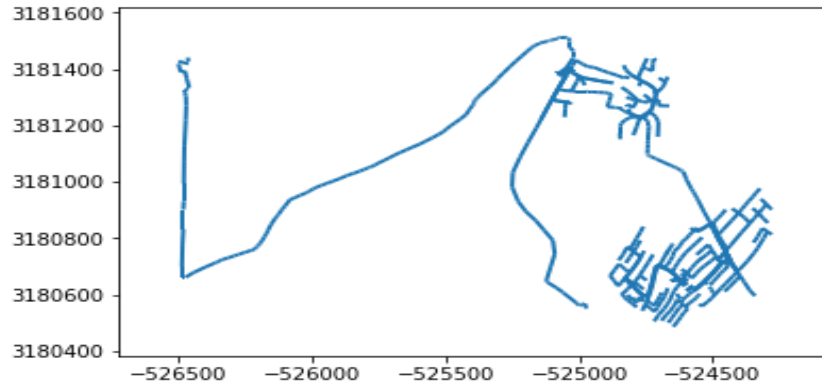
Figure 5. GIS-based reconnection model for Feeder 1
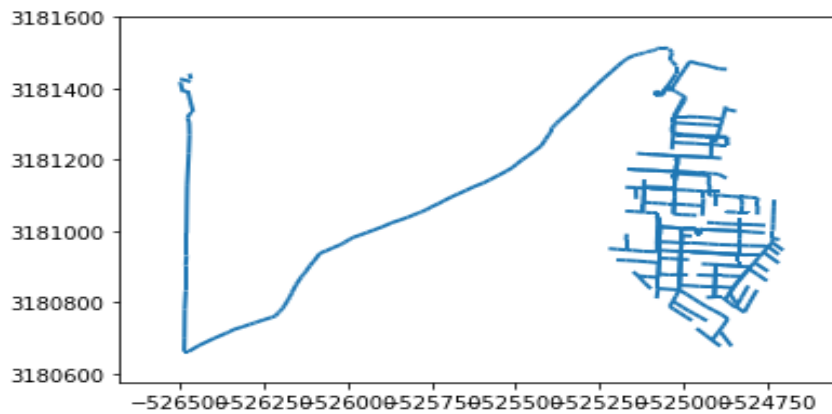
Figure 6. GIS-based reconnection model for Feeder 2

2.2.1.1 Network Creation

This section describes the feeder reconnection process from the GIS-based shapefiles using node coordinates obtained from the distribution utility coupled with the corresponding attribute table to perform the following operations using the NetworkX package.

2.2.1.1.1 Edge Creation

To create edges for nodes with various line layers of the feeder—such as underground, overhead, low-tension, and high-tension—the edge parameters are defined to capture the different line characteristics. Some considered parameters include capacitance, continuous line ratings, positive-, negative-, and zero-sequence impedances. Cables used for edge creation are classified according to their size and voltage level (e.g., 11 kV, 415 V). Also included in this class are distribution transformers for connecting nodes, whose parameters are defined such as the connection types, windings, maximum and minimum taps, and percentage load and no-load losses.

2.2.1.1.2 Feeder Head Location

The feeder head is determined by identifying any node within the vicinity of the substation with only one neighbor connected. This procedure was implemented by constructing a rectangle with the substation nodes and then identifying the node with one neighbor connected to it.

2.2.1.1.3 Adding Nodes and Merging Neighboring Nodes

The next step is combining the nodal elements—such as the circuit breakers, distribution transformers, and switches—with their properties in the attribute table for the respective feeders. For circuit-breaker nodes, attention was given to never use bus bars as an edge parameter because they are internally connected, as shown in Figure 7. Figure 8 shows distribution transformers connecting overhead lines for a certain portion of the feeder.

To determine if nodes should be merged, the Euclidean distance metric (D) was used to compute the distance between nodes. Nodes with D < 0.001 are considered neighboring nodes and are thus merged into a single node.
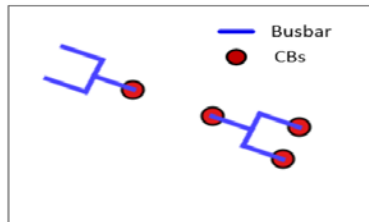
Figure 7. Bus bar and circuit-breaker connection

2.2.1.1.4 Remove Loops in Feeder Layout

There is a high possibility of forming loops or cycles in the process of network creation. For instance, circuit-breaker nodes can easily form a loop that causes power flow to be trapped in a section of the network with a high tendency to increase network losses. To remove these cycles, edges connecting circuit breakers to create loops are removed from the network topology.

Because power flow cannot run in a disconnected network, it is important to compute the number of connected and disconnected components. To determine the main connected components, a list of connected components generated as subgraphs was created. Not all disconnected line segments or nodes can be fixed automatically or algorithmically. Reconnecting components that are disconnected might require human intervention to decide whether to connect islanded components. In some cases, axis coordinates are flipped to connect disconnected line segments.
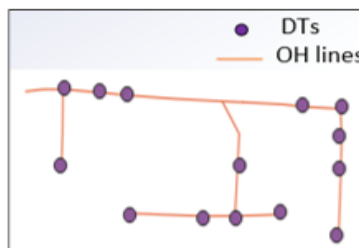
Figure 8. Distribution transformers connecting overhead lines for a certain portion of the feeder

The complete procedure for translating GIS data to the OpenDSS format is illustrated in Figure 9. The reconnection models are updated with a device data sheet to create the OpenDSS model, with the load profiles as inputs to the OpenDSS model.
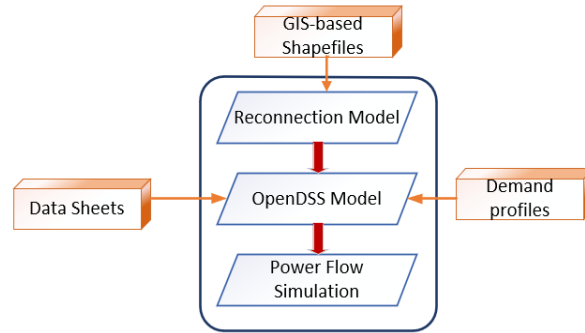
Figure 9. GIS-based data set translation to OpenDSS model

2.3 Distribution System Loading Data Sets

We received three loading data sets from BRPL: (1) three-phase, three-wire, 2-W metered data obtained at both 11-kV feeder heads; (2) three-phase, three-wire, 3-W metered data obtained at all distribution transformers; (3) and monthly customer billing data.

2.3.1 Feeder Head Loading Data

BRPL shared feeder head loading data sets for Feeder 1 and Feeder 2 that included time series of import and export readings, Phase A and Phase C voltage readings (kV), current readings (A), demand (kW), the power factor, and the time stamp. All these data were sampled at a time resolution of 15 minutes and span 1 year: from October 30, 2017, to September 30, 2018.

Figure 10 shows the combined loading of Feeder 1 and Feeder 2. Peak loading is observed in the evening hours during the summer months, and the lowest loading conditions are during the early hours during the winter months.
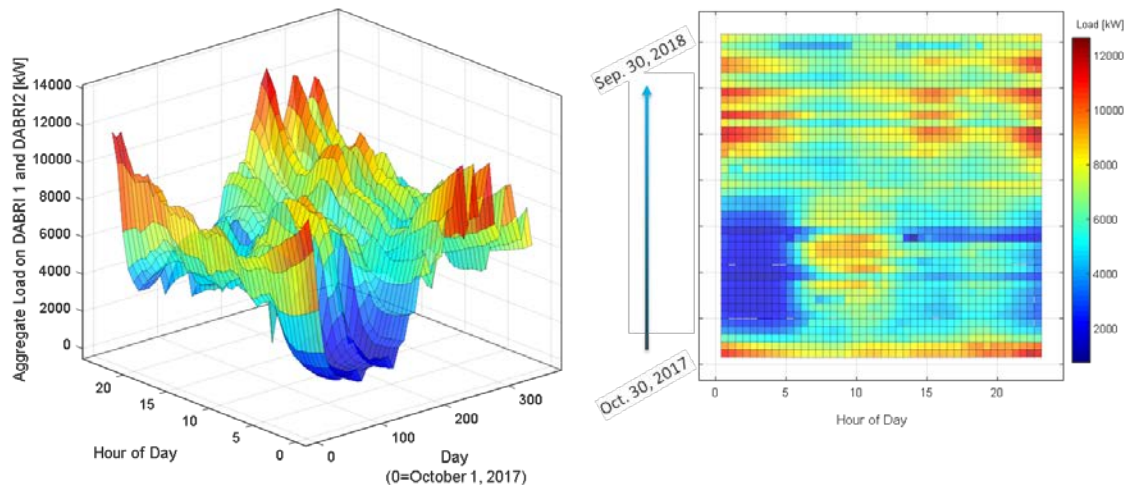
Figure 10. Surface plot of aggregate demand on Feeder 1 and Feeder 2 showing diurnal and seasonal variability (left) and heat map of aggregate demand on Feeder 1 and Feeder 2 showing diurnal and seasonal variability (right)

2.3.2 Distribution Transformer Loading Data

NREL received seven distribution transformer loading data sets for both Feeder 1 and Feeder 2, for a total of 14 distribution transformer loading profiles. Each data set comprises time-series data that include the

active power, reactive power, and voltage on each of the three phases of the secondary distribution lines spanning the same year as the feeder head time-series data. A time series that indicates outages is also included.

2.3.3 Customer Billing Data

In addition to the feeder head and distribution transformer loading time-series data sets, BRPL provided the customer billing information for all customers serviced by each distribution transformer.

2.3.4 Method for Cleaning Distribution Transformer Data

The distribution transformer data are cleaned to enable the quasi-static time series simulations. Once cleaned, the time series are normalized relative to the maximum loading condition observed on each distribution transformer. The data cleaning process is described in the following sections.

2.3.4.1 Data Cleaning Process

The data were analyzed to decompose the typical trends in the loading profiles from the abnormal variabilities including measurement errors. Typical trends are a composite of several timescales; load variability features subhourly, hourly, diurnal, and seasonal dynamics. Here, we focus on the daily trend, which is characteristic for each month of the year; and the seasonal variability, which is characterized by a daily relative drift from the mean monthly value.

To obtain the typical daily profile for each month, the loading observed during each half-hourly time point is averaged with all the same half-hourly values within the month (e.g., all points at 1:30 a.m. in April are averaged for a single value for April, 1:30 a.m.). This process is repeated for each month in the year, producing a profile that is used as a template, or donor, profile to fill missing time points. The donor profiles for Feeder 1 and Feeder 2 are shown in Figure 11 and Figure 12.
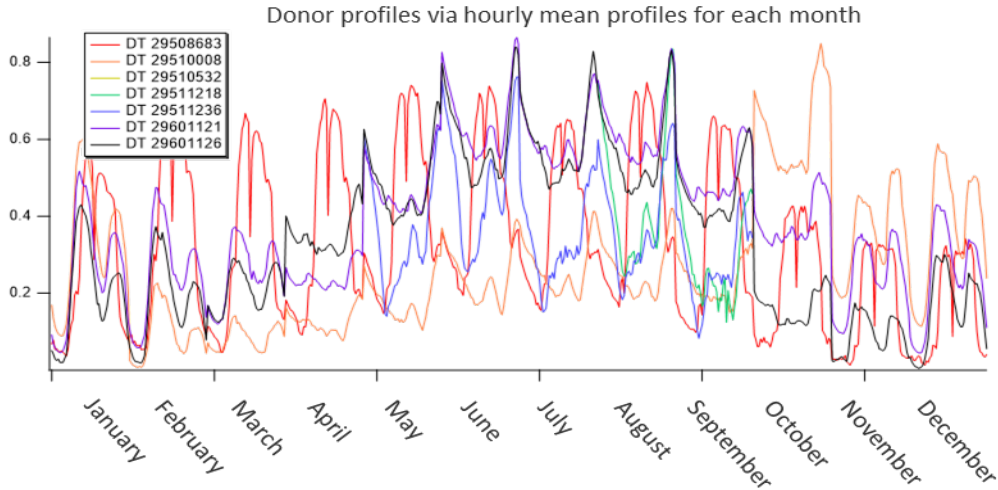
Figure 11. Donor profiles for each distribution transformer for Feeder 1 during each month
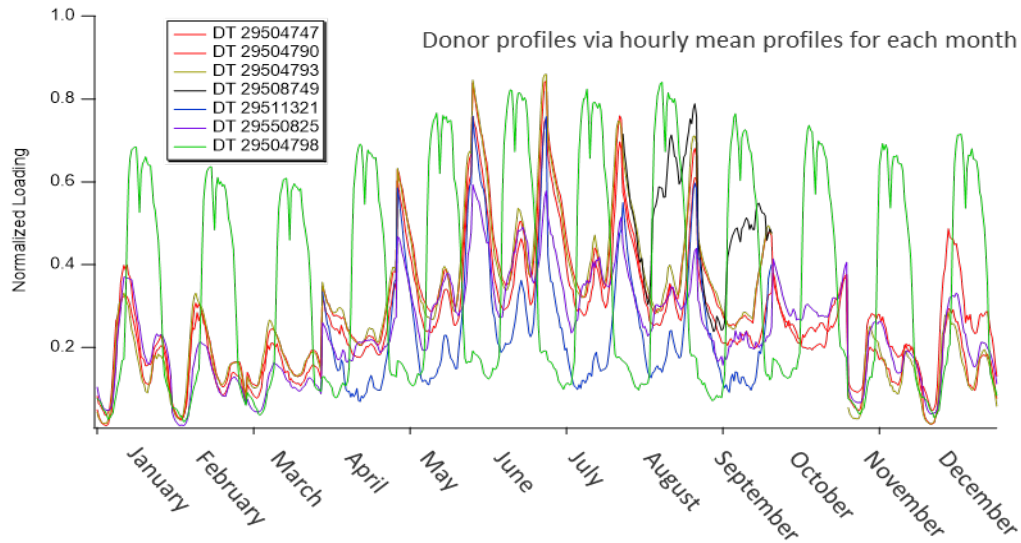
Figure 12. Donor profiles for each distribution transformer for Feeder 2 during each month

Some notable consequences of using a donor profile to fill in the missing data include that the data at the boundaries of the domain of the missing data might feature a step discontinuity. A smoothing technique is used to prevent this. Additionally, if a single donor profile is used repeatedly to fill consecutive days, those days would not feature seasonal variability and inter-monthly trends. To incorporate more natural variability into the data sets when there are large gaps, the daily mean drift from the monthly mean value interpolated to a 30-minute resolution and expressed as a percentage is used as an alternative to duplicate days being repeated. The filled data taken from the donor profile are then scaled by this drift factor.

The effect of the daily mean drift and smoothing is shown in Figure 13. This figure shows an instance where there were several consecutive data with afflicted data points that were replaced by synthetic data. Although each day has a similar profile, the scale and absolute load differ slightly throughout the synthetic profile.
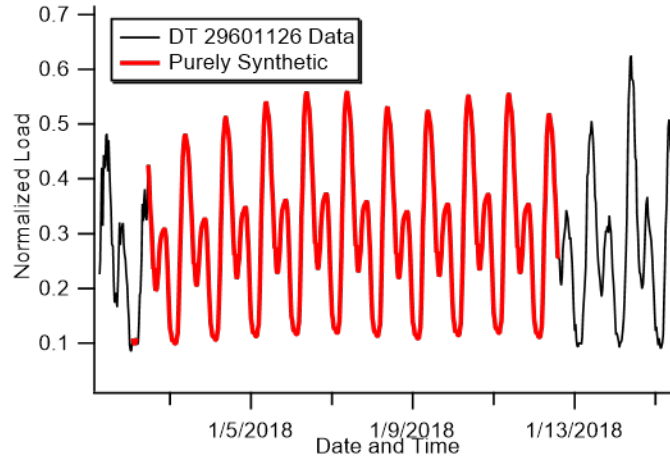
Figure 13. Purely synthetic data filled using the fill processes for DT 29601126 in Feeder 1

The result for each distribution transformer represents a single, serially complete time series that is normalized relative to the maximum loading condition for each transformer. All the various afflictions were removed and replaced with the donor data rescaled by the daily mean drift relative to the monthly mean. In cases where no donor profile data were available, the mean of the remaining distribution transformer profiles was used. Again, a smoothing method was used to avoid step discontinuities.

2.3.4.2 Initial Validation

To validate the data cleaning method, some of the available data were removed so that synthetic data could be compared against the real data. The residuals between the synthetic data and the real data were calculated to ascertain the accuracy of the synthetic data. The distribution of these residuals normally has a mean bias error of -0.036, or -3.6%, as shown in Figure 14. Figure 15 shows the distribution transformer loading profile for DT 29601126 after this data filling method has been applied, and the performance of this method is shown in the green traces (filled in synthetic data) compared with the black ones (real data).
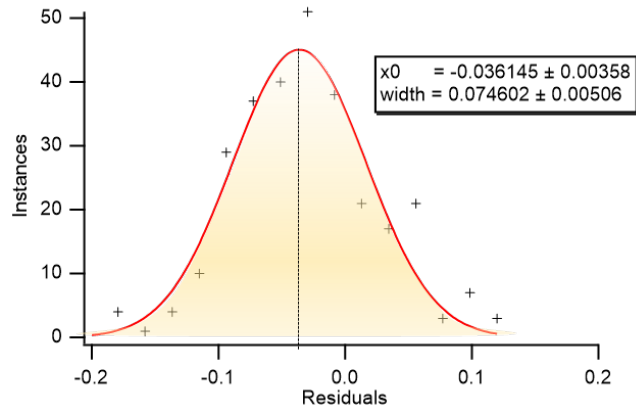
Figure 14. Distribution of residuals obtained by comparing the synthetic data to the real data
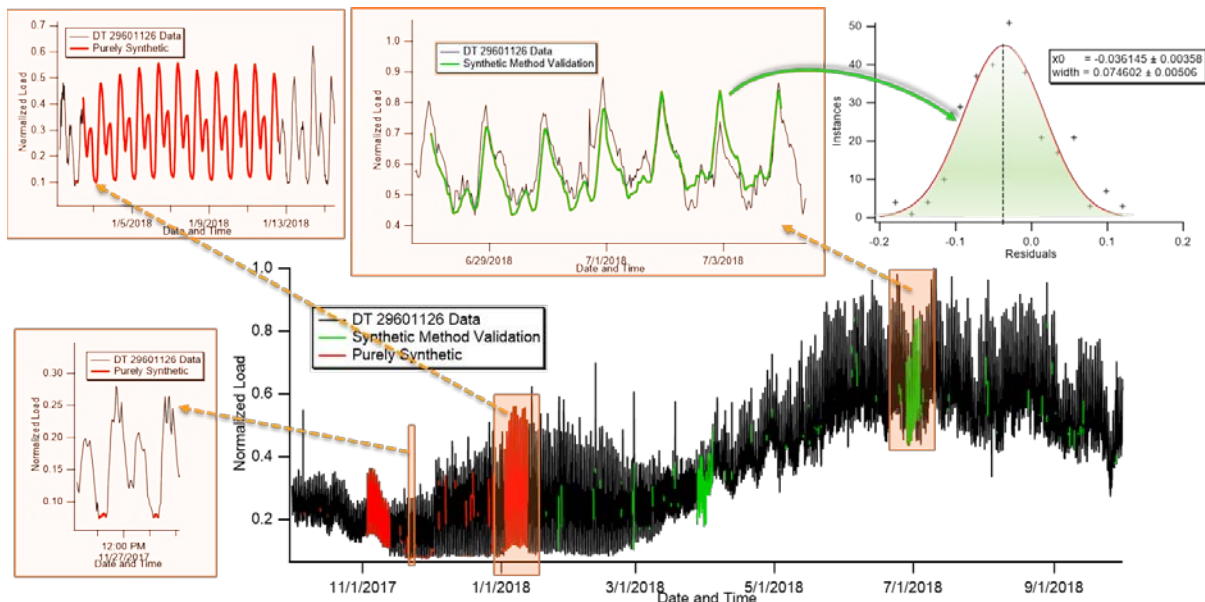
Figure 15. Loading profile for DT 29601126. The green trace represents data that are synthetic and for which real data are available; the red trace represents data that are purely synthetic, i.e., no real data are available.

2.4 Load Allocation

Once the feeder topology has been defined, the next step is to accurately define the secondary loads. This is required because the feeder load along with the circuit impedance will define the power flows. Determining these customer peak load values is both critical and challenging because advanced metering infrastructure and SCADA data are, at this time, usually only available for the substation or, at best, for the distribution transformers, but not for individual customers. To add to this challenge, secondary customers might be moved to different distribution transformers because of changes in demand or network upgrades during the study period. These changes might not necessarily get updated in the utility's GIS, and secondary customer locations might not have been mapped at all. This section describes a method to capture the phase customer load once the per-phase impedance of each circuit component is accurately modeled using the methodology described in the previous section.

Three data sources were available for the load profiles: (1) SCADA data for the feeder head (66/11-kV transformer), (2) the distribution transformers (11/0.433-kV transformers), and (3) monthly kWh values from the billing data for each of the 12 months considered in the study for all customers downstream of the distribution transformers. No information was available for the geographic coordinates of each customer or to which phase they were connected. The following section describes the process for identifying locations and peak load values for all secondary connected customers and validating the resulting customer loading profiles.

2.4.1 Load Allocation Using Individual Distribution Transformer Data

We use the peak-loading condition obtained from each distribution transformer's 30-minute resolution loading profiles to help allocate loads to the secondaries. This is done by using a known parameter—phase voltages—to iterate through a power flow model until loading estimates produce the target voltage. Few distribution transformers experience peak demand at the same time points; therefore, multiple time points corresponding to each distribution transformer's peak-loading condition were analyzed and iterated. The following sections describe the algorithm used and the initial assumptions.

Because of data issues, the voltage drops from the feeder head to the distribution transformer secondaries obtained from power flows on the feeder model did not match with the actual voltage measurements. This is because the same primary cable was supplying the load for all distribution transformers from the feeder head, so if the overall loading differed because of missing data, the voltage drops would also be different. Thus, it was essential to develop an approach to allocate loads to distribution transformer secondaries that could generate the same voltage drops as observed in the measurements while ensuring that the distribution transformer peak loading and phase imbalances are accurately captured.

2.4.1.1.1.1 Using Evolutionary Algorithm for Load Allocation

The voltage drops along a line are based on the real and reactive power flows. The values of these flows are dependent on the system impedance, which had already been captured using the GIS data and component specification sheets, and the values of the secondary loads and power factors on each phase. The approach adopted was to optimally allocate the secondary loads to each distribution transformer at its peak-loading time point using an evolutionary algorithm. An evolutionary algorithm is a generic population-based metaheuristic optimization algorithm.

In this approach, each distribution transformer was allocated optimal loads separately. The per-phase load and power factor values of DT_{opt} (DT being allocated optimal loads), were chosen using the evolutionary algorithm at its peak-loading condition, t_p. Throughout the optimization process, the per-phase load and power factor values of all other distribution transformers in the feeder were kept fixed at the same values as given in their loading profiles at t_p. If any of these inputs were not available, the following assumptions were used to fill in the missing values:

- If the measured loading kW value was zero for any one phase of a distribution transformer, the sum of the other two phases was equally divided in all three phases.

- If a load's kW value was zero or negative (bad data), or if the values were not available for all three phases, then the distribution transformer was assumed to be 50% loaded.

- If the loading values were not available for all three phases of DT_{opt}, then the evolutionary algorithm could choose loading values from ±25% of its rating, else bounds were kept as ±25% of its actual peak-loading value.

- If voltage measurements were not available for one phase, then a reasonable value based on the other two phases was applied.

- If none of the voltages were available, or if they were negative or much lower than nominal, then a value of 1 p.u. or slightly less than the feeder head value was assumed.

- Similarly, if power factor values were not available for one phase, a reasonable value based on the other two phases was applied; if none of the values were available, unity power factor was assumed.

Once these missing values were filled in, the following evolutionary algorithm steps were implemented to get the optimal loads:

- The feeder head voltage in the OpenDSS models are set to the same values as observed in the feeder head SCADA data for *tp*.

- The initial population was then generated for DT_{opt}; here, initial population means a set of values for the loads and power factors for each phase of DT_{opt}. These values were generated from within the specified bounds. The load kW values could be chosen from within ±25% of the measured kW values at *tp*. The power factor values could be chosen from (0.8,1), typical residential power factor values. The distribution transformer tap positions were not continuous and could be chosen from only seven allowed positions (0.9, 0.925, 0.95, 0.975, 1.0, 1.025, 1.05), as given in the distribution transformer specification sheets.

- The initial population consisted of multiple sets of values, and each set was used to evaluate the fitness function. The fitness or the objective function was the squared sum of differences between the target (VT) and actual (VA) voltages for each phase of DT_{opt}. The target voltage was read from the measurements at *tp*, as shown in Figure 16. The actual voltages were obtained by attaching lumped loads at the secondaries of DT_{opt}, with kW and power factor values taken from the initial population sets.

initial voltages   target voltages

METER NO	DATE TIME	P B_PH	P Y_PH	P R_PH	VBV	VYV	VRV
29XXX	10/1/2017	241.5	227.7	154.1	245.41	242.88	244.95

Figure 16. Initial and target voltages from distribution transformer measurements

The set that gives the least value of the objective function is used to generate the next generation of load kW and power factor values. The DT_{opt} secondary loads are replaced with these values, and the objective is evaluated again. This process is repeated until the difference between the last and current iteration is less than the specified tolerance. The process flowchart is shown in Figure 17. This process is applied to each distribution transformer to generate the optimal peak-load kilowatt, power factor, and tap position values.

Maximum Loading Condition Inputs

- Load kW and power factor (PF) values of all DTs at t_p.
- Target Voltages of DT_{opt} at t_p

Network Information

Network topology and component specifications generated using GIS and specification sheets

Evolutionary Algorithm (EA)

Creates New values for the DT Loads aiming to minimize the objective function using:

- Mutation
- Recombination
- Replacement
- Evaluation

Load kW, PF and tap positions determined using EA

Target Voltages (V_T)

Value of objective Function

Objective Function:

$$\min \sum_{i=1}^{3} (V_{Ti} - V_{Ai})^2$$

Power Flow Module

Determines the actual load voltages at the DT secondary by running power flow analysis on the OpenDSS feeder models after modifying the load kW and PF values to those generated by the EA module.

Actual Voltages (V_A)

Figure 17. Flowchart of load allocation using evolutionary algorithm

Figure 18 and Figure 19 show a comparison of voltages obtained using this modified approach. The optimal voltages exactly match the target voltages for most distribution transformers and are closer to the target voltages than the initial voltages for others. The reason these values do not exactly match is that other than the assumptions used for filling in missing data, the taps could be chosen from a fixed set of values, and their positions could not be set separately for each phase; however, the power factor values and tap positions are all realistic, and voltage drops are closer to the ones actually observed.
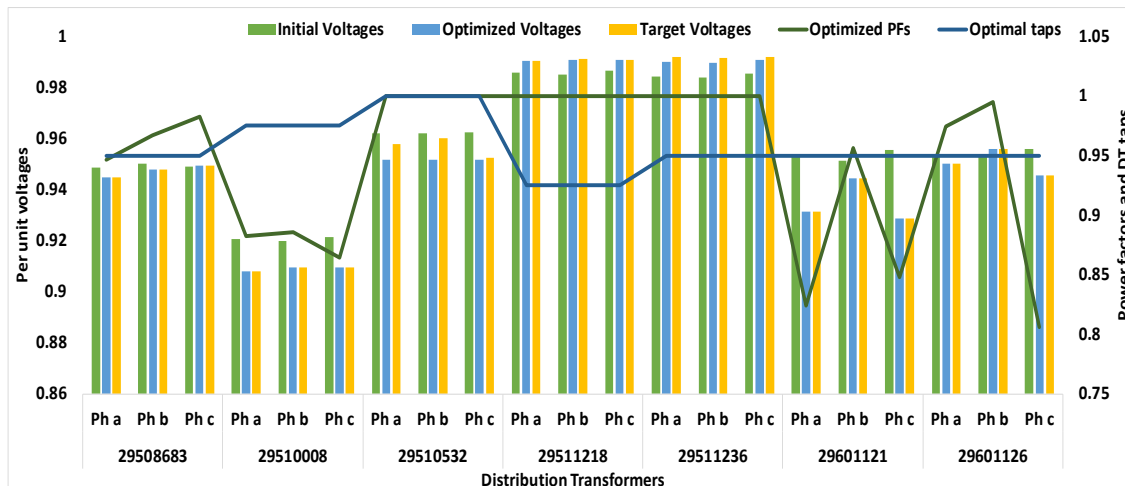
Figure 18. Comparison of voltages using modified evolutionary algorithm for Feeder 1
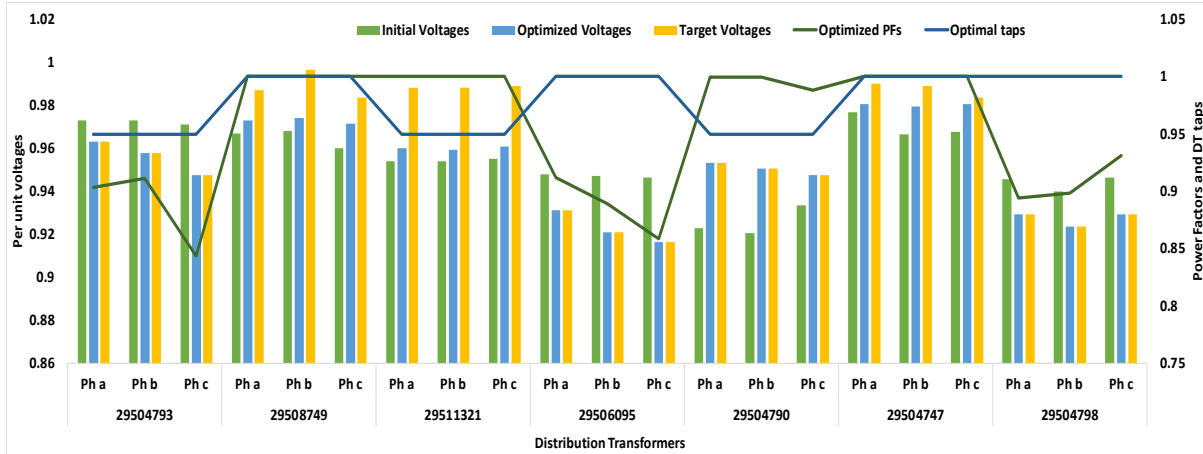
Figure 19. Comparison of voltages using evolutionary algorithm for Feeder 2

2.4.1.1.1.2 Secondary Customer Load Allocation Using the Optimal Lumped Loads

The load allocation optimization algorithm described previously determined the optimal loading values at the secondary of the distribution transformers. These loads give the same voltage drops as given in the measurements and validate the accuracy of the network models to the distribution transformer secondaries; however, these optimal loads represent the sum total of all the loads present downstream of the distribution transformers. Because most EV integration will happen at the individual customer locations, it is essential to distribute these lumped loads on each phase of the distribution transformer secondaries to downstream customers.

Figure 20 shows the feeder models with all the distribution transformers marked as red triangles. These models show that the secondaries represent a significant portion of the feeders; however, further validation of the secondary models was not possible because no information was available for the locations of the secondary customers or their voltage measurements. The only information available was the number of downstream customers for each distribution transformer and their respective monthly kWh values. These values were used to distribute the lumped optimal loads to downstream customers. The approach followed here ensured that the voltage drops and phase imbalances at the distribution transformer secondaries will remain similar to the ones observed from the measurements. This approach is shown in Figure 21.

Figure 20. Feeder models showing the primary and secondary networks separated by the distribution transformers (red triangles)
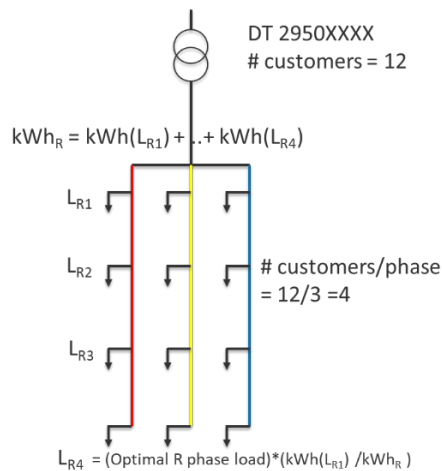
Figure 21. Distribution transformer secondary optimal lumped load among downstream customers

- Because no information was available about which phase the customer was connected to, it was assumed that the number of customers per phase were equal, and the total number of customers for each distribution transformer was divided equally in all the three phases.

- The annual kWh values were then determined for each customer (kWh_{cust}) by summing the monthly kWh values. This averaged any inconsistencies that might have existed in the monthly billing periods and the SCADA data used.

- The lumped load was then distributed to each customer based on their kWh proportion. To implement this, the total annual kWh per phase of the distribution transformers (kWh_{phase}) was determined by summing the annual kWh values of all customers on that phase. Then, for each customer, kWh_{cust} was divided by kWh_{phase} to get the customer's kWh proportion. This proportion was then multiplied by optimal lumped load to get the customer's peak kW value. This ensured that the total load per phase of the distribution transformer stayed exactly the same and the customer's peak loading corresponded with its annual energy consumption.

- The power factor values for each secondary customer load were kept the same as their correponding lumped load's power factor at t_p. Finally, because no nodes existed in the GIS files to connect these secondary customers, addditional nodes needed to be created. These nodes were kept roughly equidistant, and the distance was based on the plot sizes observed in the Google Earth overlay. The newly created secondary nodes are shown in Figure 22.
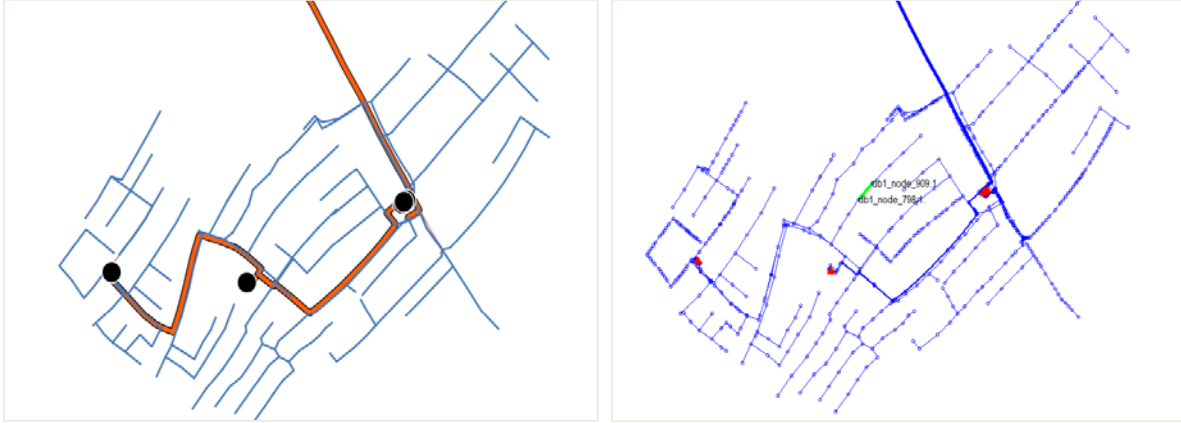
Figure 22. Feeder 1 GIS layout without secondary nodes (left) and its OpenDSS models with added secondary nodes (right)

3 Grid-Readiness

Evaluation of grid performance is essential for determining the readiness of the grid to adopt emerging technologies. Grid-readiness metrics measure the impact from emerging technologies on the reliability of the network under changing conditions, which is critical when evaluating new investments, large shifts in demand patterns and composition, or untested technologies. As a best practice, the evaluation and development of these metrics relies on time-series data collected from multiyear simulations of feeder models with multiple control schemes. A suite of technical indices is helpful in characterizing and understanding network operations coupled with possible feeder upgrades under different use cases and scenarios. The subsequent sections describe the metrics that are used to evaluate the grid impacts for different use cases and EV integration scenarios.

3.1 Technical Indices

3.1.1 M1: System Average Voltage Magnitude Violation Index

The system average voltage magnitude violation index (SAVMVI) provides a measure of the severity of nodal voltage violations on a bus. It gives an estimate of how far outside the nodal voltages are from their permissible bounds, as shown in Figure 23 (M1), which presents a hypothetical time series and corresponding violations. For this study, separate bounds were used for primary (high-voltage) and secondary (low-voltage) nodes based on the recommendations of the utility. First, all primary and secondary buses were identified. If buses are primary, the overvoltage threshold of $V_u = 1.1$ p.u. and an undervoltage threshold $V_l = 0.9$ p.u. is used. Similarly, if the bus is secondary then the bounds are assumed to be within $V_u = 1.06$ p.u. and $V_l = 0.94$ p.u. A bus could have multiple nodes based on the number of phases, so average bus voltage is considered here:

$$V_i^{avg} = \frac{1}{n} \sum_{k=0}^{n} V_i^k$$

where n is the number of buses in any node i.

For each bus i at each time point t, the violation outside the limits are defined by:

$$V_i^{viol}(t) = \begin{cases} V_{avg}(t) - V_u, & \text{if } V_{avg}(t) > V_u \\ 0, & \text{if } V_l < V_{avg}(t) < V_u \\ V_l - V_{avg}(t), & \text{if } V_{avg}(t) < V_l \end{cases}$$

The time-averaged violation for each bus is then determined by:

$$V_i^{viol\_avg} = \frac{1}{T} \sum_{t=0}^{T} V_i^{viol}(t)$$

where T is the total number of simulated time points.

SAVMVI for the feeder is obtained by dividing the sum of the time-averaged violations for all buses by the total number of buses in the feeder,

$$SAVMVI = \frac{1}{N} \sum_{i=1}^{N} V_i^{viol\_avg}$$

where N is the number of buses in the modeled network.

For instance, if a feeder has 100 nodes and each node has an average voltage of 1.06 p.u. for all time points (for example, 17,520 time points in total—for 30-minute resolution data set during a year), and the voltage threshold is 1.05 p.u., then:

$$SAVMVI = \frac{(1.06-1.05)*100*17520}{100*17520} = 0.01 \text{ p.u.}$$

3.1.2 M2: System Average Voltage Fluctuation Index

The system average voltage fluctuation index (SAVFI) provides a measure of the differences between average voltages at a current time point and the preceding one (i.e., voltage fluctuations), as shown in Figure 24 (M2). This gives the voltage deviation or fluctuation at all buses at each time point, which is then summed for all the buses across the feeder. The time average for each bus divided by the number of buses gives the SAVFI.

$$V_i^{avg} = \frac{1}{n}\sum_{k=0}^{n} V_i^k$$

where n is the number of buses in any node i.

Voltage fluctuation for any bus i:

$$V_i^{fluc}(t) = \left| V_i^{avg}(t) - V_i^{avg}(t-1) \right|$$

$$V_i^{fluc\_avg} = \frac{1}{T}\sum_{t=0}^{T} V_i^{fluc}(t)$$

$$SAVFI = \frac{1}{N}\sum_{i=1}^{N} V_i^{fluc\_avg}$$

where T is the total number of simulated time points, and N is the number of buses in the modeled network.

For example, if the feeder example mentioned in M1 has a constant voltage difference between the previous and current time points of 0.01 p.u., then:

$$SAVFI = \frac{(0.01)*100*17520}{100*17520} = 0.01 \text{ p.u.}$$

3.1.3 M3: System Average Voltage Unbalance Index

The system average voltage unbalance index (SAVUI) provides a measure of the voltage unbalance (maximum difference between a bus's individual phase and average voltage, M3, as shown in Figure 25) among all nodes. Voltage unbalance is defined as:

$$Voltage_{unbalance} = \frac{Maximum\ deviation\ from\ average\ voltage}{Average\ voltage} * 100\%$$

To evaluate the SAVUI for all buses, the maximum deviation of any phase voltage of the bus from the average bus voltage is evaluated at each time point to get the unbalance and is summed for all time points. SAVUI is obtained by dividing the sum of the time-averaged unbalance sums for all buses by the total number of buses:

$$V_i^{avg} = \frac{1}{n}\sum_{k=0}^{n} V_i^k$$

$$V_i^{unb\_max}(t) = \left|\max(V_i^k(t)) - V_i^{avg}(t)\right|$$
$$V_i^{unb\_min}(t) = \left|\min(V_i^k(t)) - V_i^{avg}(t)\right|$$

$$V_i^{unb}(t) = \frac{\max(V_i^{unb\_max}(t),\ V_i^{unb\_min}(t)) * 100}{V_i^{avg}}$$

$$V_i^{unb\_avg} = \frac{1}{T}\sum_{t=0}^{T} V_i^{unb}(t)$$

$$SAVUI = \frac{1}{N}\sum_{i=1}^{N} V_i^{unb\_avg}$$

where n is the number of buses in any node i, T is the total number of simulated time points, and N is the number of buses in the modeled network.

For instance, if a feeder has 100 nodes and each node has an unbalance of 0.01 p.u. for all time points (17,520, as previously explained), then:

$$SAVUI = \frac{(0.01)*100*17520*100}{100*17520} = 1\%$$
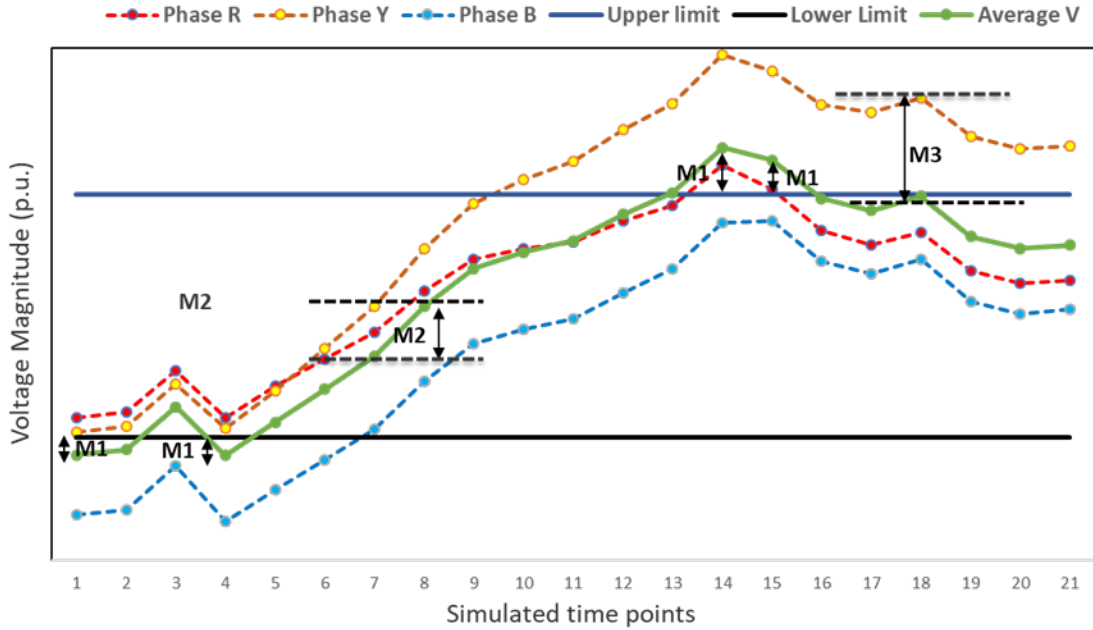
Figure 23. Technical indices used to quantify grid-readiness for hypothetical voltage profiles

3.1.4   M4: System Control Device Operation Index

The system control device operation index (SCDOI) provides a measure of the average control device operations in a day, such as voltage regulators and capacitor banks. For the feeder use cases presented in this report, operations of capacitor banks were evaluated with this index (SCDOI$_{cap}$). SCDOI$_{cap}$ is calculated by summing all capacitor bank operations (TO$_{cap}$) throughout the simulation time frame and then dividing this net operation count by the number of days (T$_{day}$) and the number of capacitor banks (*NC*):

$$SCDOI_{cap} = \frac{1}{NC} * \frac{1}{T_{day}} \sum_{i=1}^{NC} TO_{cap,j}$$

For example, if a feeder has two capacitor banks and each capacitor bank operates 10 times in a day, then:

$$SCDOI_{cap} = \frac{2 * 10 * 365}{2 * 365} = 10$$

3.1.5   M5: System Reactive Power Demand Index

The system reactive power demand index (SRPDI) provides a measure of the power factor at the substation and consequently the additional loading on the substation transformer because of reactive power demand/injections of the feeder. To calculate this metric, the absolute reactive power flow at the substation is summed at each time point and divided by the total number of time points simulated:

$$SRPDI = \frac{1}{T} \sum_{t=0}^{T} Q_{sub}(t)$$

where T is the total number of simulated time points.

For example, if the absolute reactive power flowing through the substation is 100 kVar at all time points (17,520, as previously explained), then:

$$SRPDI = \frac{100*17520}{17520} = 100 \text{ kVar}$$

3.1.6 M6: System Energy Loss Index

The system energy loss index (SELI) gives a measure of the total energy loss in the feeder as a proportion of the total energy demand of the loads. For this metric, the total feeder loss (kW and kVar) and total load kW and kVar are stored at each time point. These are then summed and multiplied by a multiplier (*mult*) to get the total energy loss and total energy demand of all loads.

$$mult = \frac{\Delta t}{60}$$

where Δt is the simulation time step in minutes.

Total energy loss equals:

$$E_{loss} = \frac{1}{T} \sum_{t=0}^{T} kW_{loss}^{sub}(t) * mult$$

where T is the total number of simulated time points.

Total load energy demand equals:

$$E_{load} = \frac{1}{T} \sum_{t=0}^{T} \sum_{i=1}^{L} kW_i(t) * mult$$

where L is the number of loads in the feeder.

This index is then defined as:

$$SELI = \frac{E_{loss}}{E_{load}}$$

For example, if a feeder has a constant real power loss of 50 kW at each time point, and the sum of loads is constant at 1 MW at each time point, then during a year or 17,520 time points (30-minutes resolution data set):

$$SELI = \frac{(50)*17520}{1000*17520} = 0.05 \text{ or } 5\%$$

3.2 Simulation Architecture

Time-series simulations are conducted leveraging NREL's high-performance computing (HPC) systems, which enable the analysis of a wide variety of scenarios and longer time horizons because of the ability to drastically reduce computational time.

Figure 24 shows the different scenarios of multiyear, quasi-static time-series simulations required to assess grid-readiness and test the efficacy of BESS to mitigate possible overloading conditions. All these scenarios require different time resolutions, control modes, varying EV penetration levels, or network upgrades. Considering all these requirements the simulation platform should have the following features:

- Be scalable to allow for the addition of new control modes, feeder models, EV penetration levels, time resolution, and length of simulations.

- Provide the end user with an easy to use interface.

- Be able to start multiple simulations together leveraging all available computational resources and minimize the total simulation time.

- Be able to store all the raw data and processed results and make it readily available in the future.

The simulation platform characterized in Figure 25 makes use of open-source tools such as OpenDSS and OpenDSSDirect.py, which provides a Python-based library interface to OpenDSS. It leverages the HPC resources available at NREL and is capable of starting thousands of quasi-static time-series simulations together. To further increase resource utilization, another open-source Python package, Dask, was used to run many simulations in parallel on the different cores of the same node. All the results are saved in separate directories to avoid overlaps. The platform also includes a Linux-based command line interface that allows the user to start all the simulations for a feeder with a single command line. Owing to its modular nature, new feeders can be added simply, and new control modes can also be easily integrated and simulated using the existing command line interface. By leveraging these capabilities, simulation times can be reduced from weeks or even months to several hours.
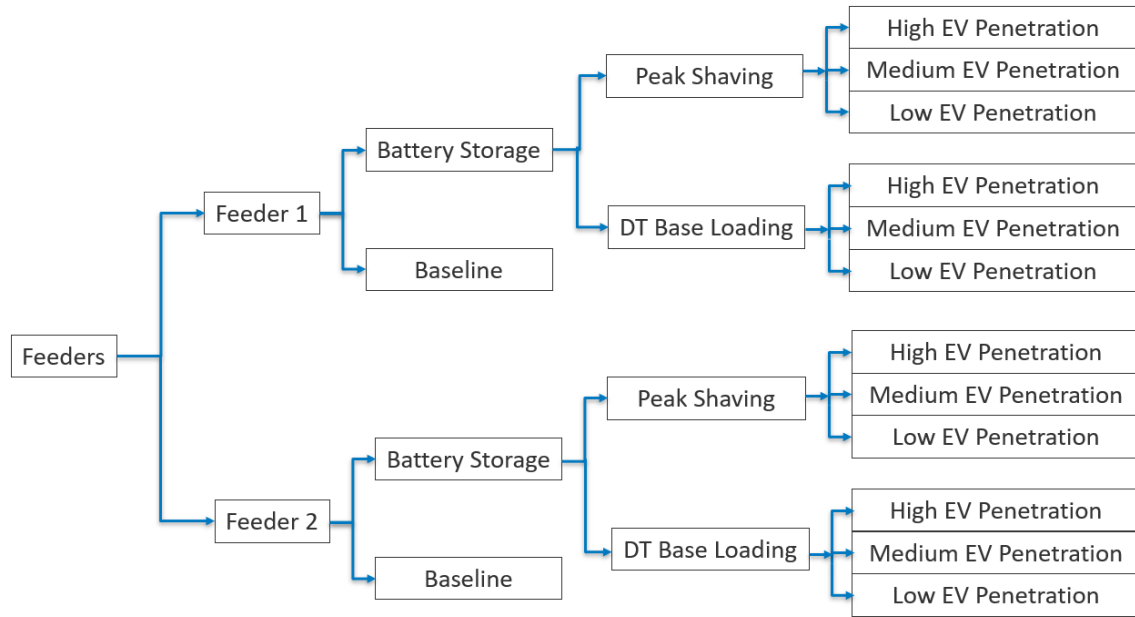
Figure 24. Multiyear time-series simulation scenarios
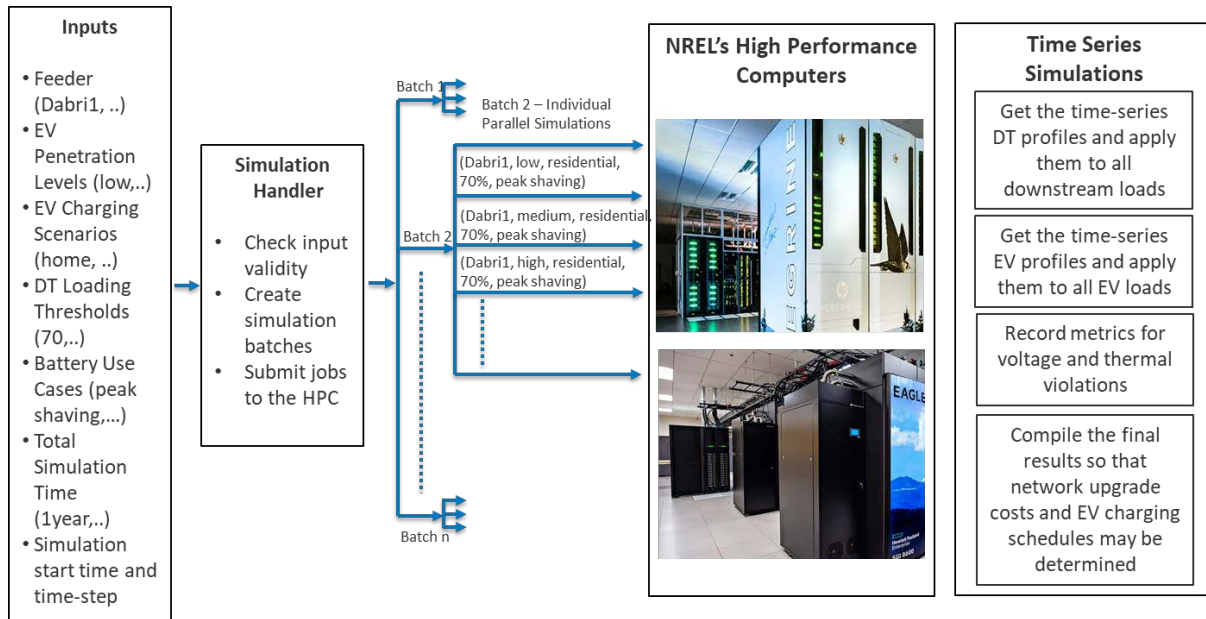
Figure 25. Simulation architecture leveraging NREL's HPC system. *Photos by NREL*

4 Electric Vehicle Integration

This chapter describes the development and implementation of EV integration scenarios within the simulation framework. Impacts of EV loads are evaluated on the same two feeders discussed in detail in Chapter 2. Modeling this framework is conducted by following an object-oriented approach, i.e., an individual EV, charging station, and single charger are treated as separate objects with corresponding static properties. Three key variables were identified to initialize the framework, as shown in Figure 26:

- Number of EVs: This parameter determines how many EVs need to be modeled for the area. Based on levels of penetration, this number would vary. The fleet can have different EVs and e-rickshaws, which will have different charging behaviors/preferences, battery capacities, and driving ranges. Initial results presented in the subsequent sections assume a homogeneous fleet, i.e., the battery capacities are the same, but the preferences vary randomly within a predefined set.

- Charging scenarios: Three dominant modes are studied in the framework: (1) residential dominant, (2) public station dominant, and (3) commercial/workplace dominant. These modes help the framework determine how many chargers are needed to charge the vehicle fleet at its entirety. For Case 1, the required number of chargers is almost equal to the number of total EVs, whereas for Case 2 and Case 3, a smaller number of chargers can be considered because there is an underlying time-sharing concept among the users.

- Length of simulation: This refers to the time duration for which the scenario will be simulated. If the simulation spans a multiyear time frame, growth factors may be included in the base level of penetration.
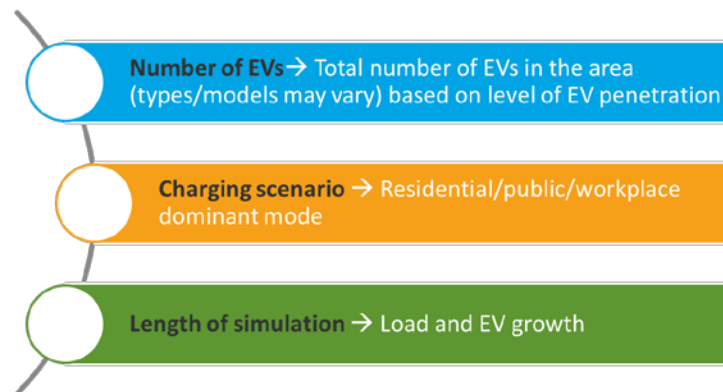
Figure 26. Key parameters of EV scenario simulation framework

4.1 Charging Scenarios

Charging scenarios are formulated based on the types of chargers as initially specified by BRPL (Figure 27). Bharat AC chargers are assumed to be the most prevalent models because they provide the most inexpensive charging options. In a residential-dominant charging scenario, a single AC charger is assumed to fully charge a single vehicle overnight. These chargers will be used by consumers in public- or workplace-dominant modes mostly to top off because the charging rates are slow. Level 1 DC chargers are assumed to be available in public or workplace/commercial stations.
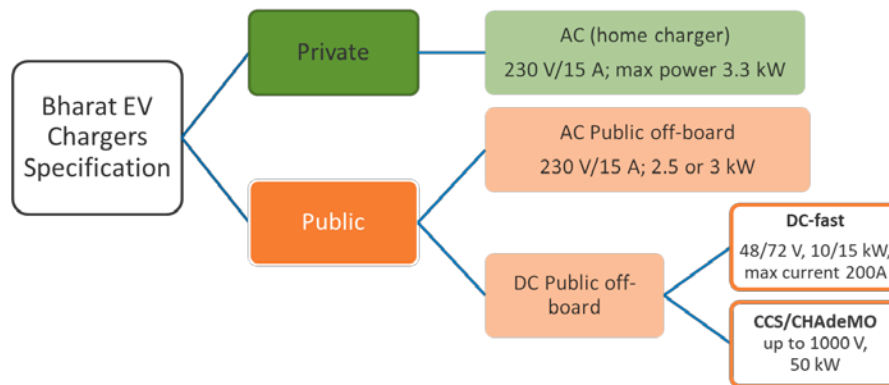
Figure 27. Bharat EV charger types and specifications

These chargers are distributed according to three levels of penetration:

- Low: residential, overnight charging, 3.3-kW chargers, new EV users added every year, double the vehicles in the 10th year from first year

- Medium: residential + workplace, mostly overnight + afternoon peaks, 3.3-kW + 10-kW DC chargers, new EV users added every year, four times the vehicles in the 10th year from first

- High: residential + workplace + public, overnight + afternoon peaks + intermittent topping up, 3.3-kW + 10-kW DC + 50-kW CCS/Chademo chargers, new EV users added every year, eight times the vehicles in 10th year from first.

4.2 Demand Profiles

Demand profiles of EV chargers or charger clusters represent how much load an EV penetration scenario translates into for the grid. For residential charging:

- Everyday charging takes place for each user with varying starting time and state-of-charge (SOC) levels

- Individual 3.3-kW chargers—nonlinear relationship between SOC and consumption level

- Overnight charging: starts anytime between 5 p.m. and 12 p.m.

- Starting SOC is assumed to vary every day for a single user.

In contrast to residential charging, a cluster of chargers or a charging station requires a detailed model of gas-station-like characteristics, where EV arrival/waiting can be modeled along with individual charging events. Figure 28 shows how the workflow is designed to calculate the net consumption of a charging station.
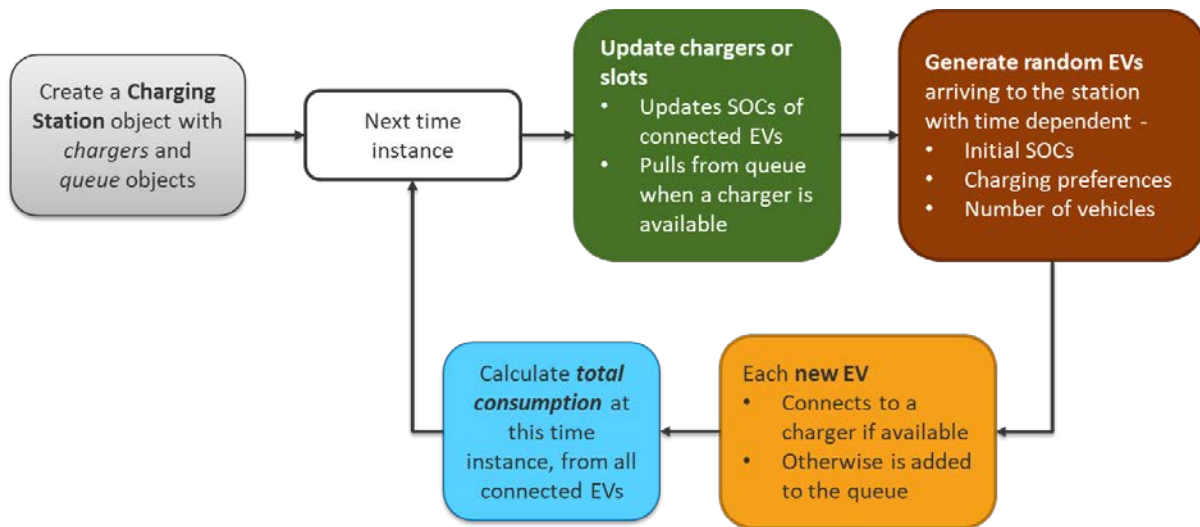
Figure 28. Workflow of a charging station model

The following assumptions were considered while modeling the charging stations:

- Chargers draw constant power when EVs are charging (independent of initial SOC).

- Linear SOC build, e.g., if it takes an EV 5 hours to reach 100% of its battery capacity, in 1 hour the SOC will see a 20% increase from the starting point.

- Time resolution: simulation time resolution can be more granular (for example, 5 minutes for the initial set of results), but new EV flock generation might take place in a longer time horizon (every 20 minutes).

- Number of chargers: fixed for a given type of station; the maximum waiting queue is equal to the number of chargers.

- No maximum waiting time for individual EVs

- Each EV can specify its charging preference: desired SOC or duration of charge event.

Examples of how such a public charging station behaves throughout a day are shown in Figure 29. This station has 30 slow chargers with a possible net peak load of 99 kW. The dark blue trace shows how many EVs arrive at the station at different times (~250 in total; the numbers are high in the early morning and evening time frame, moderate around noon, and low at other times), and their initial SOCs are plotted by the red trace. Both variables are drawn from random distributions. Such distributions are created as a plug-and-play part of the larger model and are randomly created for each network simulation. The net consumption profile for this charging station is plotted with the light blue trace, showing constant high load in the evening and through the night. This refers to the fact that EVs require a longer time to charge in the evening because their initial SOCs are low, and consequently all the chargers in the station are occupied for this duration. The long EV queue at night is represented by the black trace at the bottom of Figure 29, which suggests that the queue keeps growing after 8 p.m. but tapers when midnight approaches.

BRPL data (Figure 30) suggest that a commercial station where overnight parking and charging are prevalent will have a different demand profile than a publicly accessible one. These profiles represent 36 days and measurements from a single meter. Examples of a few of these charging station placements are given in Figure 31 for Feeder 2.
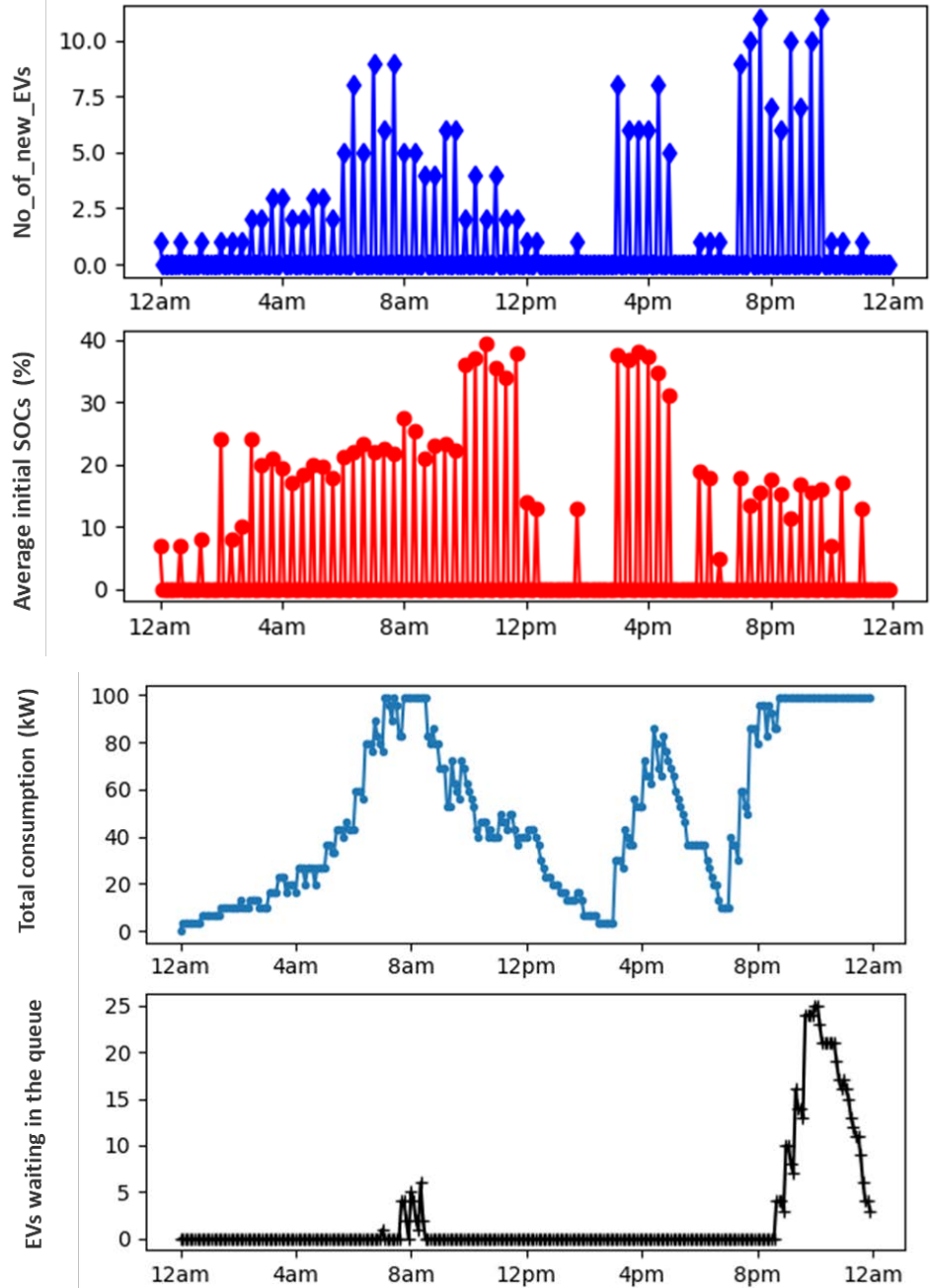
Figure 29. Preliminary results from a sample public charging station model
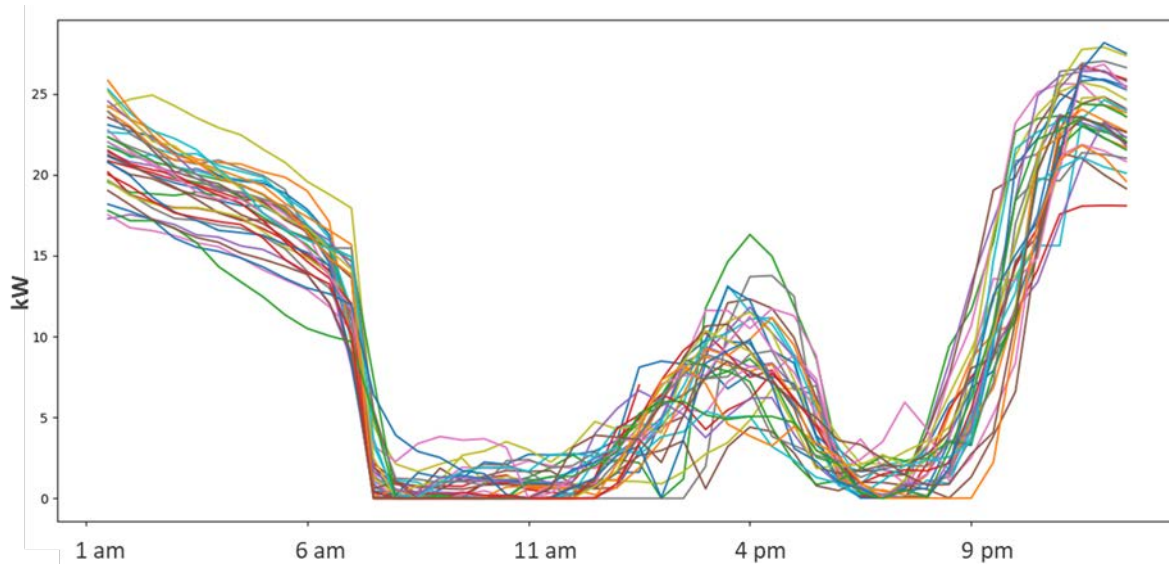
Figure 30. Preliminary data from BRPL from a charging cluster during 36 days
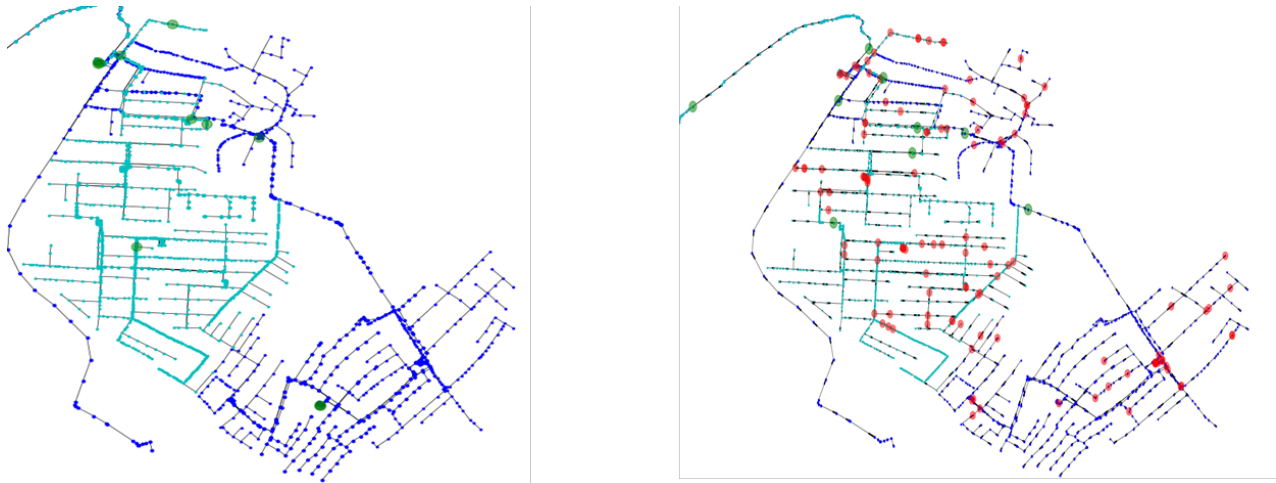
Figure 31. Sample locations of charging stations: secondary connected stations (left) and primary connected stations (right)

4.3 Electric Vehicle Load Aggregates

This section presents results from integrating the EV scenario generation framework with the feeder simulation platform. There are 300 chargers clustered among 10 charging stations (public + workplace/commercial, secondary connected). The number of chargers in a station could vary to reflect diversity in locations. In this scenario, approximately 2,000 EVs are considered that create discrete charging events within a single day. A hot summer day profile was selected for this initial simulation. Figure 32 through Figure 35 show typical net demand profiles for some charging stations that are generated for this scenario. Each station is broken into sets of DC (10-kW) and AC (3.3-kW) chargers and presented separately in these figures.
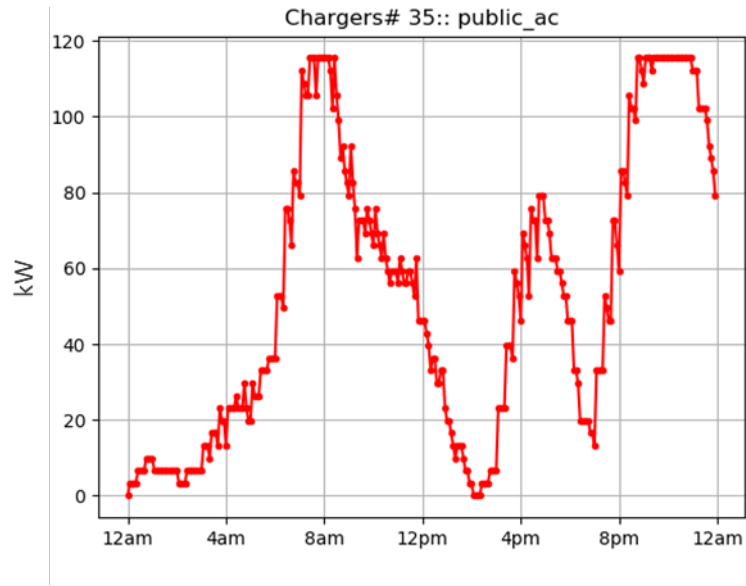
Figure 32. Net demand profile for a public charging station (35 AC chargers)
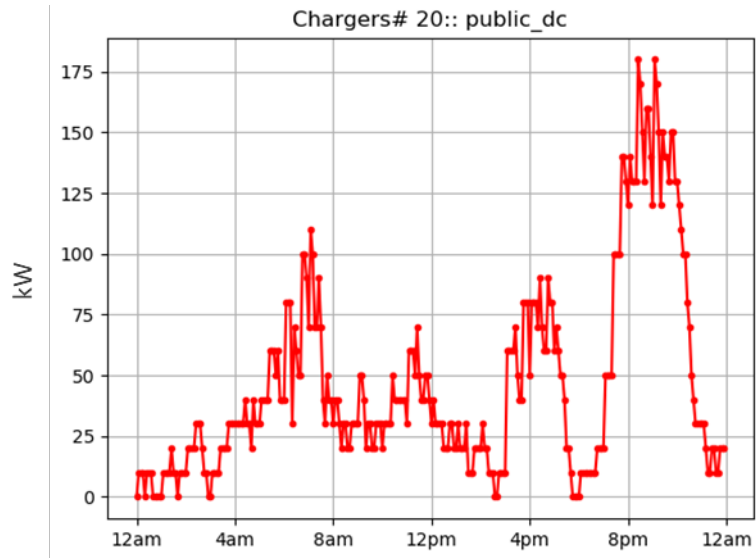
Figure 33. Net demand profile for a public charging station (20 DC 10-kW chargers)
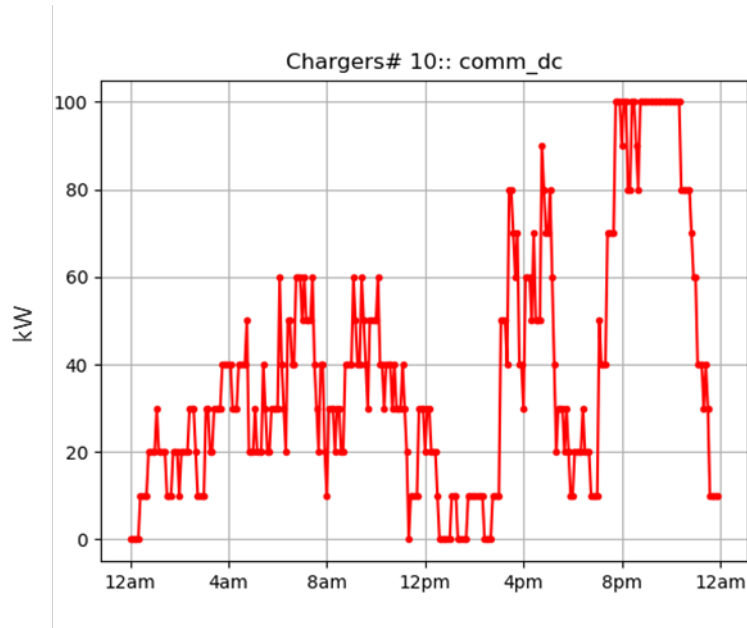
Figure 34. Net demand profile for a commercial charging station (10 DC 10-kW chargers)
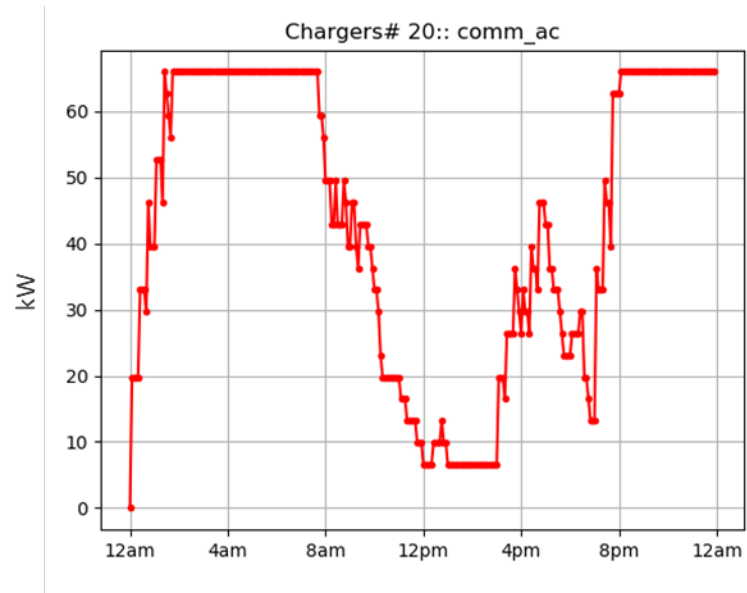
Figure 35. Net demand profile for a commercial charging station (25 AC chargers)

Total EV loads for all these stations and baseloads for the given day are shown in Figure 36. As this figure suggests, for this scenario, the EV load adds more than 1 MW to the existing baseload of 1.5 MW. Voltage impacts are shown in Figure 37 and Figure 38, which plot minimum voltages (among all the nodes) for every 30 minutes. Figure 37 shows that there is a clear voltage drop in the evening because of the high EV load compared to the no EV scenario in Figure 38. Such a drop depends on the daily profile and variations in EV charging profiles.
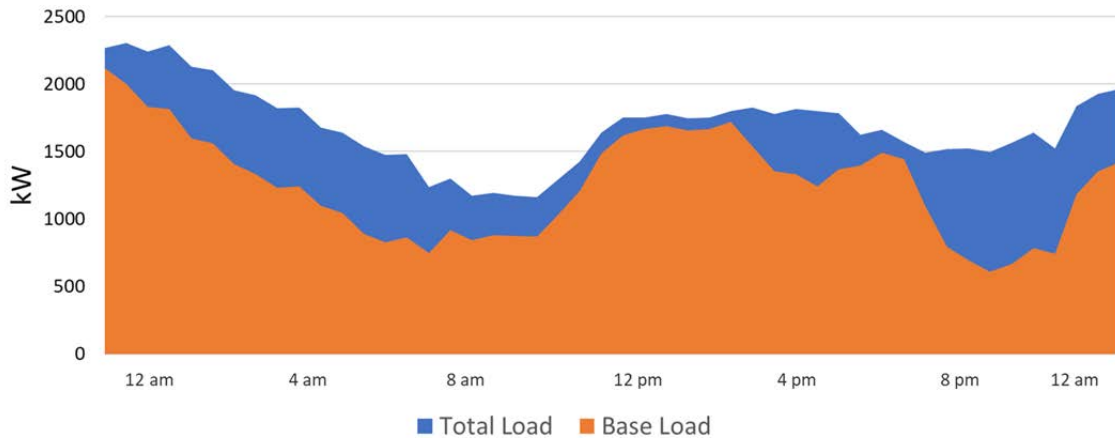
Figure 36. Baseload and total load (after EV integration) profiles for a summer day
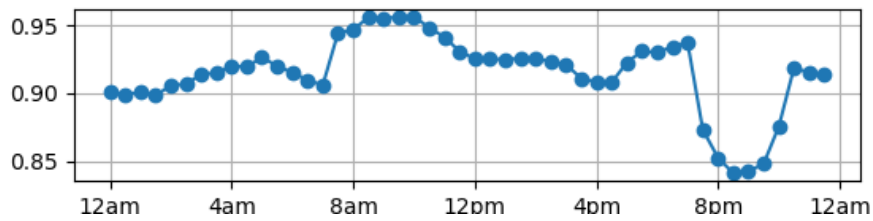
Figure 37. Minimum voltage profile with EVs charging in charging stations
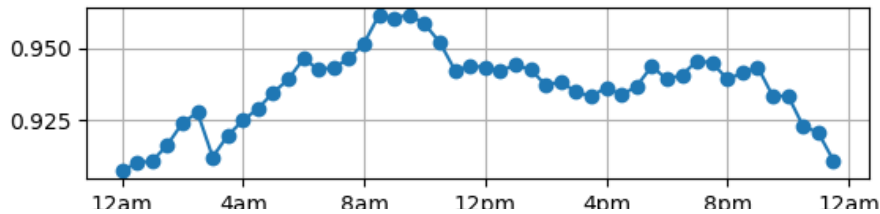
Figure 38. Minimum voltage profile without any EV charging scenario

On a system level, aggregated EV loads vary on temporal loading levels based on scenarios. For example, for the high EV scenario, the loads will get distributed when there are available stations (Figure 39), but they will increase in magnitude if those vehicles are charging mostly overnight for a residential-dominant scenario (Figure 40).
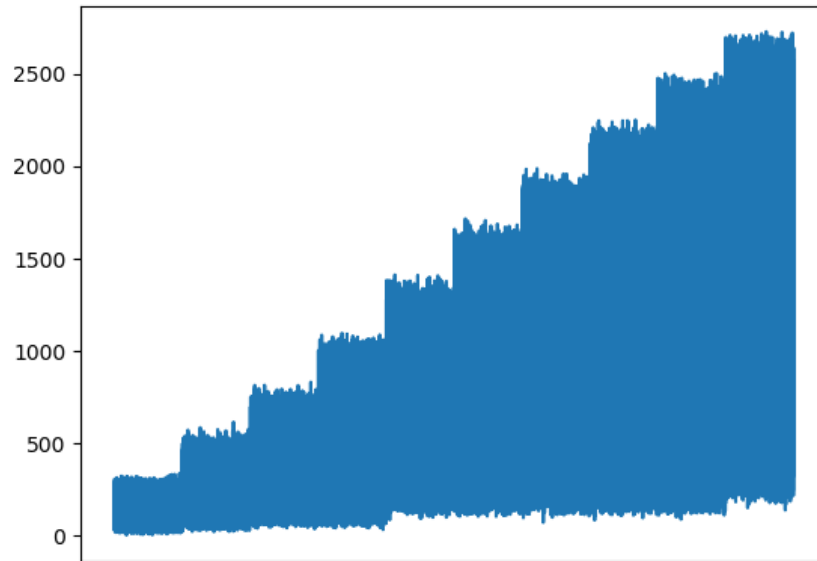
Figure 39. Ten-year aggregate EV demand (in kilowatts): fast-charging stations and distributed charging throughout a day
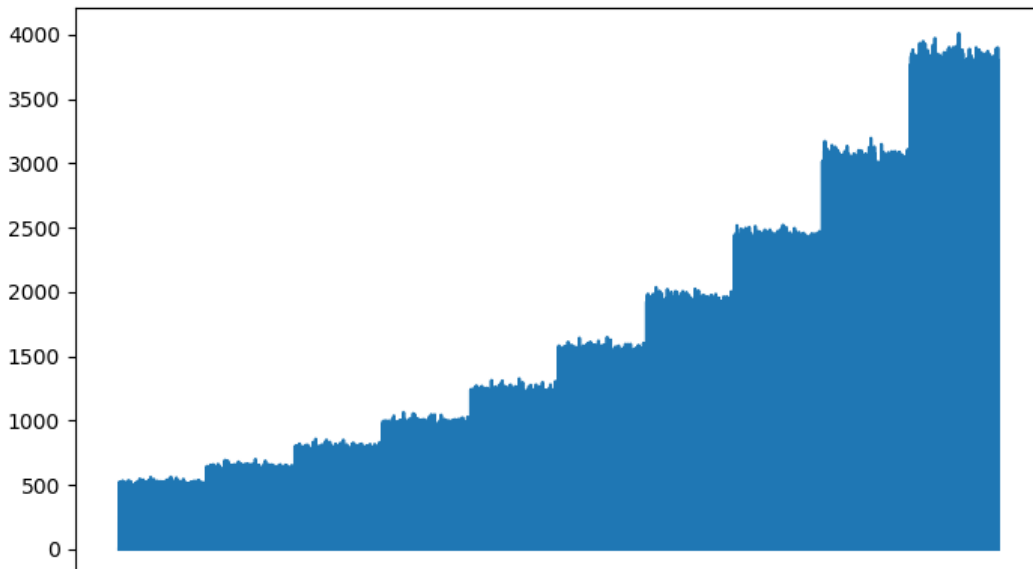
Figure 40. Ten-year aggregate EV demand (in kilowatts): residential charging and mostly overnight events

5 Energy Storage Integration

This chapter describes the method for sizing lithium-ion (Li-ion) batteries that would be deployed at each distribution transformer in Feeder 1 and Feeder 2. The chapter is broken into four sections. The first section describes how the batteries will be sized to mitigate distribution transformer overloading. The second section introduces a sizing chart that can be used to identify the battery size for any arbitrary distribution transformer loading profile. The third section discusses the impact of load growth. Finally, in the fourth section, the resulting battery sizes for Feeder 1 and Feeder 2 are tabulated and discussed.

5.1 Battery Sizing Algorithm

5.1.1 Distribution Transformer Overloading

In this study, the Li-ion batteries are sized to mitigate overloading conditions defined by cases were the distribution transformer load is more than 70% of the rated capacity, as shown in Figure 41.
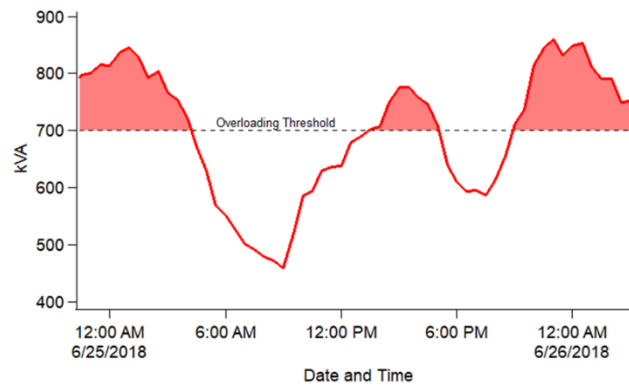
Figure 41. Various overloading conditions observed for a distribution transformer rated at 990 kVA. (The overloading threshold is 70% of the rated capacity.)

An overloading instance covers a span of time defined from when the distribution transformer loading first crossed above the overloading threshold to when the loading again falls below the overloading threshold. During an overloading instance, the loading peaks at some point above the overloading threshold. This is the power associated with the overloading condition. The total energy associated with the overloading condition can also be measured (shown in the red highlighted areas in Figure 41). These two quantities, the power and energy, associated with the overloading condition can be coupled as a point pair, i.e., $X_i=(power_i, energy_i)$.

5.1.2 Battery Sizing Map

This subsection describes the form of the battery sizing map that can be used to obtain the battery size appropriate for any distribution transformer subject to any loading profile. The complete battery sizing map for an example distribution transformer is illustrated in Figure 42. The blue dots in Figure 42 correspond to every overloading instance observed during a year exceeding 70% of nominal rating, i.e. when the kVA loading of the distribution transformer surpasses a threshold defined as 70% of the rated capacity of that distribution transformer. The bivariate distribution of the overloading point pairs is superimposed over the scatterplot. It is assumed that commercially available batteries are generally available with a 4:1 ratio between energy and power—e.g., a 2-kW, 8-kWh battery could be readily procured, whereas a 2-kW, 20-kWh is not expected to be commercially available. Thus, all the battery sizes analyzed in this study will be on the 4:1 energy-to-power ratio line. Three points are of interest in the battery sizing map: (1) the peak power overloading instance point pair shown in red, (2) the projected peak power point pair to the 4:1 ratio line shown in purple (i.e. mapping at constant energy from the peak

power point to the 4:1 ratio line), and (3) the 70th percentile point pair. The 70th percentile point represents the point on the 4:1 ratio line that would decrease 70% of the overloading instances given a full SOC at the time of overloading.

Each of the three sizing points of interest offer relative advantages and disadvantages. If a battery were to be sized to meet the most extreme overloading cases (point (1) or point (2)), then the battery would sit idle while charged to where a portion of the energy stored in the battery would be unused for all periods, except for during the most extreme case. Thus, the 70th percentile point pair (point (3)) allows for a battery to fully mitigate most overloading cases and a portion of the extreme overloading cases while avoiding the problem of unused idle stored energy. The 70th percentile point is selected precisely at a point on the 4:1 ratio line that enables the battery to fully mitigate all overloading instances during which loading on the distribution transformer is at or below the level of the overloading instance which is larger than 70% of all the observed overloading cases. This means that some overloading instances, particularly higher peak loading cases, will not be fully mitigated by a battery sized corresponding to the 70th percentile point pair. Still, even in these extreme cases, the battery will discharge to mitigate a significant portion of such an extreme overloading case but cannot fully mitigate the case.
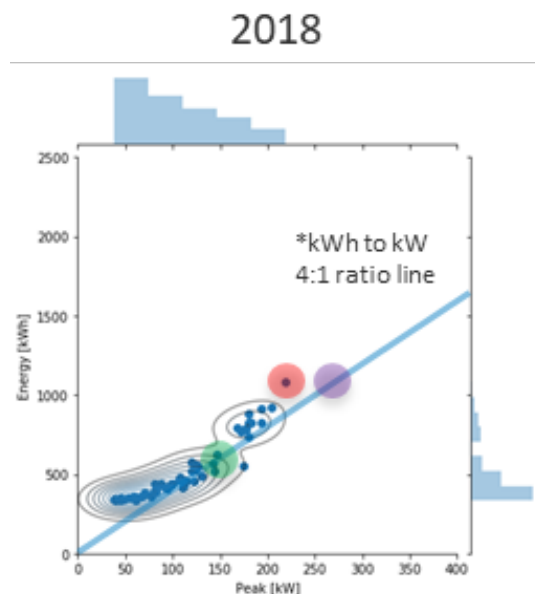
Figure 42. Battery sizing map for a distribution transformer

5.1.3 Load Growth

In this work, the batteries are sized to mitigate overloading conditions that are present after allowing for 10 years of load growth, assuming a 2% compounding annual growth rate per BRPL's expected load growth. Toward this end, the load profiles were scaled by a factor of 1.02^n, where n represents the number of years since 2018. Thus, n spans from [0,10]. The raw, uncleaned, distribution transformer loading profiles were used to scale the load, which is shown for distribution transformers of Feeder 1 and Feeder 2 in Figure 43 and Figure 44.
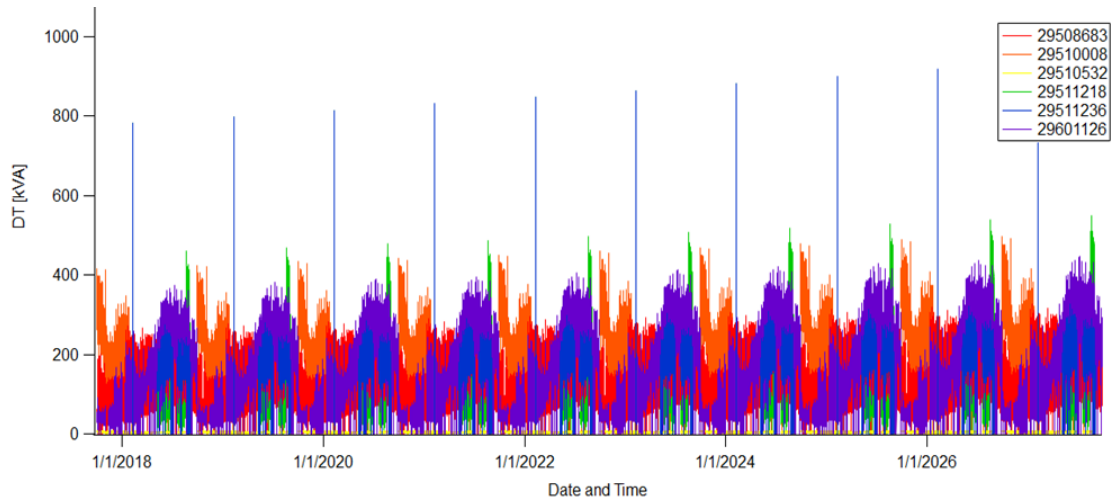
Figure 43. Distribution transformer load profiles with load growth at 2% during a 10-year horizon for Feeder 1 (without any data cleaning)
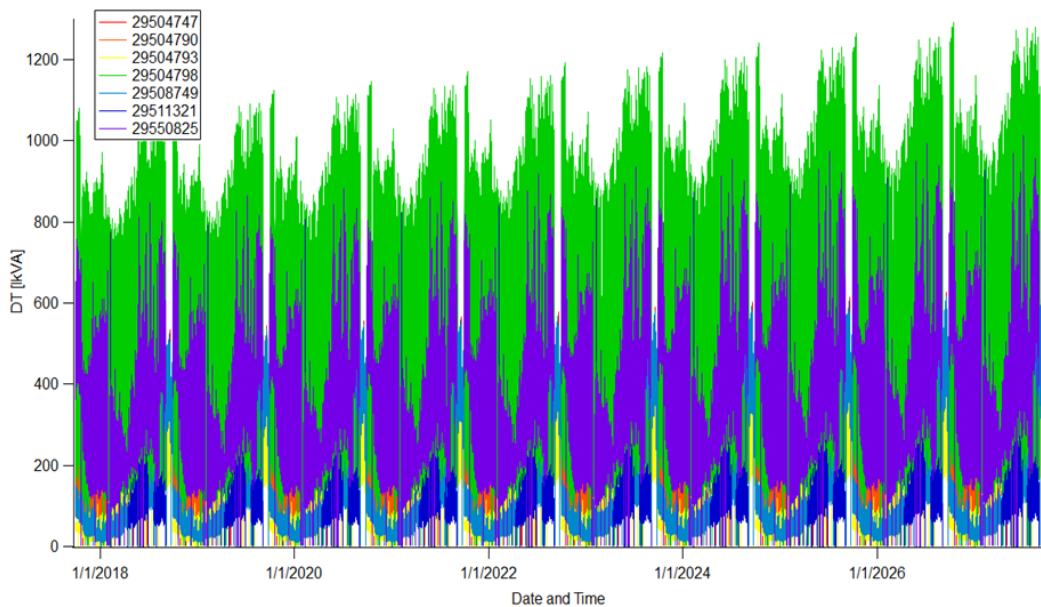
Figure 44. Distribution transformer load profiles with load growth at 2% during a 10-year horizon for Feeder 2 (without any data cleaning)

A battery sizing map can be produced for each distribution transformer for each year. An example is shown in Figure 45.
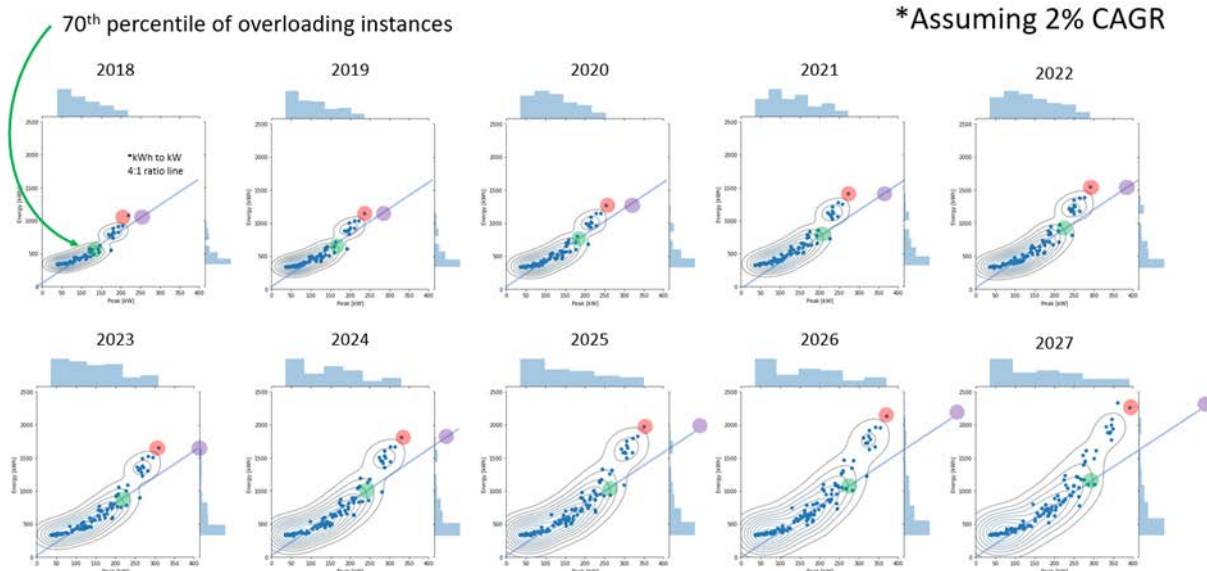
Figure 45. Sizing maps for each year for the same distribution transformer assuming a 2% compounding annual growth rate of the distribution transformer loading

5.1.4 Sizing Results

The battery sizes associated with the 70th percentile overload instance point pair are obtained using the method described for each distribution transformer in both Feeder 1 and Feeder 2 after allowing for 10 years of load growth at 2%, as tabulated in Table 2 and Table 3.

Table 2. Battery Sizes for Each Distribution Transformer in Feeder 1		
DT	**kW**	**kWh**
29508683	0	0
29510008	177	707
29510532	49	198
29511218	157	630
29511236	139	558
29601121	122	488
29601126	0	0

Table 3. Battery Sizes for Each Distribution Transformer in Feeder 2

DT	kW	kWh
29504747	0	0
29504790	104	415
29504793	196	782
29504798	890	3560
29508749	0	0
29511321	125	500
29506095	235	939

5.2 Battery Energy Storage System Control Algorithms

There are different potential modes of operation for the grid-connected BESS, including peak-shaving, capacity-firming, and voltage support modes. This report focuses on the peak-shaving and base-loading BESS control applications to help alleviate the possible distribution transformer overloading condition with load growth and the rapid adoption of EVs in the modeled distribution feeders.

5.2.1 Peak-Shaving Control Application

Power system planning ensures that there is enough capacity to service peak-loading conditions to maintain grid reliability. The peak-shaving mode of BESS requires the service operator to provide trigger values for peak shaving and base loading. The BESS will discharge power into the grid if the total power demand at the measured point—in this case, the distribution transformer—is greater than the peak-shaving upper reference limit, as shown in Figure 46. Conversely, the BESS will charge if the total power consumption at the measured point is less than the base-loading limit. It is important to ensure that the charging of the BESS occurs during the base-loading periods (i.e., the valleys) to avoid overloading the distribution transformers during peak periods.

This BESS control application can be used to defer large investments required for system upgrades and to mitigate the use of peaking generators for "flattening" the load profile. This research will provide insight into the impact of such BESS applications on upgrade deferrals; line, distribution transformer, and system-wide losses; and other grid-readiness metrics, such as system energy loss index and other voltage indices.
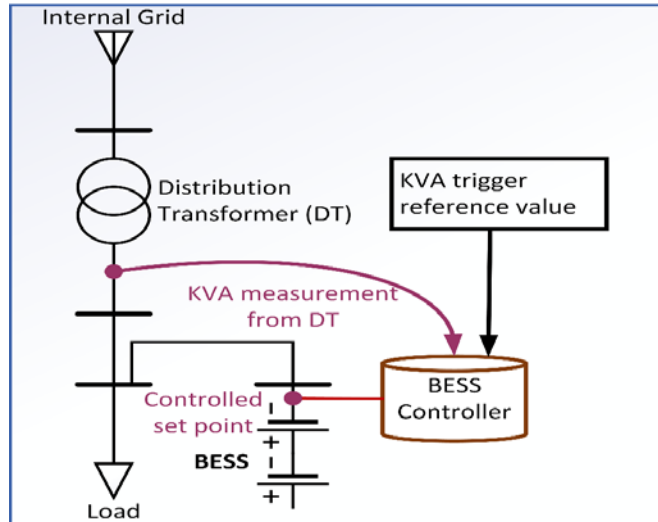
Figure 46. Peak-shaving control configuration

The BESS units were integrated based on industry standard and customized settings provided by BRPL. As shown in Figure 47, two thresholds for BESS charging and discharging have been chosen to investigate the sensitivity of the control algorithm to these set points. These thresholds can impact the BESS life because they determine the number charge and discharge operations.
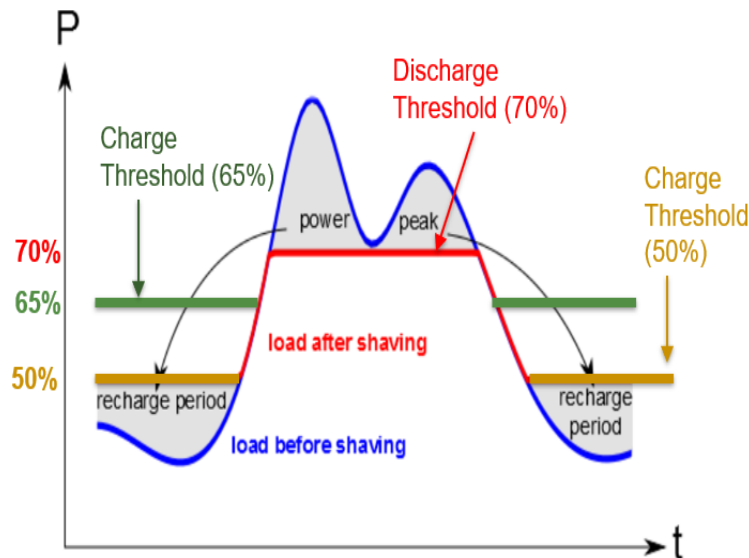
Figure 47. Peak-shaving principle. *Adapted from* **(Karmiris, 2013)**

A load duration curve is used to determine the KVA trigger value set points for the distribution transformer. The load duration curve is developed by sorting the percentage loading on the distribution transformer in descending order. The plot of the load duration curve gives the duration, or how long, a distribution transformer is loaded at a particular loading level, for example, as shown in Figure 48a, for a typical time-series load. The corresponding load duration curve is created by sorting the load in descending order, as shown in Figure 48b.
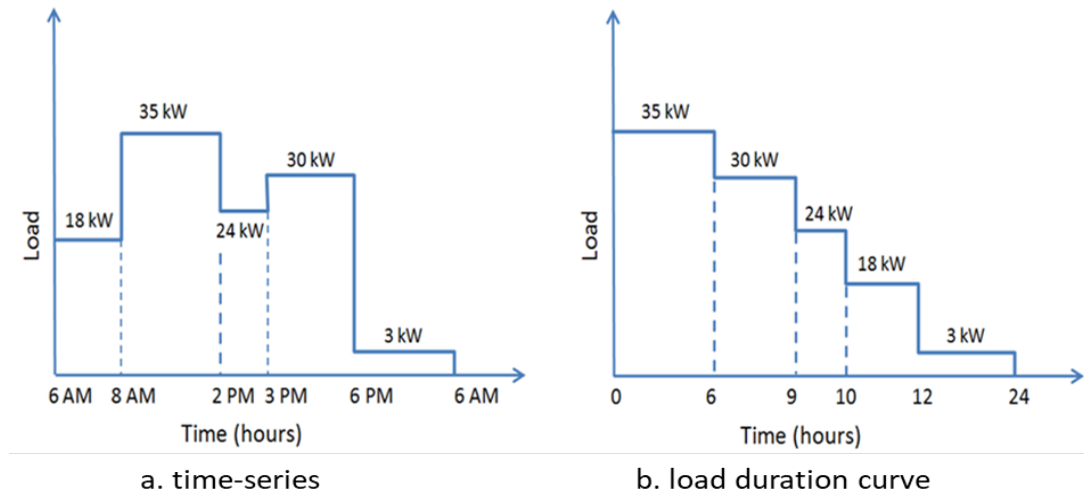
Figure 48. Creation of the load duration curve

Figure 49 shows representative distribution transformers with different load patterns characterizing residential and commercial load profiles. Also shown is the relative behavior of these distribution transformers with respect to the applied peak-shaving control thresholds.

As shown in Figure 49, there are relatively more time points when the BESS discharges to shave the peak for both 70/65 and 70/50 discharge and charge thresholds for some transformers (e.g., DT 29504793). For example, DT 29504798 has the largest percentage loading, with a commercial profile peaking during the daytime, whereas the other distribution transformers follow a residential pattern. This distribution transformer consequently has the largest BESS unit installed to shave this consistent peaking condition. These BESS units were deployed at different distribution transformers to help prevent possible overloading conditions of these distribution transformers as the load grows coupled with EVs integration. Figure 49 also suggests that the efficacy of this peak-shaving algorithm as a function of the charging/discharging thresholds will depend on the load duration curve of the individual transformer, and these threshold values should be designed according to historical consumption patterns.
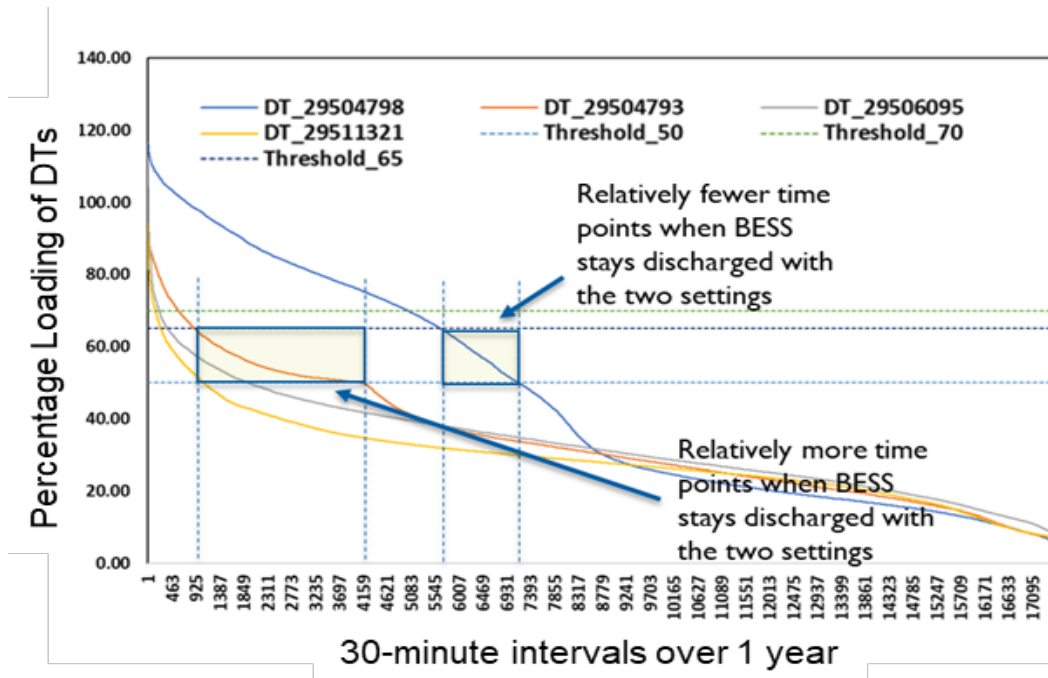
Figure 49. Load duration curves for each distribution transformer and set points for peak-shaving control

5.3 Peak-Shaving Application

This section presents simulation results for the peak-shaving algorithm implementation in 30-minute time step during a period of 10 years when two BESS deployment strategies were employed: (1) a staged deployment that only meets needs in the current year, and (2) one-time deployments of BESS units that would be big enough to cover overloading for the whole 10-year horizon. These two approaches are analyzed to measure the value of waiting for BESS cost-reduction projections, as documented in Cole 2019. Further discussions on the economic viability of this approach are presented in Chapter 6. Also, two charge and discharge set points were used for the implementation of the peak-shaving algorithm to investigate the impact of varying control algorithms on system impact to value and other grid-readiness metrics.

Figure 50 through Figure 53 show the impact of integrating BESS on the number of the 100% overloading instances for the considered distribution transformers. These figures also show the significance of peak-shaving control set points on the distribution transformer overloading time points. Figure 50 and Figure 51 show a significant difference between the two set points: 70/65 resulted in a significant reduction in the number of distribution transformer overloading instances for DT 29504793 and 29506095 (with one-time standard BESS) compared to the 70/50 case. Figure 52 shows DT 29504798 (with staged BESS), which has a commercial profile. As the load continues to increase on this distribution transformer, starting from the year 2024 through 2027, the 70/65 threshold results in a further reduction of the overloading instances than the 70/50 set points. In Figure 53, both set points produced the same result for DT 29511321. These analyses show that using the same set points for all distribution transformers might not be optimal and verifying the control algorithm through modeling could help improve performance.
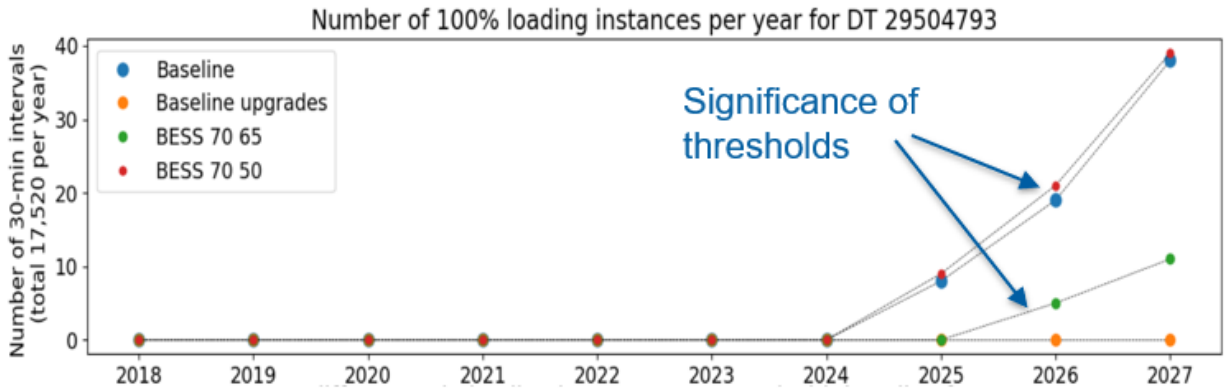
Figure 50. Number of 100% loading instances per year for DT 29504793
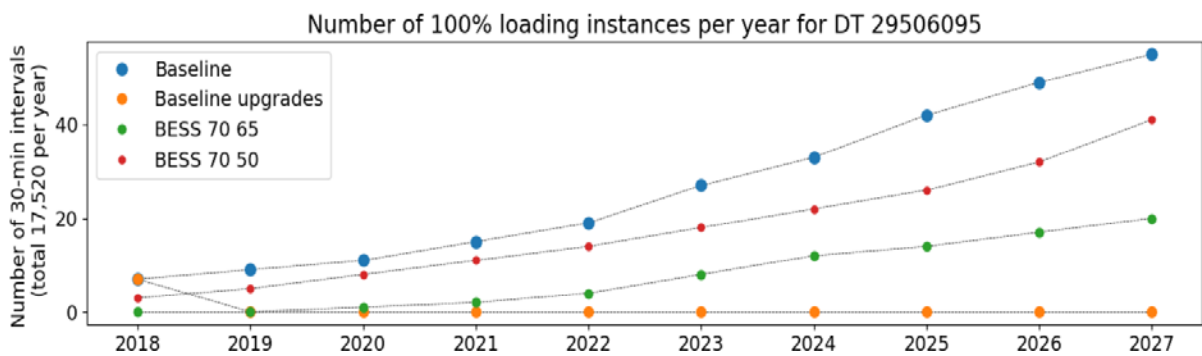
Figure 51. Number of 100% loading instances per year for DT 29506095
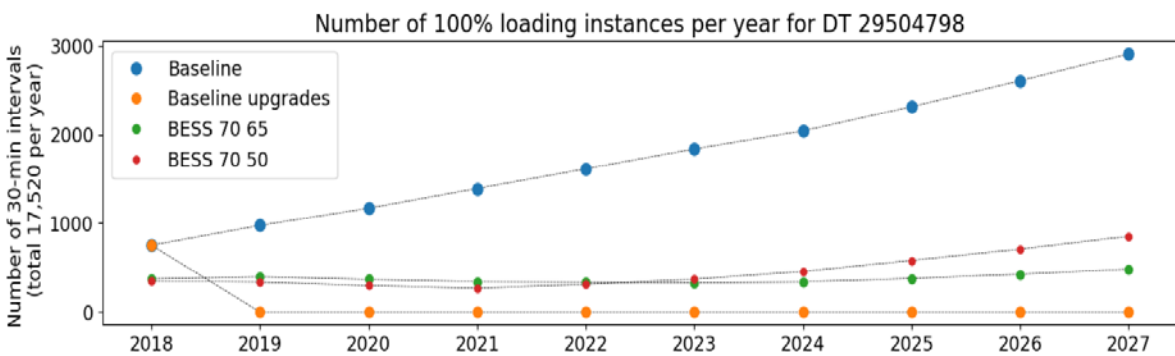
Figure 52. Number of 100% loading instances per year for DT 29504798
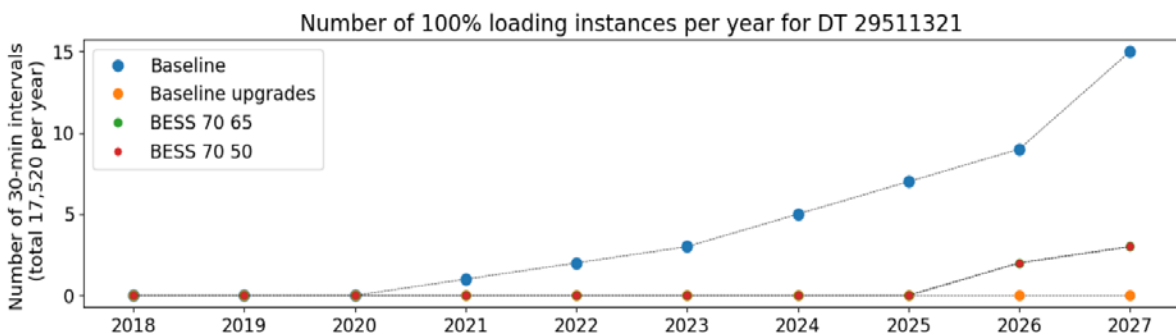
Figure 53. Number of 100% loading instances per year for DT 29511321

5.3.1 Impact on Losses

Distribution transformers are generally designed to operate with maximum efficiency at or near average power; however, a transformer's efficiency depends on its loading. Distribution transformers operating at rated capacity can have a unity loading coefficient (Yang, 2004). As shown in Figure 54, the deployment of BESS helps the distribution transformer operate at a higher efficiency than the baseline and upgrade scenarios.

Although the BESS charges during the distribution transformer minimum loading period, this additional load helps improve the distribution transformer loading coefficient without exacerbating the distribution transformer loading. The 70/65 set points result in the distribution transformer operating at a higher efficiency for more periods in the 10-year study span than the 70/50 threshold. As a result of operating more frequently in the higher efficiency region, the deployment of BESS reduces the distribution transformer losses compared with the baseline values, as shown in Figure 55. At the distribution transformer level, both set points reduced losses compared to the baseline-thermal upgrade. Also, placing BESS near load centers has the potential to reduce distribution and transmission losses.
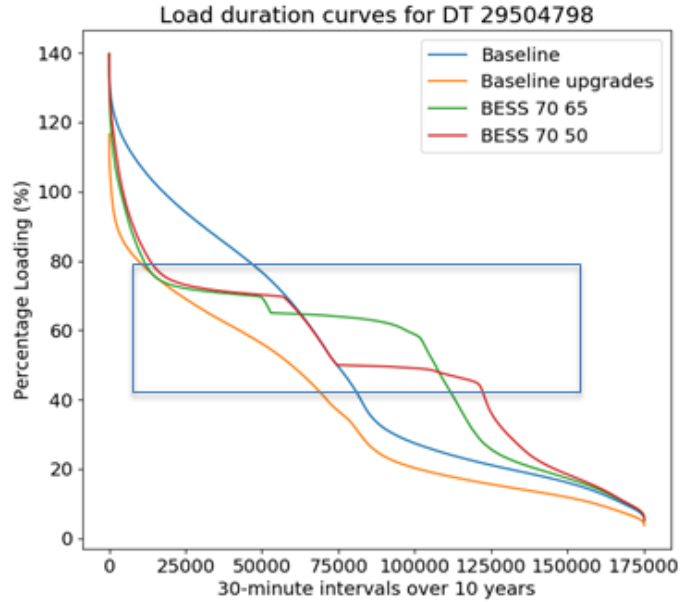
Figure 54. Percentage loading of DT 29504798 in different BESS control set points
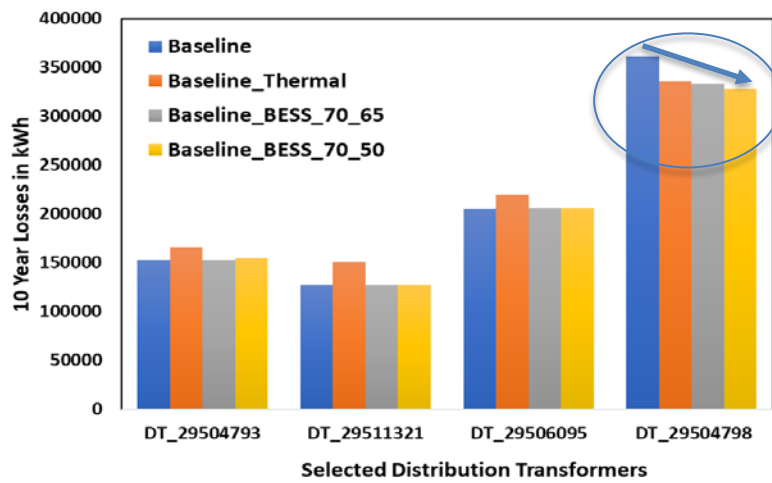
Figure 55. Impact of different deployment scenarios on distribution transformer losses

Apart from losses at the distribution transformers, it important to capture the impact of BESS integration on line losses and overall system-wide losses. As shown in Figure 56, BESS integration resulted in insignificant losses for both 70/65 and 70/50 set points of the peak-shaving control application.
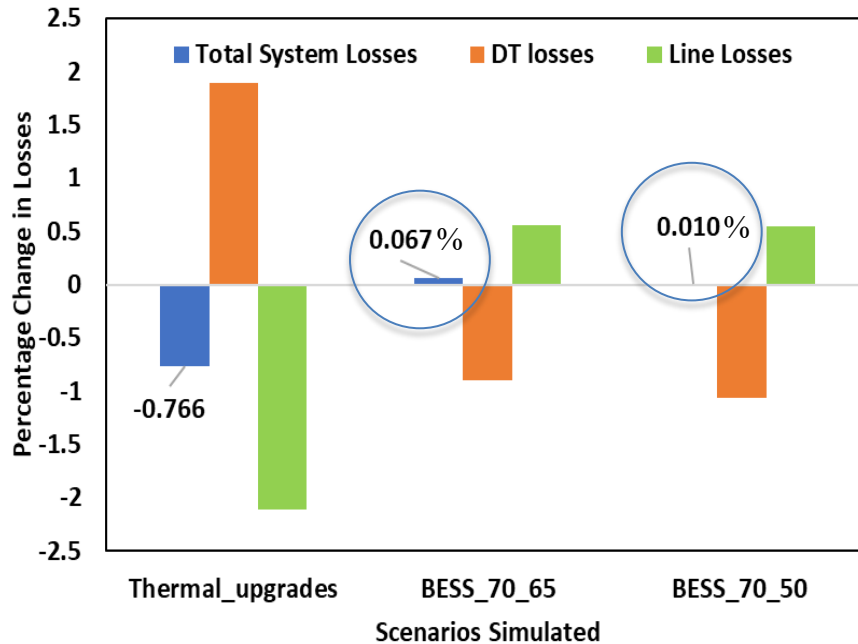
Figure 56. Impacts on distribution transformer and system-wide losses

For both charge/discharge strategies, system losses are negligible—a 0.067% and 0.010% increase over the baseline—for the 70/65 and 70/50 thresholds, as shown in Figure 56.

5.3.2 Battery Energy Storage System Transitions Between States

Although BESS can be used to mitigate distribution transformer overloading conditions, it important to consider the effect of cycling on battery degradation. It is beyond the scope of this study to assess BESS degradation resulting from charge/discharge cycles, but we have implemented an algorithm to determine the number of transitions between charge/discharge states. This number does not indicate the number of charge/discharge cycles.

As predicted from the load duration curves, BESS units installed with DT 29511321 and DT 29504798 tend to have a similar pattern with respect to the charge and discharge thresholds. The set points 70/65 have more BESS operations or change of states than 70/50; whereas for BESS units 29504793 and 29506095, the number of change of states was more for the 70/50 than 70/65 thresholds, as shown in Figure 57. Again, this shows that using the same charging and discharging thresholds might not be optimal for all distribution transformers; however, a balance among system losses, distribution transformer loading, and battery cycling will be helpful to determine an optimal control algorithm for each deployment.
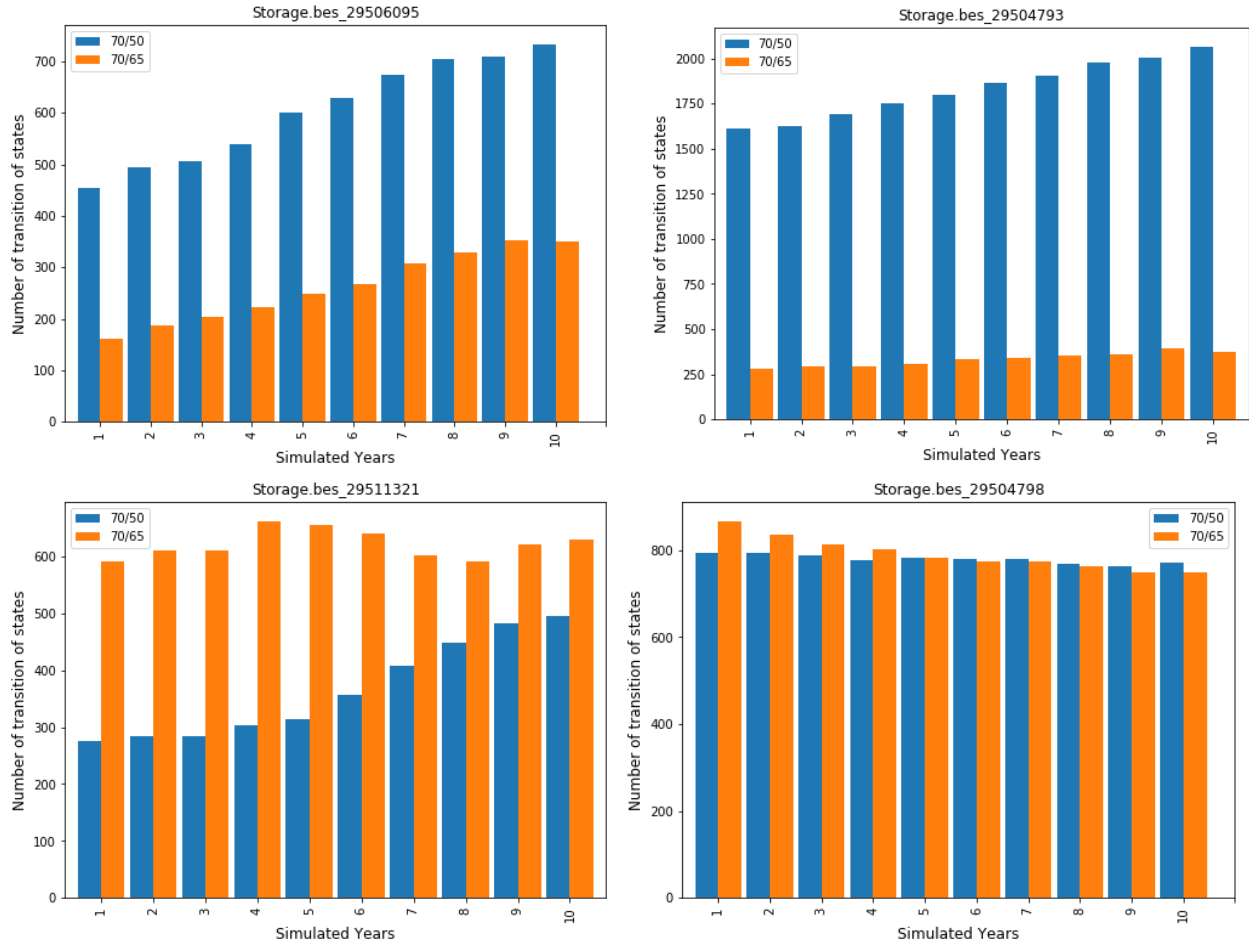
Figure 57. Number of BESS transitions of states for the considered distribution transformers

5.4 Battery Energy Storage System and Electric Vehicle Integration

This section considers a high EV penetration scenario with EV charging stations. In order to enable optimal operation of the system with the integration of EV and BESS, it is important to ensure proper coordination of both systems. Figure 58 and Figure 59 show the impact of BESS and EV charging on the distribution transformer load. Both figures show that the EVs and BESS charge (with the 70/65 threshold) during the distribution transformer loading valleys, and BESS operates to shave the peak.
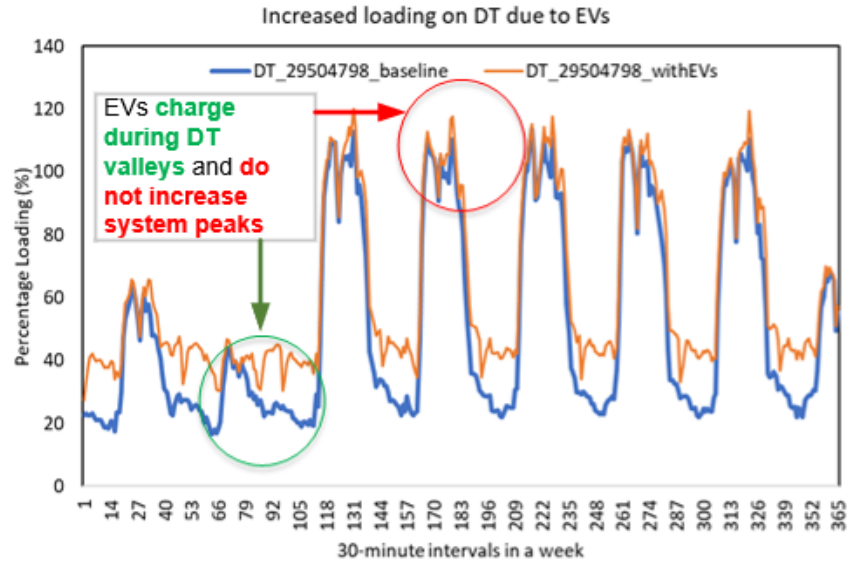
Figure 58. Impact of EV charging on distribution transformer load
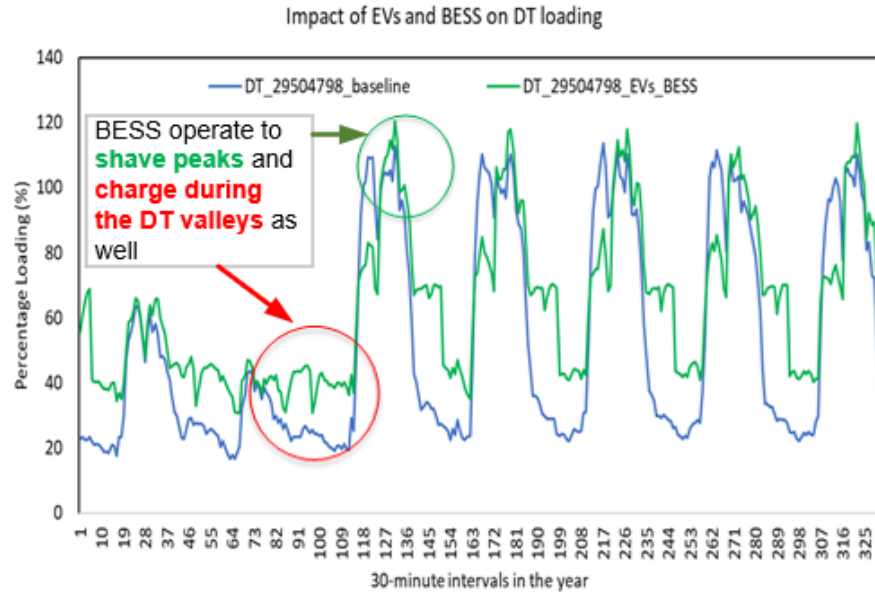
Figure 59. Impact of BESS and EV charging on distribution transformer load

As shown in Figure 60, because EVs and BESS charging occurs in the distribution transformer loading valleys, the distribution transformer operates for a longer duration in the higher efficiency region. This shows that with proper management and control design of these two technologies, the utility can maximize their benefits without comprising the reliability of their network.
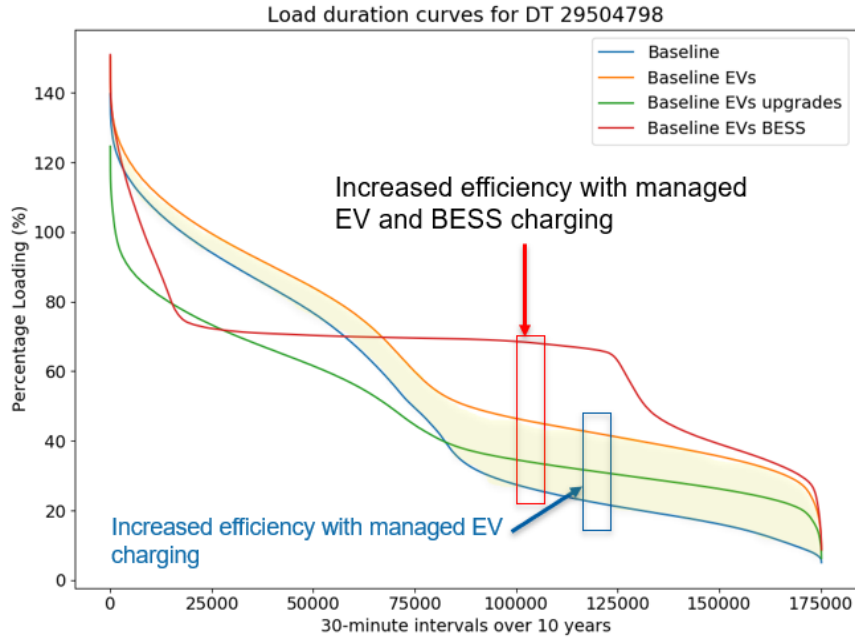
Figure 60. Distribution transformer loading impacts of EV and BESS integration

Figure 61 shows the impact of BESS and EV integration on the number of the 100% overloading instances for DT 29504798. The EVs alone increased the overloading instances by 35% more than baseline during the 10-year period. With the addition of a BESS, however, there is a significant reduction in the number of distribution transformer overloading instances. The BESS unit could mitigate 65% of the overloading instances, reducing even the baseline overloading instances and facilitating EV integration.
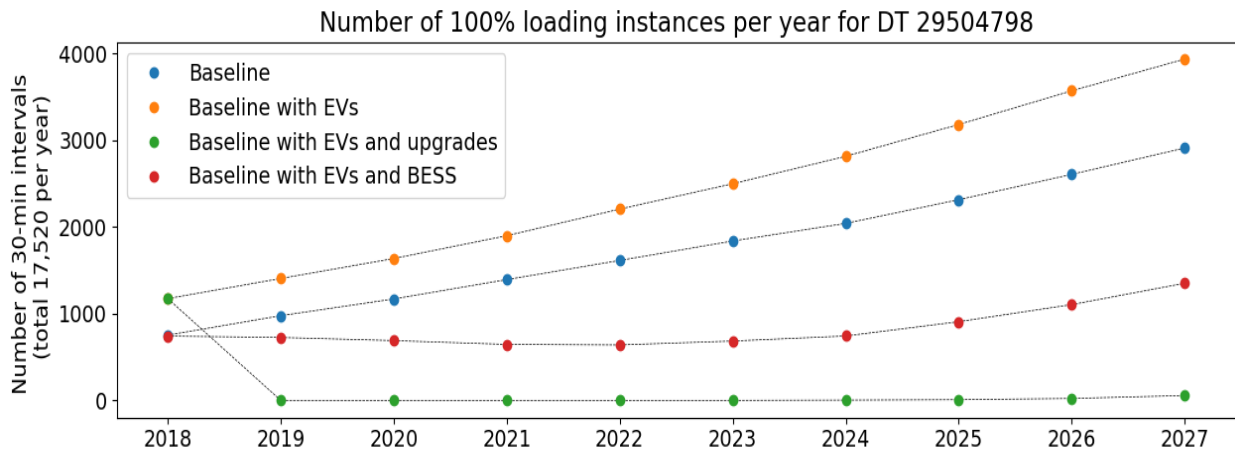
Figure 61. Number of 100% loading instances per year for DT 29504798 with EV and BESS integration

Figure 62 shows comparisons of different scenarios using the system energy loss index. Figure 62 shows that with EVs and BESS integration, the system losses increase insignificantly, by only 0.8%, compared with the baseline.
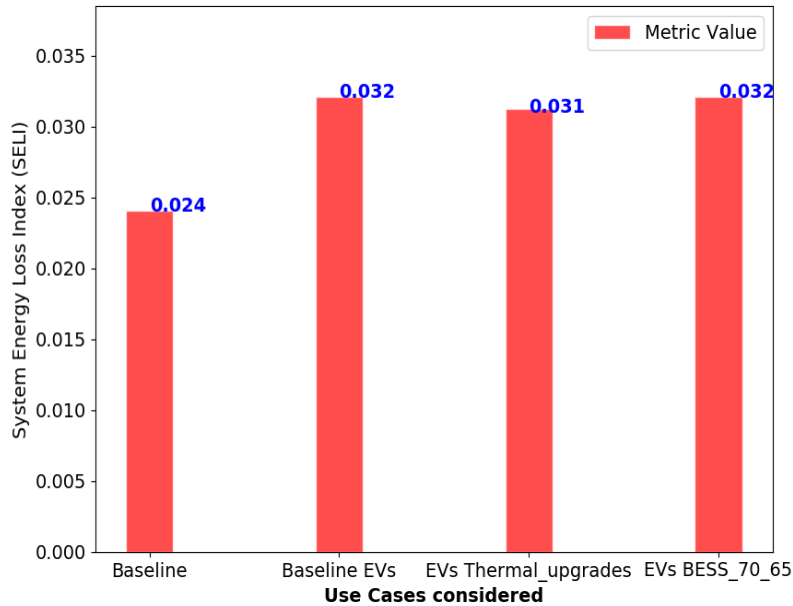
Figure 62. Evaluation of system energy loss index for various scenarios

Another critical consideration in EV integration is the increase in line loading caused by EV charging, which is a key factor for utility system planners and operators. This is because line extensions or upgrades can be a challenging mitigation alternative for network upgrades in a place such as Delhi, where there are space constraints.

In the baseline scenario with EV integration, 126 line segments experienced greater than 100% overloading, which can have a significant impact on line losses and voltage drop. Figure 63 shows the overloaded line segments in red for both the primary and secondary sides.

Figure 63. Impacts of EV charging (high penetration) on line loading

Traditional thermal upgrades of baseline violations could not mitigate EV thermal violations, but the BESS reduced line violations to only 19 line segments, as shown in Figure 64, which represents an 85%

reduction in violations. Thus, BESS units could be useful for network capacity relief as the grid continues to experience unprecedented load growth and for upgrade deferral for locations where scalability or feeder expansion is expensive and infeasible.

Figure 64. Line loading relief as a result of BESS integration under the high EV penetration scenario

5.5 Results: Grid-Readiness Metrics

The simulation architecture described in Section 3.2 was used to simulate different use cases, such as the baseline, baseline with thermal upgrades, and different BESS peak-shaving control set points. This section provides results for these use cases and presents a quantitative comparison in terms of technical indices (as defined in Section 3.1).

Figure 65 shows how the grid-readiness metrics can be used to assess the overall impact of these DERs on the grid, under different scenarios. Metrics M1–M3 (SAVMVI, SAVFI, SAVUI) assess voltage impacts from the DERs for different use cases. As shown in this figure, SAVMVI has a value of approximately 0.000028 which implies that the average violation outside permissible limits is in the order of 10^{-5} p.u. Similarly, a SAVFI value of approximately 0.0024 p.u. implies that the average voltage fluctuation is approximately 0.0024 p.u. Average voltage unbalance is also approximately 0.3%, as shown by the SAVUI metric, whereas 3% is usually acceptable.

From the comparisons within the SAVMVI, SAVFI, SAVUI charts, however, it is evident that traditional thermal upgrades reduce voltage impacts by a small margin and that the BESS peak-shaving application does not significantly contribute to changing the voltage impacts (compared with the baseline).

Capacitor operation count, as shown by $SCDOI_{cap}$, is a bit too high and might not be realistic. These very high capacitor operations on a daily basis can be caused by the relatively larger time step of 30 minutes used for the 10-year simulations compared with the capacitor controller time delays (in the order of few minutes) and other controller settings such as ON and OFF set points; however, BESS do not increase average capacitor operations significantly over the baseline.

M5, or SRPDI, shows that the average reactive power flow through the substation is approximately 765 kVar, which increases marginally with thermal upgrades and reduces with BESS. A smaller substation kVar value indicates a better power factor and reduced loading of the network devices.

SELI, or M6, results imply that the network losses do not change by any significant order compared to the baseline for both the thermal upgrades and BESS peak-shaving application.
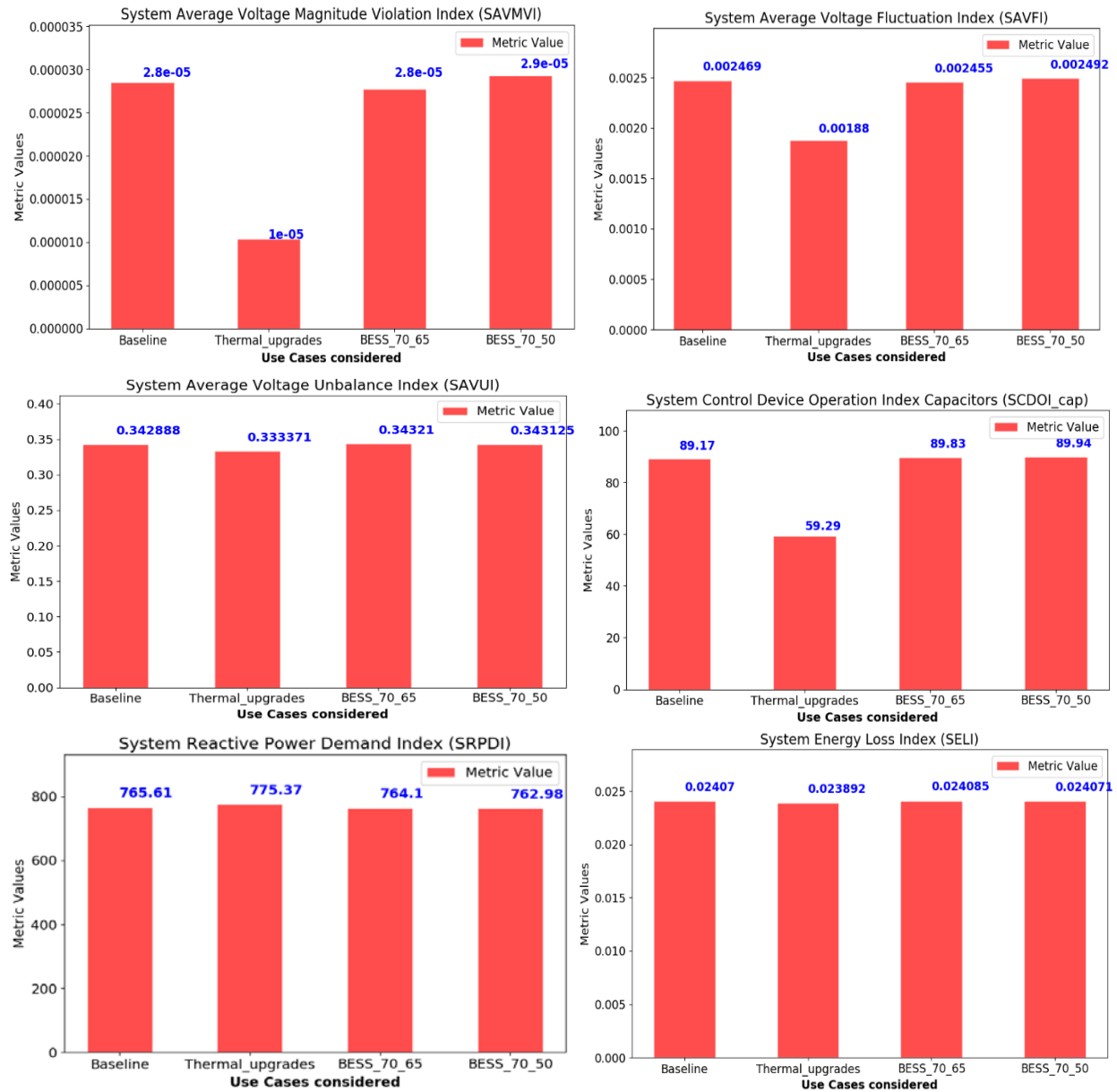
Figure 65. Grid-readiness metrics for BESS (peak shaving), traditional upgrades, and baseline use cases

6 Economic Analysis of Network Upgrades

Network upgrade decision points are determined based on technical analyses from the multiyear simulation performed on the OpenDSS model (Figure 66). Such analyses reveal when and where violations of a predefined suite of technical metrics occur. These technical metrics are used to localize where thermal violations, overloading, undervoltages, or overall power quality issues are observed on the time axis. Because power quality is an important consideration for power system operation, these metrics would represent the grid-readiness for the expected load/EV growth. To ensure reliable operation, this planning phase study considers traditional and advanced upgrade options. A traditional path would consider upgrading the network asset (line or transformer) so that the overall demand growth can be fed. An advanced upgrade option would do so with the integration of BESS that can also provide added benefits on top of mitigating the violations. This chapter looks at the economics of these network upgrade options with an emphasis on cost models evaluated for BESS deployments.
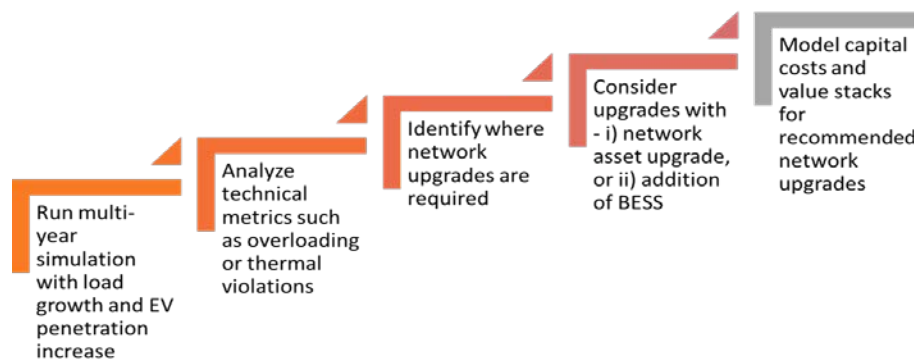
Figure 66. Flowchart for network upgrade decision points

6.1 Bottom-Up Cost Model

Utility-scale BESS integration requires developing a cost model using a bottom-up approach for a realistic capital cost estimate. Total system upfront capital costs include hardware costs (i.e., battery cells, battery racking, storage container, and bidirectional battery inverter); electrical and structural balance-of-system (BOS) costs; labor and equipment costs; engineering, procurement, and construction costs; and soft costs (i.e., fees, taxes, contingencies, and developer costs). BOS includes site preparation, mounting, wiring, containerization, and foundation. Among these components, the battery pack is usually the most expensive across different power/energy sizes.

The energy storage market has grown in recent years in part because of improvements in Li-ion battery technologies. These improvements include cost reductions and performance achievements. The purpose of this portion of this study is to perform bottom-up modeling of a Li-ion BESS that is connected to the grid and to provide economic insight into the specific system components.

The bottom-up cost model includes a mapping of all components that comprise a system (i.e., labor, material, processes, construction, and balance of system). The goal of this analysis is to find the key cost drivers of a system design. Figure 67 shows the bottom-up cost structure of utility-scale BESS installation. Total system upfront capital costs are broken into engineering, procurement, and construction costs and developer costs. Engineering, procurement, and construction nonhardware, or soft, costs are driven by labor rates and labor productivities.
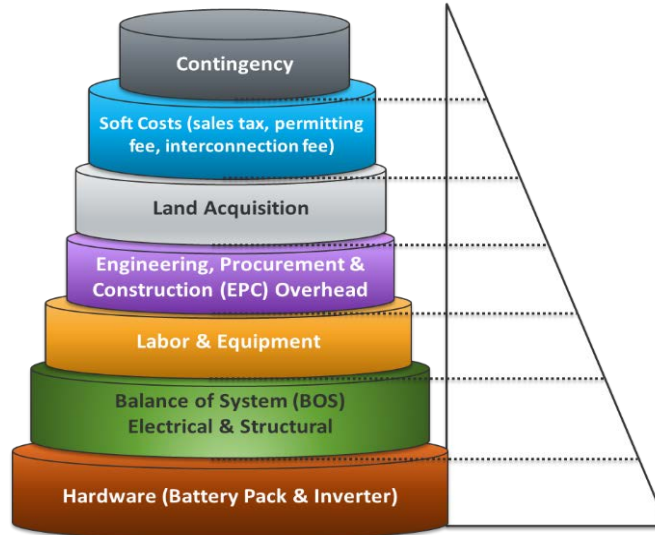
Figure 67. Capital cost components to consider for a utility-scale BESS installation

A typical BESS comprises battery racking, battery containers, power conversion systems, and step-up transformers. The bottom-up cost model is built on data collected from industry. A detailed bottom-up cost structure of our stand-alone storage model is shown in Figure 68 (Fu, 2018).

BOS = balance of system, SG&A = selling, general, and administrative
EPC = Engineering Procurement & Construction
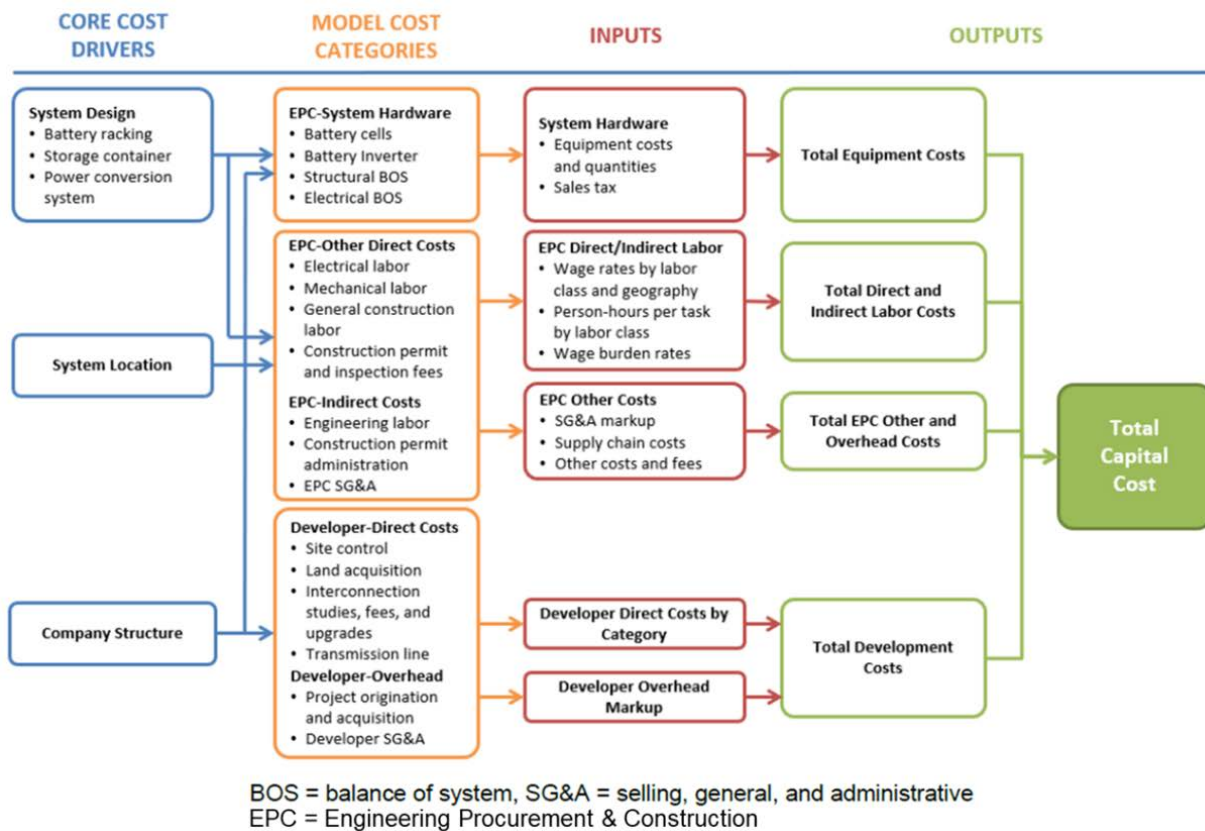
Figure 68. Structure of the bottom-up cost model for stand-alone storage systems (Fu et al. 2018)

We use the inputs from Figure 68 to calculate energy storage cost via the following equation:

$$Energy\ Storage\ Cost\left(\frac{\$}{kWh}\right)$$
$$= Battery\ Cost\left(\frac{\$}{kWh}\right) + \frac{Other\ Costs\ (\$)(Battery\ Inverters\ \dots etc.)}{Storage\ System\ Size\ (kW) \times Duration\ (hours)}$$

Table 4 lists the cost model inputs and assumptions for a utility-scale BESS in the United States (Fu et al. 2018).

Table 4. Utility-Scale Lion Energy Storage System Model Inputs and assumptions in the U.S.		
Category	**Modeled Input**	**Description**
Battery total size	Up to 1.2-MW DC (4,800 kW)	A baseline case to match the optimum load
Battery size per container	5 MWh per 40-feet container	To compute the number of containers
Li-ion battery price	$176/kWh	Ex-factory gate (first-buyer) prices. We use an aggregated Li-ion battery price in the model, and cell types for different durations are not included.
Duration	4 hours	Duration determines energy (MWh)
Battery central inverter price	$0.06/W	Ex-factory gate (first-buyer) prices
Inverter size	2.5 MW per inverter	Used to determine the number of battery inverters
Transformer size	2.5 MW per step-up transformer	Used to determine the number of transformers
Foundation	Up to 1,536 feet^2	Determined by the number of containers, inverters, transformers, and the spacing between containers
Installation labor	Nonunion at rates taken from statistics survey average by state	Modeled labor rate assumes nonunion and union labor and depends on state. National benchmark uses weighted average of state rates.
Sales tax	7.5%	Model assumption. Determined by the sales tax in California
Engineering, procurement, and construction overhead	8.67% for equipment and material; 23%–69% for labor costs; varies by system size, labor activity, and location	Costs associated with engineering, procurement, and construction, SG&A, warehousing, shipping, and logistics
Developer overhead	3% of total installation cost	Includes overhead expenses, such as payroll, facilities, travel, legal fees, administrative, business development, finance, and other corporate functions

Section 5.2.1. describes how the inputs from Fu et al. are improved to reflect the conditions in India.

6.2 Installed Capital Cost Projections

There are several challenges to developing battery cost and performance projections based on publicly available data. The currency year (nominal value), duration, depth of discharge, lifetime, size of the battery systems, and operation and maintenance are not always defined in the same way, and sometimes they are not defined at all. We concentrated our projections on 4-hour Li-ion storage systems in this report. This section presents a total system overnight capital cost expressed in units of $/kWh. All values were converted to 2019$ using the consumer pricing index. (e.g., a $380/kWh, 4-hour battery would have a power capacity cost of $1,520/kW).

The normalized cost trajectories with the low, mid, and high projections are shown in Figure 69 (Cole, 2019). The high projection follows the highest cost trajectory through 2050 and has a constant slope from 2020–2050. The mid and low projections have slope changes between each interval, with initial slopes being steeper than projections farther out, indicating that most publications see larger cost reductions in the near-term that then slow over time. By 2030, costs are reduced by 67%, 45%, and 11% in the low, mid, and high cases, respectively. By 2050, they are reduced by 80%, 59%, and 32%, respectively.
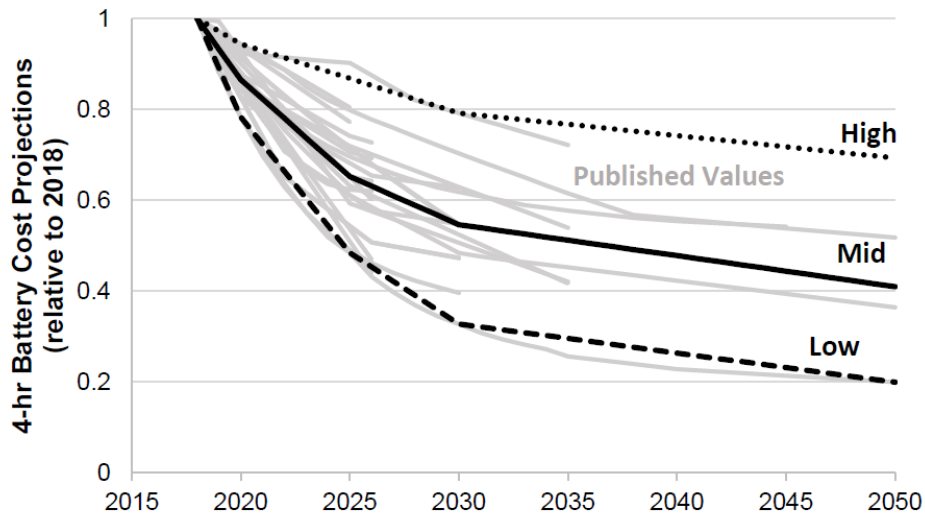
Figure 69. Battery cost projections for 4-hour Li-ion systems, with values relative to 2018. The high, mid, and low-cost projections developed in Cole et al. 2019, are shown as the bold lines.

To fully specify the cost and performance of a BESS, additional parameters besides the installed capital costs are needed, including fixed operation-and-maintenance costs. In recent studies, fixed operation-and-maintenance costs vary between $6/kW-yr fixed operation-and-maintenance and a $40/kWh-yr. We selected fixed operation-and-maintenance cost as $15/kW-yr based on the California Independent System Operator (CAISO) average. Normalized cost reductions for the Li-ion battery and inverter, annual inflator (3%) for labor cost, and annual deflator (2%) for electrical and structural BOS is applied by varying the size of the battery systems. Figure 70 presents 10-year cost projections (2019–2028) for battery system size varying between 800 kWh and 4,800 kWh using these component values.
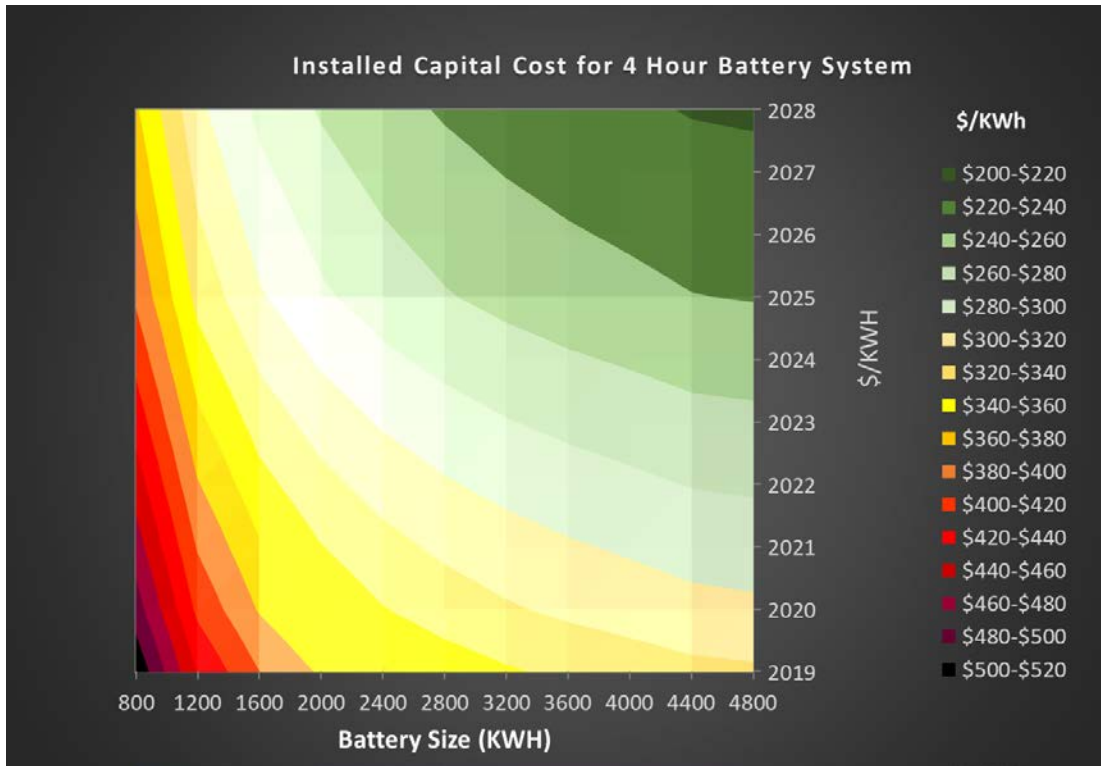
Figure 70. Battery cost projections with respect to system size between 2019 and 2028

6.2.1 Methodology Adjustments for India

6.2.1.1 Applications of Battery Energy Storage Systems

BESS are primarily sized for peak-shaving and subsequent energy time-shifting applications in this study. However, a possible secondary application can be to provide reactive power support and phase balancing, which can be made possible by proper controls and programming. BESS system specifications are selected based on distribution transformer loading and consequent BESS sizing. Modeled system specifications for power, capacity, lifetime cycles, round-trip efficiency and degradation are listed below.:

- Power range: 50 kW–1,200 kW

- Capacity range: 200 kWh–4,800 kWh

- Lifetime cycles: 6,000 (approximately 10 years)

- Round-trip efficiency: 90%

- Degradation: down to 80% of the original capacity over ten years.

6.2.1.2 Capital Cost Adjustments

- The labor rate is set as $2.45/hour as a fixed rate for all types of labor in India (CEMAC, 2018).

- A 3.3% annual inflator is applied to the unit labor cost (BNEF, 2019).

- Normalized cost reductions are applied to the Li-ion battery and inverter (NREL, 2019).

- A 2% annual deflator is applied to electrical and structural BOS (Fu, 2018).

- Some fees and costs have been excluded from the capital model for simplification. Excluded cost items are:

- o   Land acquisition
- o   Permitting fee
- o   Environmental cost
- o   Interconnection fee
- o   Transmission line
- o   Contingency (3%)
- o   Developer overhead
- o   Engineering, procurement, and construction/developer net profit
- o   Taxes (estimates for India).

6.2.1.3 Financial Assumptions for Levelized Cost Calculations

- Inflation: 3.3%
- Real discount rate: 7%
- Debt ratio: From 50%
- Fixed operation-and-maintenance cost: 15 $/kWh-yr (low)
- Electricity price: 7 cents/kWh (low) or 14 cents/kWh (high).

Based on these assumptions, the bottom-up cost model outputs are depicted in Figure 71 in terms of the capital cost breakdown for a 1.2-MW (4.8-MWh) BESS deployment.
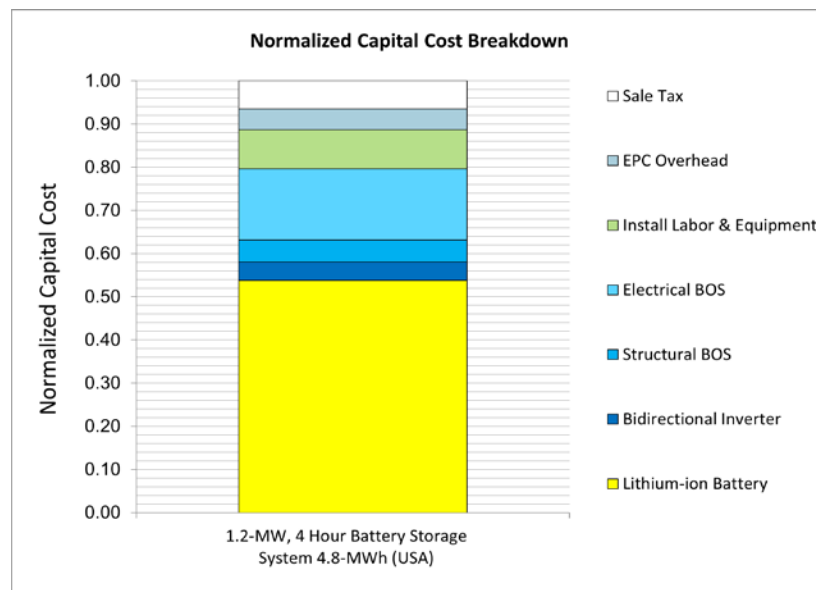
Figure 71. Normalized capital cost breakdown for utility-scale battery system

6.3 Cost Model Outcomes from Multiple Methodologies

This section uses the bottom-up cost model defined in the previous sections to estimate the costs for building a BESS for DT 29504798. DT 29504798, which was identified in section 4.1.4 as needing 3560 kWh of BESS capacity to defer the need for all traditional upgrades to the system. This represents the highest installed capacity on the two modeled feeders. Capital expenditure (Capex) and levelized cost of

energy (LCOE) are the two approaches that are used in the literature to define the feasibility of BESS projects. Both methods have strengths and weaknesses, which is why both methods are explored in this analysis. It is likely that as utilities become more familiar with how BESS fits into their systems new methods will be created or one will be favored over the other depending on the applications.

Capex is the highest contributor to the battery cost. As the capex comes down, the affordability of the battery systems becomes more appealing. Analysis of capital expenditure calculation assumes 100% equity, without financing variables. This is a simplified calculation of most significant cost drivers in energy storage projects.

LCOE is the total lifetime cost of an investment divided by the cumulated generated energy by this investment. The LCOE is the average internal price at which the energy is to be sold to achieve a zero net present value. To derive an LCOE model, the value of the electricity generation and the energy storage need to be defined explicitly. LCOE for storage systems is calculated in a similar manner as for electricity generation. The total cost of ownership of the battery system during the investment period is divided by the delivered energy. The simplified LCOE can then be calculated as:

$$LCOE\left(\frac{\$}{kWh}\right) = \sum_{1}^{n} \frac{\frac{C_{cap} + FOC}{(AEP \times e_r) + VOC}}{(1 + r)^n}$$

where:

- Project lifetime: years (n)

- Capital cost: $ (C_{cap})

- Fixed annual operating cost: $ (FOC)

- Variable operating cost: $/kWh ($VOC$)

- Nominal discount rate: (r)

- Annual electricity production, kWh (AEP).

LCOE is used to model long-term costs of multi-hour BESS operation. Bloomberg New Energy Finance (BNEF) published its findings on LCOE for Li-ion batteries from public and proprietary data in the 2019 *New Energy Outlook* (BNEF, 2019). BNEF's global LCOE benchmark for battery storage sits at $187/MWh as of 2019 in the Delhi region. This is down by 35% relative to the beginning of 2018.

On the other hand, LCOE is highly dependent on annual revenue coming from electricity generation. Batteries do not generate electricity to create revenue. They are used for energy arbitrage, to store energy and use it when needed or various other services. LCOE is also very sensitive to changes in financial parameters and debt structure. Also, it is more complicated when staged deployment becomes a strategy for the project. In our analysis, we used a 50% debt ratio, 10-year loan period, 10.3% loan rate, 3.3% inflation, 7% real discount rate, and 10.53% nominal discount rate for the LCOE calculations.

We estimated the capital cost of a 3,600-kWh battery system (4 hour) as $336/kWh in 2019 and $213/kWh in 2030 (Figure 72). BNEF estimates that capital cost for a battery storage system is $338/kWh in 2019 and $168/kWh in 2030; however, the battery system size is not identified at BNEF's report (BNEF 2019).

The following sections show the outcomes of storage deployment on the Capex methods and the LCOE methods to help give a full picture when comparing BESS investments to other investments.
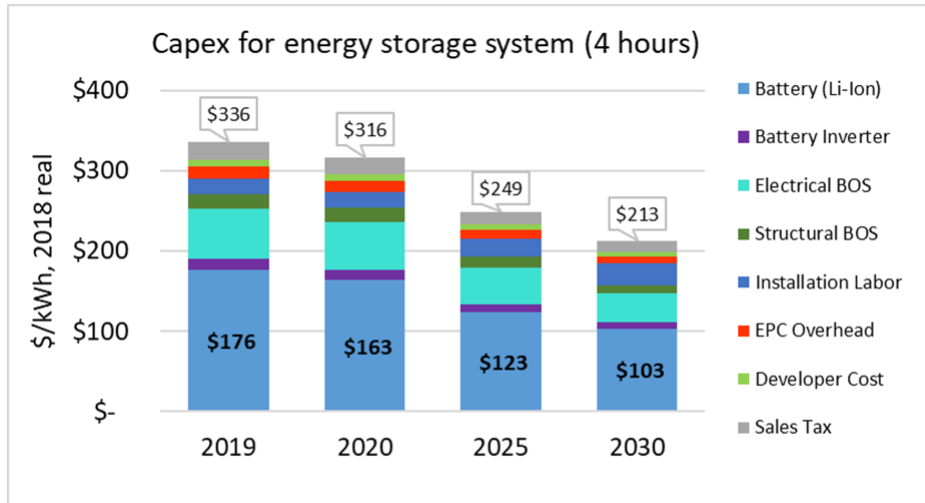
Battery System Size: 3,600 kWh

Figure 72. Capital cost estimated for 3,600-kWh battery using NREL battery cost model

6.3.1 Battery Deployment Scenarios: Standard vs. Staged

The staged deployment is designed for meeting the capacity requirements from the feeder line/transformer upgrades as time advances. We created three deployment scenarios: (1) standard deployment at the first year of the project (3,600 kWh), (2) staged deployment for meeting the battery requirements, and (3) staged deployment by adding 200 kWh every year (Table 5).

Table 5. Standard and Staged Deployment Scenarios for 3,600-kWh Battery System

Total Battery Capacity (kWh)

Years	2019	2020	2021	2022	2023	2024	2025	2026	2027	2028
Standard deployment (Scenario 1)	3,600	3,600	3,600	3,600	3,600	3,600	3,600	3,600	3,600	3,600
Staged deployment (Scenario 2)	2,000	2,400	2,400	3,000	3,000	3,000	3,600	3,600	3,600	3,600
Staged deployment (Scenario 3)	1,800	2,000	2,200	2,400	2,600	2,800	3,000	3,200	3,600	3,600
Battery capacity required (kWh)	**1,474**	**1,760**	**2,055**	**2,329**	**2,556**	**2,840**	**3,054**	**3,287**	**3,560**	**3,560**

Figure 73 represents the impact of standard and staged deployment scenarios to the battery capacity requirements.
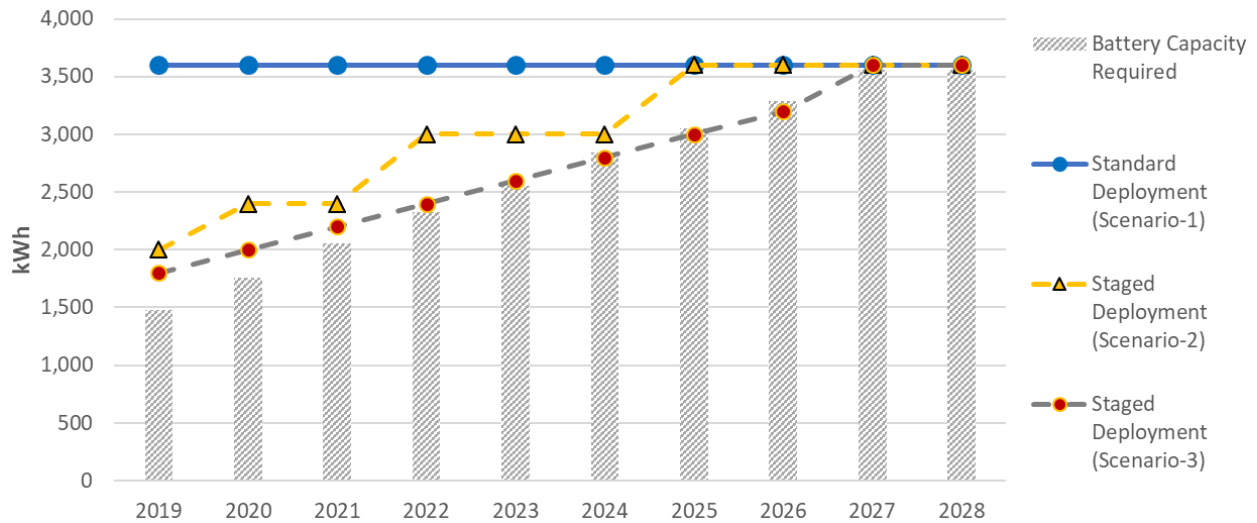

Figure 73. Standard and staged deployment scenarios for 3,600-kWh battery system with respect to battery capacity requirements between 2019 and 2018

Maximum annual energy delivered by the standard deployment scenario is calculated by the installed battery capacity (3,600 kWh, 4 hour x 900 kWh), one cycle per day for the whole year (365 days) at its maximum capacity (1,314 MWh-yr) for the battery lifetime, with the effect of degradation down to 80% at the end of the battery lifetime (10 years). Similarly, for the staged deployment scenarios, maximum annual energy delivered is calculated by the installed battery capacity at that particular year with one cycle per day and the degradation of battery packages based on their installation years (Figure 74).
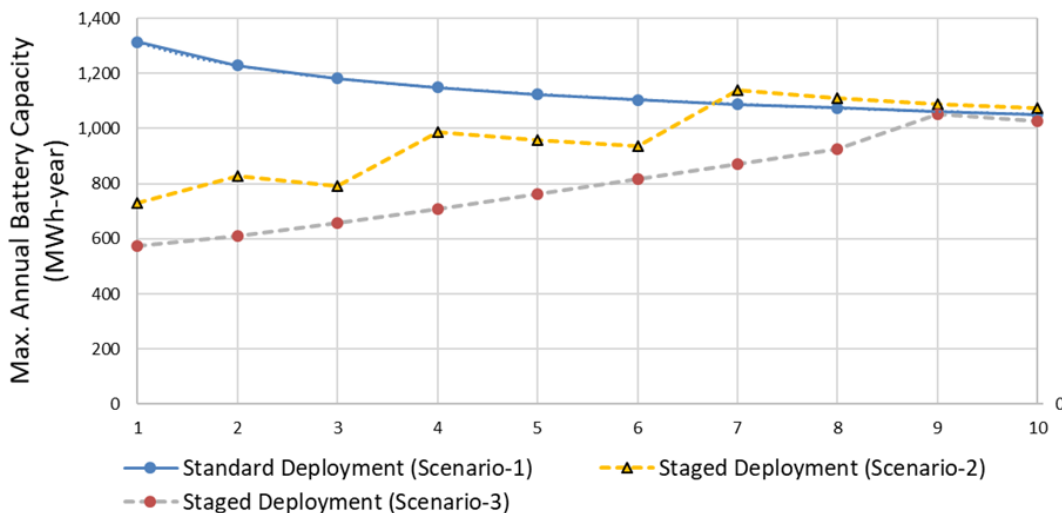
Figure 74. Annual battery maximum capacity increase with the impact of battery degradation for standard and staged deployment scenarios

The Capex method is a simple and effective way of showing the significant cost drivers in energy storage projects. The Capex results of staged deployment scenarios showed that capital costs can be 9.7% cheaper for Scenario 2 and 13% cheaper for Scenario 3 with respect to the standard deployment scenario (Figure 75).
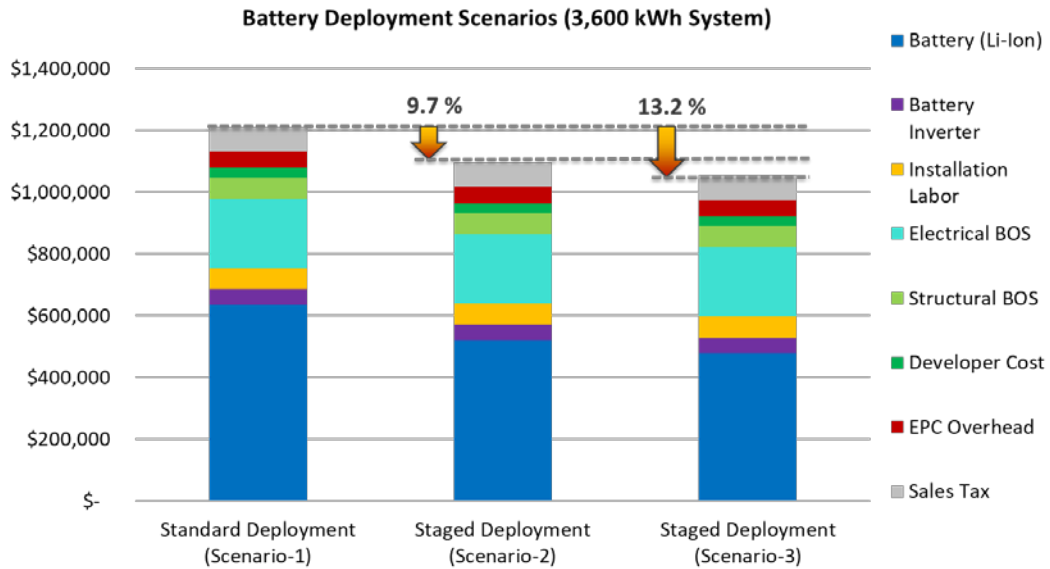
Figure 75. Capital cost savings for staged deployment scenarios

Figure 76 shows BNEF's estimates for battery storage LCOE and outputs of the System Advisor Model (SAM), developed by NREL. As shown, the first 3 years of forecast are very similar, but the SAM estimates increase more than the BNEF numbers ($225/MWh in 2019 and $163/MWh in 2028) in the later years. This likely results from greater detail that is allowed by using SAM, such as the battery size, electricity price, annual electricity generation/delivery, dispatch model, round-trip efficiencies, and annual fixed operation-and-maintenance costs. In our calculations, we modeled a 3,600-kWh battery system with standard deployment, 1,314 MWhr-yr generation/delivery with down to 80% degradation in 10 years, 7 cents/kWh electricity price, and 15 $/kWh-yr fixed operation-and-maintenance cost.
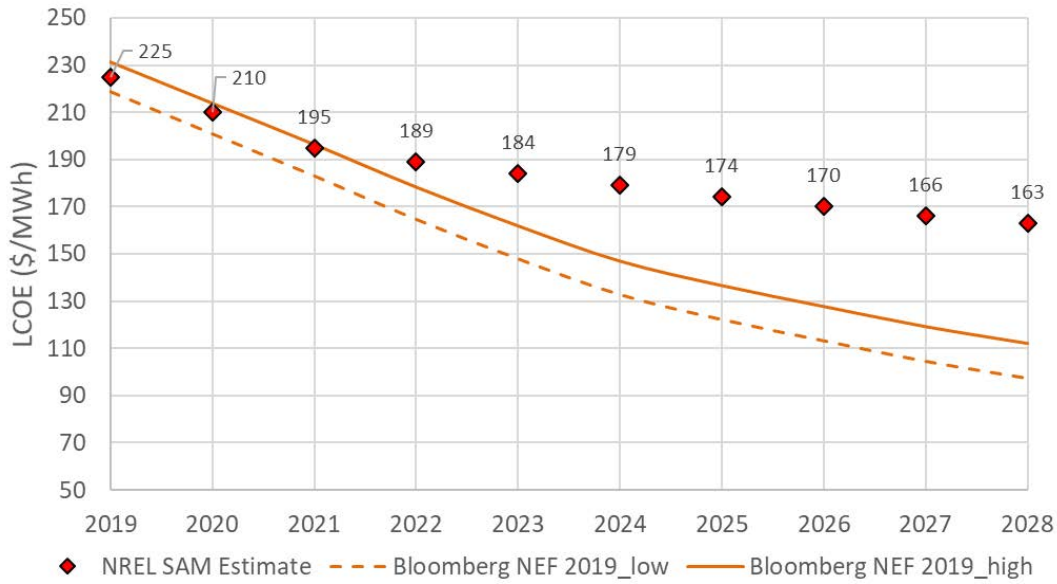
Figure 76. Storage LCOE forecast comparison (BNEF vs. NREL SAM estimates)

Figure 77 represents the sensitivity of LCOE to the electricity price. LCOE is calculated based on the generated electricity from the generator of a power plant. Because batteries do not generate electricity, we defined the buying and selling price of the electricity as the same (7 cents/kWh) and populated the 10-year cash flow. As a sensitivity to power purchase agreement (PPA) prices, we created alternative scenarios by changing the difference of the buying and selling price in 1 cent/kWh increments up to 14 cent/kWh. For example, the power purchase agreement difference (Δ PPA) of 7 cents/kWh stands for the buying price of 7 cents/kWh and selling price of 14 cents/kWh. The results showed that the additional revenue reduced the LCOE at a certain level for Δ PPAs ranging from 1 to 7 cents/kWh (Figure 77). The LCOE values are found to be as low as $126/MWH for Δ PPA of 7 cents/kWh in 2018.
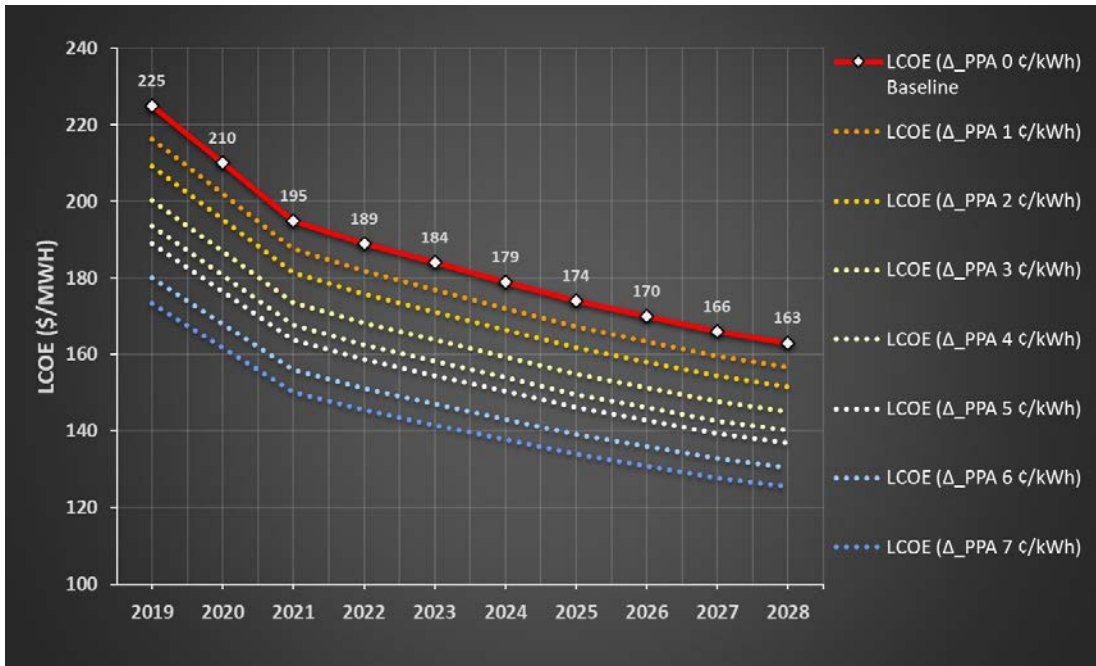
Figure 77. Change in energy storage LCOE with respect to change in electricity buying and selling price difference

Table 6 summarizes the present value of costs for BESS deployment scenarios and for the transformer upgrade scenario, all for the baseline load assumption. The present value of deployment scenarios is discounted to annual to the base year 2019 by applying the annual discount rate. The results show that the BESS scenarios are still more expensive than the traditional transformer upgrades, as shown for the selected Delhi feeders. One of the biggest benefits of BESS, however, is the possibility of providing additional performance criteria beyond traditional line/transformer upgrades alone.

Table 6. Comparison of Present Value of the Cost for Different Deployment Scenarios			
		Present Value ($U.S. 2019)	Present Value (Indian Rupee 2019)
Baseline (no upgrades are done)		$0	₹0
Baseline + BESS	Scenario 1: Standard Deployment	$1,210,000	₹86,428,571
	Scenario 2: Staged Deployment (Reaching Demand)	$1,090,000	₹77,857,143
	Scenario 3: Staged Deployment (Annual)	$1,050,000	₹75,000,000
Baseline + Transformer Upgrade		$285,000	₹20,357,143

6.4 Key Takeaways from Cost Analysis

Evaluating the cost-benefit of new technologies such as BESS is difficult because the full operational or capacity value of an asset is somewhat uncertain and likely to have either benefits or challenges that are not forecasted. In terms of benefit, one can imagine that a BESS placed on a feeder for DT loading control would, over time and experience of the operator, be utilized for other purposes such as helping to balance energy or be operated in a strategic way during emergencies. Therefore, the bottom-up cost model outlined in this section provides various methodologies for evaluating costs that may all be necessary comparing new investments in BESS, at least until investments in BESS is a more established practice by utilities.

LCOE is limited in its ability to evaluate energy storage systems because batteries do not generate electricity. Rather, to compare the merits of different types and sizes of batteries, an alternate set of metrics are required that are normalized in some respect, such as the net present value of benefits minus costs, normalized to the storage capacity, or reported as a ratio of benefits to costs. As examined in this report, capital expenditure is a simplified calculation of significant cost drivers in energy storage projects and may provide necessary insights beyond LCOE for a deployment like the one outlined in this report. Installed battery costs are expected to reduce by 45% for the mid scenario cases in 2030 (Cole, 2019). This is also supporting the idea of postponing the capital expenditures to later years in staged deployment Capex models. It is very hard to reflect that scenario in an LCOE model due to high volatility in financial parameters. Key takeaways from the cost analysis include:

- The staged deployment scenario results in additional cost savings because the price of batteries is expected to decrease over time, and delaying investment in capacity that is not needed has obvious benefits. While there could be challenges in other aspects of a staged deployment, the savings is substantial, with a 13.2% savings in the most optimal deployment strategy.

- The results of the Capex model showed that, the unit cost for 3,600 kWh battery system can be as low as $338/kW for a standard deployment scenario. Similarly, unit Capex can be as low as $302/kW and $291/kW for staged deployment scenario case 1 and case 2 respectively.

- BESS could provide additional performance criteria that additional transformer upgrades alone do not.

7 Conclusions

This report presented a detailed framework for analyzing the impacts of emerging technologies, including EVs and BESS, on distribution feeders in India. The results obtained on models of two representative distribution feeders taken from BRPL's territory in Delhi, India, were also presented. Novel distribution feeder modeling, data cleaning, and load allocation techniques were developed as a part of this effort. A suite of grid-readiness metrics was also integrated in the framework to help assess the impacts of emerging technologies on grid operation and voltage. These metrics provide a quantifiable way of comparing different DER scenarios. The developed distribution systems analysis platform can be easily scaled for testing the impacts of various types of DERs and DER use cases.

As part of this effort, more than 500 hours of quasi-static time-series simulations were completed to analyze various DER scenarios using NREL's supercomputing facilities. A 10-year time horizon was considered, starting from 2018 until 2027, to better assess requirements for network upgrades as EVs and load continue to increase on feeders. Traditional approaches of increasing asset capacities—either by adding new devices or by replacing existing, overloaded devices with higher rated devices—were compared against the scenario where an appropriately sized BESS was used to mitigate overloading conditions. An easy-to-use approach was developed that can suggest effective control points to be used for BESS by simply looking at the load duration curves of the distribution transformers. It was shown that choosing the correct control set points for BESS is essential because an incorrectly chosen set point might worsen the overloading instances.

From these simulations, it was found that even a conservatively sized BESS designed to mitigate only the 70th percentile of overloading instances was sufficient to defer network upgrades for several years into the future. A significant reduction in overloading instances was observed for that BESS, which followed a staged approach. In this approach, instead of adding a BESS sized for the 10th year in the first year, additional batteries were added each year based on the loading requirements. The impact of the BESS on feeder losses compared with the baseline and the traditional upgrades scenario was insignificant. This was because even though there was a marginal increase in net line losses, the distribution transformer losses reduced significantly as a result of their increased operation in their higher efficiency region.

The baseline, traditional upgrades, and BESS scenarios were simulated along with EVs in the feeder. Load increase because of EVs was modeled by considering realistic driving patterns, charging behaviors and the rated capacity of different charger types to meet the expected SOC of EVs. The EVs charging at charging stations were charged during the valleys or low loading periods of their corresponding distribution transformers. This helped in increasing equipment utilization and efficiency. Such a charging approach can be implemented using novel rate structures that incentivize charging during off-peak periods. An important observation was that BESS could defer approximately 85% of expensive line upgrades required because of high EV penetration by mitigating overloading instances. Traditional upgrades based on baseline thermal violations could not defer these upgrades. It was also found that connecting EV charging stations to the primary or high-voltage lines of the feeder reduced undervoltage violations and secondary line upgrades compared with the secondary connected charging stations.

Another major accomplishment of this effort was the development of a bottom-up cost model for BESS applicable for India. This model was used to determine the most cost-effective approach for installing BESS. Three scenarios were compared. In the first scenario, the BESS installed in the first year was sized to meet the expected requirements of the 10th year. A staged approach was followed in the second and third scenarios. In the second scenario, the BESS was sized to meet energy requirements of the first couple of years, and additional batteries were added after several years. In the third scenario, batteries were added each year to fulfill the energy requirements of the respective year. It was found that the present value of the BESS was 10% less in the second scenario than the first scenario, whereas it was

13% less in the third scenario than the first scenario. This showed that appropriate sizing, control, and a staged BESS deployment approach could provide significantly more technical and cost benefits.

8 Notable Outcomes of This Study

This study led to numerous interesting findings. This chapter summarizes the modeling, simulations, and analyses to selected outcomes. Some findings are specific to the evaluation of BESS and EVs, whereas some outcomes are generic policy suggestions. The following sections summarize six outcomes. References to chapters and subsections are also included for more detail.

8.1 Unmet and Unidentified Needs to Monetize Storage Services

A BESS is an expensive asset, and every techno-economic analysis or cost-benefit analysis considers net present value and return on investment. The common understanding is that BESSs are not in a position provide a positive net present value. That aspect of a negative return on investment is a true and present challenge all over the world, despite the increase in BESS deployments. Although there is no one rationale for increasing BESS deployments globally, part of the cause is investors understand that not all the services a BESS can provide are monetizable. Figure 78 lists and categorizes all the services a typical BESS can provide; however, not all services can be converted to currency. With all future predictions pointing towards further reduction of BESS costs, it is certainly worth evaluating value from BESS prior to thermal upgrade proposal is put up before appropriate authorities.
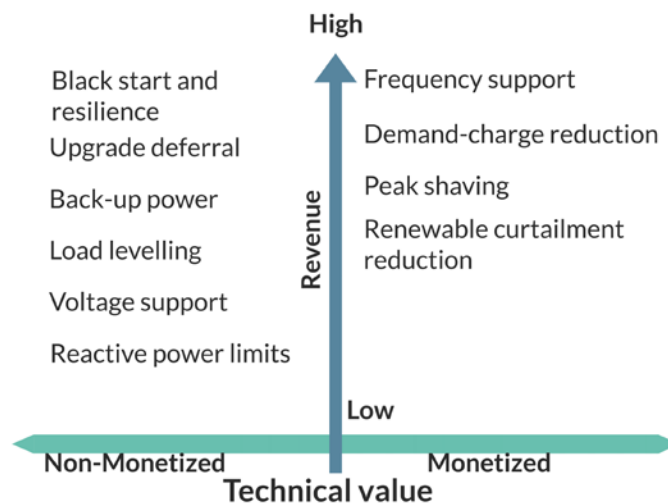

Figure 78. Technical value of BESS and categorization of nonmonetizable and monetizable services

8.2 Scalability of reusable Framework for Distribution Utilities

This effort developed a reusable framework for distribution utilities to assess the impact of emerging technologies (BESS, EV, and PV) on their power distribution grids. The framework contains three layers, as shown in Figure 79. The first and base layer is distribution feeder topology assessment. The second layer is for distributed generation, such as rooftop PV or any generation resources commonly referred to as a DER. The third layer is dedicated to BESS. The fourth layer is built to include EVs. Overall, all four layers interact and provide a comprehensive assessment of challenges and opportunities from emerging technologies.
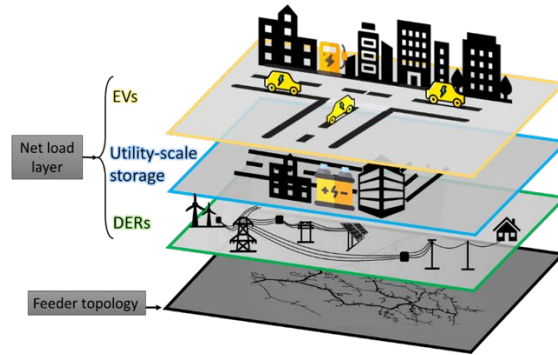
Figure 79. Modular layers in our power distribution analyses framework

Although this framework was simulated on NRELs HPC and simulation runs exceeded 500 hours, the computational requirements for using this framework are not beyond a typical server or modern laptop. It is expected that BRPL engineers could run distribution feeder operations scenarios without the need for upgrades of simplification of models.

Analysis using this framework can be conducted outside of a supercomputing system, given that we would like many utilities and other interested users to do this analysis. The solution framework is built entirely based on open-source platforms and programming language. All the dependencies are open and accessible, keeping in mind other utilities or interested users.

8.3 Impact of Battery Energy Storage System on Distribution System Losses Are Negligible

The main case study performed in this effort is on helping distribution utilities understand the implications of deferring a distribution transformer upgrade by deploying a BESS in the neighborhood. Hence, the presiding question was understanding how a BESS affects system losses. Distribution transformers are generally designed to operate with maximum efficiency at or near 70% of rated power—in other words, transformer efficiency depends on its loading. As shown in Figure 80, the deployment of BESS helps the distribution transformer to operate at a higher efficiency region than the baseline and upgrade scenarios.

Although a BESS charges during the distribution transformer minimum loading period, this additional load helps to improve the distribution transformer loading coefficient without exacerbating the distribution transformer loading. As a result of operating more frequently in the higher efficiency region, the deployment of BESS reduces the distribution transformer losses compared with the baseline values, as shown in Figure 81. At the distribution transformer level, both set points reduced losses compared to the baseline-thermal upgrade. Also, placing a BESS near load centers has the potential to reduce distribution and transmission losses.
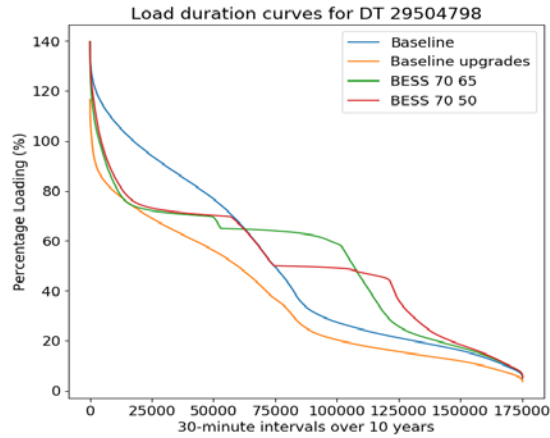
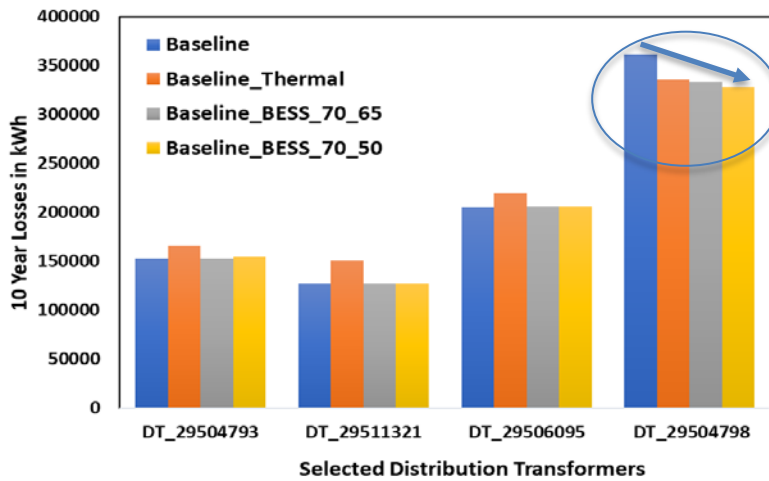**Figure 80. Percentage loading of DT 29504798 in different BESS control set points**

Figure 81. Impact of different deployment scenarios on distribution transformer losses

8.4 Choice of Battery Energy Storage System Controls Decide the Value, Purpose, and Life of the Asset

Power system planning operations ensure that there is enough capacity to service peak-loading conditions to maintain grid reliability. The peak-shaving mode of BESS requires the service operator to provide trigger values for peak shaving and base loading. The BESS will discharge power into the grid if the total power demand at the measured point—in this case, the distribution transformer—is greater than the peak-shaving upper reference limit. Conversely, the BESS will charge if the total power consumption at the measured point is less than the base-loading limit. It is important to ensure that charging the BESS occurs during the baseload loading periods (i.e., the valleys) to avoid overloading the distribution transformer during peak periods.

A load duration curve is used to determine the set points for the distribution transformer. Figure 82 shows the impact of peak-shaving thresholds on its effectiveness. This figure also shows the significance of peak-shaving control set points on the distribution transformer overloading time points. Figure 82 shows a significant difference between the two set points: 70/65 resulted in a significant reduction in the number of distribution transformer overloading instances for DT 29504793 and DT 29506095 (with one-time standard BESS) compared to the 70/50 case. Specifically, the 70/50 use case lead to an increase in overloading scenarios, perhaps negating the purpose of BESS deployment.
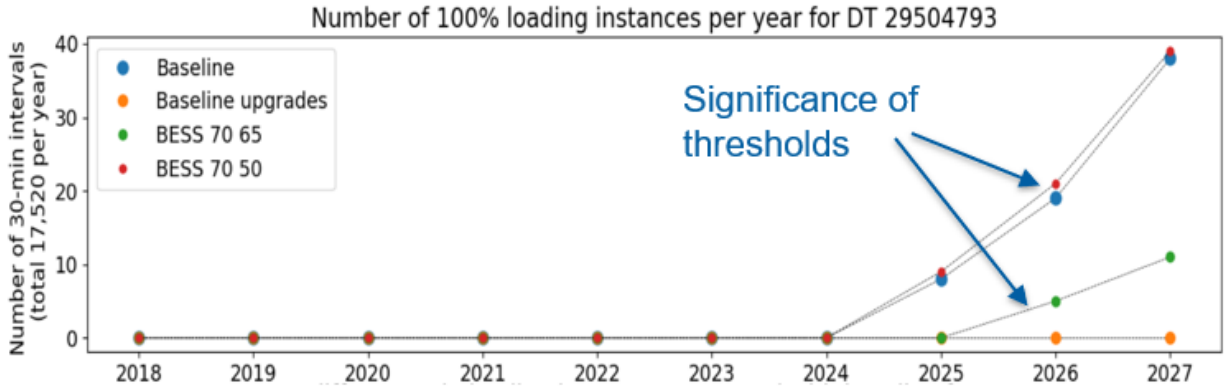
Figure 82. Number of 100% loading instances per year for DT 29504793

Note: BESS 70 65 represents a control scheme where the battery operates to keep the loading of the DT between 70% and 65%. Simillarly for BESS 70 50 keeping the DT between 70% and 50%.

8.5 Staging Battery Deployments Can Be Cost-Effective

We created three deployment scenarios: (1) standard deployment during the first year of the project (3,600 kWh), (2) staged deployment to meet the battery requirements, and (3) staged deployment by adding 200 kWh every year (Table 7).

Table 7. Standard and Staged Deployment Scenarios for 3,600-kWh Battery System										
Years	**2019**	**2020**	**2021**	**2022**	**2023**	**2024**	**2025**	**2026**	**2027**	**2028**
Standard deployment (Scenario 1)	3,600	3,600	3,600	3,600	3,600	3,600	3,600	3,600	3,600	3,600
Staged deployment (Scenario 2)	2,000	2,400	2,400	3,000	3,000	3,000	3,600	3,600	3,600	3,600
Staged deployment (Scenario 3)	1,800	2,000	2,200	2,400	2,600	2,800	3,000	3,200	3,600	3,600
Battery capacity required (kWh)	1,474	1,760	2,055	2,329	2,556	2,840	3,054	3,287	3,560	3,560

The results of the staged deployment scenarios showed that capital costs can be 9.7% less for Scenario 2 and 13% less for Scenario 3 (Figure 83). Section 6.3.2 contains detailed descriptions on how we reached this result.
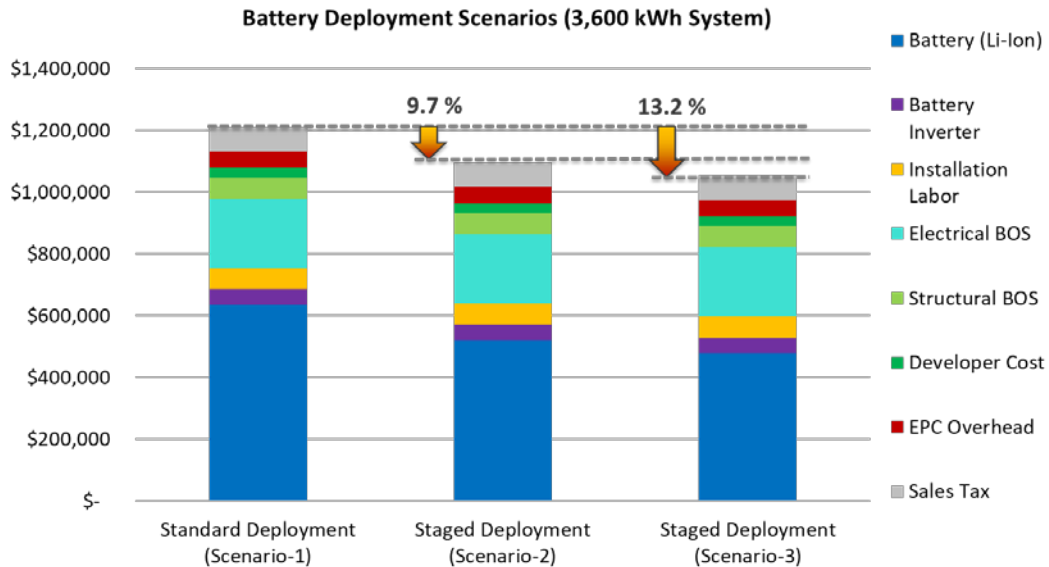
Figure 83. Capital cost savings for staged deployment scenarios

8.6 Coupling Battery Energy Storage System with Electric Vehicle Leads to More Benefits

A critical consideration in EV integration is the increase in line loading caused by EV charging, which is a key factor for utility system planners and operators. This is because line extensions or upgrades can be a challenging mitigation alternative for network upgrades in a place such as Delhi where there are space constraints. As EV penetration increases loading of lines, transformers also increase. Not all distribution feeders can accommodate an increase in EV penetration at the same rate or to the same extent. Different distribution feeders have different limits due to ageing and other physical limitations. Chapter 3 in this report lists six grid-readiness metrics to assess the state and opportunities of distribution feeder.

Additionally, a use case was assessed particularly to understand how a BESS can displace the need for grid upgrades with high EV penetration on selected distribution feeder. In the baseline scenario with EV integration, 126 line segments of the selected distribution feeder experienced greater than 100% overloading, which can have a significant impact on line losses and voltage drop. Figure 84 shows the overloaded line segments in red for both the primary and secondary sides.

Figure 84. Impacts of EV charging (high penetration) on line loading

The traditional thermal upgrades of the baseline violations could not mitigate EV thermal violations, whereas deploying BESS reduced line violations to only 19 line segments, as shown in Figure 85, which represents an 85% reduction in violations. Thus, BESS units could be useful for network capacity relief as the grid continues to experience unprecedented load growth, and for upgrade deferral for locations where scalability or feeder expansion is expensive and infeasible.

Figure 85. Line loading relief as a result of BESS integration under the high EV penetration scenario

References

BNEF. (2019). *New Energy Outlook.* New York City: BloombergNEF.

Cole, W. a. (2019). *Cost Projections for Utility-Scale Battery Storage.* Golden, Colorado: National Renewable Energy Laboratory.

EPRI. (2016). *StorageVET V1.0 Software User Guide: User and Technical Documentation for the Storage Value Estimation Tool.* Palo Alto, California: Electric Power Research Institute.

Espinosa, A. N. (2015). *Low Voltage Networks Models and Low Carbon Technology Profiles. ENWL LV Network Solutions Dissemination Document.* Manchester, United Kingdom: The University of Manchester.

Fu, R. T. (2018). *2018 U.S. Utility-Scale Photovoltaics-Plus-Energy Storage System Costs Benchmark.* Golden, Colorado: National Renewable Energy Laboratory.

Hledik, R. (2017). *Stacked Benefits: Comprehensively Valuing Battery Storage in California.* Sacramento, California: California Energy Commission.

Karmiris, G. a. (2013). *Peak Shaving Control Method for Energy Storage.* Vasterås, Sweden: ABB.

NREL. (2019). *Annual Technology Baseline.* Golden, Colorado: National Renewable Energy Laboratory.

Stephen, O. a. (2014). Geospatial Modeling of Electricity Distribution Network In Ife Central Local Government Area, Osun State, Nigeria. *Science Journal of Environmental Engineering Research*, 1-7.

Yang, M. Y. (2004). Efficient Operation Regions of Power Distribution Transformers. *IEEE Transactions on Power Delivery*, 1713-1717.

About USAID

The United States Agency for International Development (USAID) is an independent government agency that provides economic, development, and humanitarian assistance around the world in support of the foreign policy goals of the United States. USAID's mission is to advance broad-based economic growth, democracy, and human progress in developing countries and emerging economies.

About the Ministry of Power, Government of India

The Ministry of Power is primarily responsible for the development of electrical energy in the country. The Ministry is concerned with perspective planning, policy formulation, processing of projects for investment decision, monitoring of the implementation of power projects, training and manpower development, and the administration and enactment of legislation in regard to thermal, hydro power generation, transmission, and distribution.

About NREL

The National Renewable Energy Laboratory (NREL) is the U.S. Department of Energy's (DOE's) primary national laboratory for renewable energy and energy efficiency research. NREL deploys its deep technical expertise and unmatched breadth of capabilities to drive the transformation of energy resources and systems.